



Comprehensive Power System Reliability Assessment

Final Project Report

Power Systems Engineering Research Center

*A National Science Foundation
Industry/University Cooperative Research Center
since 1996*





Power Systems Engineering Research Center

Comprehensive Power System Reliability Assessment

Final Project Report

Research Team Faculty

Sakis Meliopoulos, Georgia Institute of Technology
David Taylor, Georgia Institute of Technology
Chanan Singh, Texas A&M University

Research Team Students

Fang Yang, Georgia Institute of Technology
Sun Wook Kang, Georgia Institute of Technology
George Stefopoulos, Georgia Institute of Technology

PSERC Publication 05-13

April 2005

Information about this project

For information about this project contact:

A. P. Sakis Meliopoulos, Project Leader
Professor
School of Electrical and Computer Engineering
Georgia Institute of Technology
Atlanta, Georgia 30332
Phone: 404 894-2926
Fax: 404 894-4641
Email: sakis.meliopoulos@ece.gatech.edu

Power Systems Engineering Research Center

This is a project report from the Power Systems Engineering Research Center (PSERC). PSERC is a multi-university Center conducting research on challenges facing a restructuring electric power industry and educating the next generation of power engineers. More information about PSERC can be found at the Center's website: <http://www.pserc.org>.

For additional information, contact:

Power Systems Engineering Research Center
Cornell University
428 Phillips Hall
Ithaca, New York 14853
Phone: 607-255-5601
Fax: 607-255-8871

Notice Concerning Copyright Material

PSERC members are given permission to copy without fee all or part of this publication for internal use if appropriate attribution is given to this document as the source material. This report is available for downloading from the PSERC website.

© 2005 Georgia Institute of Technology. All rights reserved.

Acknowledgements

The work described in this report was sponsored by the Power Systems Engineering Research Center (PSERC). We express our appreciation for the support provided by PSERC's industrial members and by the National Science Foundation under grant NSF EEC-0080012 received under the Industry / University Cooperative Research Center program.

We wish to thank all the PSERC members who provided support for this project, in particular Duke Power and Arizona Public Service.

Executive Summary

This project advances the state of the art in reliability assessment of electric power systems. The developed techniques enable probabilistic risk assessment. Risk issues have become of utmost importance as market forces are introduced into the power industry. The project's objective is to provide an integrated approach to reliability assessment addressing the issues of component reliability as well as system reliability. The developed methodology uses sensitivity analysis to identify components that limit system reliability. An added feature of the methodology is a probabilistic approach for estimating available transfer capability.

The reliability analysis methods can provide reliability indices at a customer site or at any system bus. Probability, frequency and duration indices are computed using methods based on a Markov state space approach. Examples are: (a) probability of customer interruption, (b) frequency of customer interruption, and (c) duration of customer interruption.

Two approaches for assessment of the overall power system reliability have been used: (a) an enumerative approach and (b) Monte Carlo simulation. In particular, an efficient enumerative approach was developed in which an operating state of an electric power system (after a contingency) is classified as either a 'success' or 'failure' via an effects analysis to determine whether the system will operate. Each 'failure' state is further analyzed to determine how many customers will be affected, what the limiting design parameters are, etc. The system's reliability is determined from the frequency and duration of the transitions from 'success' operating states to 'failure' operating states. The proposed method is based on the efficient identification of 'boundary transitions' (i.e., transitions from a 'successful' operating state to a 'failure' operating state and vice versa) with a series of ranking/evaluation procedures. The success or failure of an operating system state is determined with an improved contingency analysis method that takes into consideration the slow dynamics of the system, such as induction motor load retardation during a fault and subsequent acceleration after fault clearing.

This project's major accomplishments are:

1. Formulation of a comprehensive reliability assessment methodology.
2. Implementation of an improved and efficient contingency selection.
3. Implementation of a stochastic power flow analysis algorithm.

Table of Contents

| | |
|--|------------|
| <i>Acknowledgements</i> | <i>i</i> |
| <i>Executive Summary</i> | <i>ii</i> |
| <i>Table of Contents</i> | <i>iii</i> |
| <i>Table of Figures</i> | <i>v</i> |
| <i>Table of Tables</i> | <i>vii</i> |
| 1. Introduction | 1 |
| 1.1 Project Description | 1 |
| 1.2 Main Accomplishments | 2 |
| 1.3 Background on Reliability Assessment | 2 |
| 1.4 Summary Guide to this Report | 2 |
| 2. Reliability Assessment – Background Information | 3 |
| 2.1 Truncation of the State Space | 3 |
| 2.2 Contingency Selection and Ranking | 4 |
| 2.2.1 Performance Index (PI) Method..... | 4 |
| 2.2.2 Screening Methods..... | 6 |
| 2.2.3 Hybrid Contingency Selection and Ranking Method [6, 7] | 6 |
| 2.3 Monte Carlo Simulation (MCS) | 7 |
| 3. Comprehensive Reliability Assessment Methodology | 8 |
| 3.1 Component and Event Model | 9 |
| 3.2 State Enumeration | 9 |
| 3.2.1 Contingency Enumeration..... | 9 |
| 3.2.2 Electric Load Enumeration..... | 11 |
| 3.3 Effects Analysis | 11 |
| 3.3.1 Adequacy Approach..... | 11 |
| 3.3.2 Security Approach..... | 12 |
| 3.4 Reliability Indices | 12 |
| 3.4.1 Probability index | 13 |
| 3.4.2 Frequency index | 13 |
| 3.4.3 Duration index..... | 14 |
| 4. Single Phase Quadratized Power Flow Problem | 15 |
| 4.1 Introduction | 15 |
| 4.2 Power Flow Equations using QPF | 17 |
| 4.3 Solution Method | 22 |
| 4.4 Numerical Example | 24 |
| 5. Advanced Contingency Selection | 27 |
| 5.1 Security Assessment | 27 |

Table of Contents (continued)

| | |
|--|------------|
| 5.2 Contingency Ranking/Selection..... | 28 |
| 5.3 Examples of Detailed Performance Index Sensitivity Calculations | 34 |
| 5.3.1 Current based loading index..... | 34 |
| 5.3.2 Voltage index | 38 |
| 5.4 Improvements in Performance Index Contingency Ranking Methods | 42 |
| 5.4.1 QPF Sensitivity Method [13] | 43 |
| 5.4.2 Reducing the nonlinearity of the variations of performance indices | 48 |
| 6. Remedial Actions..... | 50 |
| 6.1 Quadratized Remedial Action Models..... | 51 |
| 6.1.1. Shunt Capacitor/Reactor Switching | 51 |
| 6.1.2. Regulating Transformer-- Phase Shift / Transformer Tap Adjustment..... | 51 |
| 6.1.3. MVAR Generation / Bus Voltage Adjustments | 55 |
| 6.1.4. Load Transfer | 56 |
| 6.1.5. MW generation adjustments..... | 58 |
| 6.1.6. Interruptible / Firm / Critical Loads | 60 |
| 6.2 Remedial Action Computation Methodology..... | 62 |
| 6.2.1 Problem Formulation | 62 |
| 6.2.2 Nondivergent Optimal Power Flow Approach..... | 62 |
| 6.2.3 Solution Methodology..... | 64 |
| 7. Probabilistic Power Flow..... | 66 |
| 7.1 Introduction | 66 |
| 7.2 Problem Statement and Solution Approach..... | 66 |
| 7.3 Proposed Model Description..... | 68 |
| 7.3.1 Electric Load Stochastic Model | 68 |
| 7.3.2 Probabilistic Generation Model | 70 |
| 7.3.3 Transmission System Model | 75 |
| 7.4 Example Results..... | 76 |
| 7.4.1 System Description | 76 |
| 7.4.2 Numerical Results | 78 |
| 7.5 Stochastic Power Flow via Multi-Point-Linearization | 82 |
| 8. Example of Overall Reliability Evaluation | 90 |
| 9. Conclusions | 102 |
| References | 103 |

Table of Figures

| | | |
|--------------|--|----|
| Figure 2.1. | Actual performance index curve vs. linearized curve | 6 |
| Figure 3.1. | Overall computational algorithm for reliability assessment methodology | 8 |
| Figure 3.2. | Two-state Markov model | 9 |
| Figure 3.3. | Wind-chime enumeration scheme | 11 |
| Figure 3.4. | State-space diagram | 13 |
| Figure 4.1. | General power system bus | 16 |
| Figure 4.2. | Performance comparison of quadratized and traditional power flow method | 16 |
| Figure 4.3. | Generator connected to bus k | 17 |
| Figure 4.4. | π -equivalent of circuit branch | 19 |
| Figure 4.5. | Capacitor or reactor at bus k | 20 |
| Figure 4.6. | Constant impedance load at bus k | 20 |
| Figure 4.7. | Constant power load at bus k | 21 |
| Figure 4.8. | A simplified two-bus example power system | 24 |
| Figure 5.1. | Definition of the contingency control variable u_c | 31 |
| Figure 5.2. | Illustration of a unit outage model with the contingency control variable u_c | 32 |
| Figure 5.3. | Illustration of a common mode line outage model with the contingency control variable u_c | 33 |
| Figure 5.4. | Plots of circuit-loading index vs. the contingency control variable u_c | 44 |
| Figure 5.5. | Plots of voltage index vs. the contingency control variable u_c | 45 |
| Figure 5.6. | Test system used for contingency ranking evaluation | 46 |
| Figure 5.7. | The IEEE 24-bus reliability test system | 47 |
| Figure 5.8. | Nonlinear curve of current based loading performance index with respect to a circuit outage control variable | 48 |
| Figure 5.9. | Nonlinear curve of original performance index with respect to a circuit outage control variable u and first order approach line | 49 |
| Figure 5.10. | Nonlinear curve of transformed performance index with respect to a transformed circuit outage control variable v and first order approach line | 49 |
| Figure 6.1. | Shunt capacitor or reactor at bus k | 51 |
| Figure 6.2. | Regulating transformer model (Tap side = bus k) | 52 |
| Figure 6.3. | Generator connected to bus k | 55 |
| Figure 6.4. | Load transfer | 57 |
| Figure 6.5. | Constant power critical load at bus k | 60 |
| Figure 6.6. | Illustration of a general bus k of an electric power system with a fictitious current source | 63 |
| Figure 7.1. | Schematic illustration of an electric power system | 67 |
| Figure 7.2. | The IEEE 24-bus reliability test system | 77 |
| Figure 7.3. | Comparison of proposed method and Monte Carlo simulation results; probability density function of circuit 140-160 current assuming Gaussian distributions | 78 |
| Figure 7.4. | Comparison of proposed method and Monte Carlo simulation results; cumulative probability function of circuit 140-160 current assuming Gaussian distributions | 78 |
| Figure 7.5. | Comparison of proposed method and Monte Carlo simulation results; probability density function of circuit 10-20 current assuming Gaussian distributions | 79 |
| Figure 7.6. | Comparison of proposed method and Monte Carlo simulation results; cumulative probability function of circuit 10-20 current assuming Gaussian distributions | 79 |
| Figure 7.7. | Comparison of proposed method and Monte Carlo simulation results; probability density function of circuit 140-160 current assuming uniform distributions | 80 |

Table of Figures (continued)

| | | |
|--------------|---|----|
| Figure 7.8. | Comparison of proposed method and Monte Carlo simulation results; cumulative probability function of circuit 140-160 current assuming uniform distributions.... | 81 |
| Figure 7.9. | Comparison of proposed method and Monte Carlo simulation results; probability density function of circuit 10-20 current assuming uniform distributions..... | 81 |
| Figure 7.10. | Comparison of proposed method and Monte Carlo simulation results; cumulative probability function of circuit 10-20 current assuming uniform distributions..... | 82 |
| Figure 7.11. | Schematic representation of non-conforming load sectionalization | 84 |

Table of Tables

| | | |
|-------------|--|-----|
| Table 2.1. | Cumulative probabilities of states as a function of total simultaneous outages m for a system with 300 units (FOR=0.05) and 2000 circuits (FOR=0.001)..... | 3 |
| Table 2.2. | Cumulative numbers of states as a function of total simultaneous outages m for a system with 300 units and 2000 circuits | 4 |
| Table 4.1. | Comparison of traditional and quadratized power flow convergence properties | 26 |
| Table 5.1. | Performance index change computed directly, with the traditional method and with the proposed method..... | 45 |
| Table 5.2. | Ranking results | 46 |
| Table 5.3. | Performance index change and ranking results for the circuit loading index..... | 46 |
| Table 5.4. | Performance index change and ranking results for the voltage index..... | 46 |
| Table 5.5. | Performance index change and ranking results for the voltage index for the IEEE 24-bus reliability test system..... | 48 |
| Table 6.1. | List of possible remedial actions | 50 |
| Table 7.1. | Comparison of proposed method and Monte Carlo simulation results for voltage magnitude assuming Gaussian distribution | 80 |
| Table 7.2. | Comparison of proposed method and Monte Carlo simulation results for circuit currents assuming Gaussian distribution..... | 80 |
| Table 7.3. | Comparison of proposed method and Monte Carlo simulation results for circuit currents assuming uniform distribution..... | 82 |
| Table 7.4. | List of congestion management actions..... | 85 |
| Table 8.1. | Reliability indices of IEEE-RTS (first level and common mode contingencies)..... | 90 |
| Table 8.2. | Reliability indices of IEEE-RTS (first level, second level and common mode contingencies)..... | 91 |
| Table 8.3. | Table of first level generator unit outages | 91 |
| Table 8.4. | Table of first level circuit outages | 92 |
| Table 8.5. | Table of first level common mode outages..... | 93 |
| Table 8.6. | Second level contingencies based on set 1. Generator G70_3 + another generator on outage..... | 94 |
| Table 8.7. | Second level contingencies based on Set 1. Generator G70_3 + one transmission line on outage | 95 |
| Table 8.8. | Second level contingencies based on set 1. Transmission line 20-60 + one generator on outage..... | 96 |
| Table 8.9. | Second level contingencies based on set 1. Transmission line 20-60 + another transmission line on outage | 97 |
| Table 8.10. | Second level contingencies based on set 1. Transmission line 90-120 + one generator on outage..... | 98 |
| Table 8.11. | Second level contingencies based on Set 1. Transmission line 90-120 + another transmission line on outage | 99 |
| Table 8.12. | Second level contingencies based on set 1. Transmission line 140-160 + one generator on outage..... | 100 |
| Table 8.13. | Second level contingencies based on set 1. Transmission line 140-160 + another transmission line on outage | 101 |

1. Introduction

A framework for comprehensive reliability assessment has been developed based on Markov models of system components and identification methods of events that contribute to unreliability. Specifically, an improved wind-chime approach is described coupled with an improved power system model. The model is based on the single phase quadratic modeling approach that provides superior performance in two aspects: (a) faster convergence, (b) ability to model complex load characteristics, and classes of loads such as interruptible load, critical load, etc. The same model has been extended for identifying events that contribute to the unreliability of the system. The method is integrated in the wind-chime scheme for the quick identification of critical events and effects analysis of the critical events. Since the methods are based on the Markov state space approach, probability, frequency and duration indices are computed, such as: (a) probability of customer interruption, (b) frequency of customer interruption and (c) duration of customer interruption. The advanced load modeling capability enables: (a) a realistic evaluation of industry practices such as load management programs on system reliability, and (b) a realistic evaluation of load characteristic on voltage problems and their impact on reliability. Examples illustrating the capabilities of the approach are provided.

1.1 Project Description

The scope of this project is to advance the state of the art in reliability assessment of electric power systems. The developed techniques enable probabilistic risk assessment. This issue has become of the utmost importance as deregulation and competition is invading the power industry. The specific objectives of the project are to provide an integrated approach to reliability assessment addressing the issues of component reliability as well as system reliability. A useful feature of the developed methodologies is the sensitivity analysis that identifies the components that limit system reliability. A byproduct of the methodology is a probabilistic methodology for available transfer capability. The reliability analysis methods provide reliability indices at the customer site or at any bus of the system. Since the proposed methods are based on the Markov state space approach, probability, frequency and duration indices are computed. Examples are: (a) probability of customer interruption, (b) frequency of customer interruption and (c) duration of customer interruption. Two approaches for the overall power system reliability have been considered: (a) the enumerative approach and (b) Monte Carlo simulation. In particular, an efficient enumerative approach has been developed. Specifically, an operating state of an electric power system (a contingency) is classified as “success” or “failure” via an effects analysis to determine whether the system will operate under normal conditions. Each ‘failure’ state is further analyzed to determine how many customers will be affected, what are the limiting design parameters, etc. The reliability of the system is determined from the frequency and duration of the transitions from ‘success’ operating states to ‘failure’ operating states. The proposed method is based on the efficient identification of ‘boundary transitions’, i.e., transitions from a ‘successful’ operating state to a ‘failure’ operating state and vice versa with a series of ranking/evaluation procedures. The success/failure of an operating system state will be determined with an improved contingency analysis method that takes into consideration the slow dynamics of the system, for example induction motor load retardation during a fault and subsequent acceleration after fault clearing. We have focused on the development of improved

methodologies for these basic problems. The developed methodologies are described in this report.

1.2 Main Accomplishments

The main accomplishments of this project are:

1. Formulation of a comprehensive reliability assessment methodology.
2. Implementation of an improved and efficient contingency selection.
3. Implementation of a stochastic power flow analysis algorithm.

1.3 Background on Reliability Assessment

Reliability assessment methods have appeared many decades ago. In the seventies the first comprehensive mathematical models were introduced, first for generation reliability and then for transmission reliability. Generation reliability analysis models are well developed. However, transmission system reliability methods are not as well developed due to the difficulties arising from the huge computational problem associated with transmission reliability analysis. Section 2 of this report summarizes transmission reliability approaches and identifies the difficulties. It summarizes the known approaches and discusses the advantages and disadvantages of these approaches.

1.4 Summary Guide to this Report

Section 2 provides some basic background information on issues on transmission system reliability.

Section 3 provides an overview of the comprehensive reliability assessment methodology.

Section 4 provides a brief description of the single phase quadratized power flow (SPQPF) model.

Section 5 provides an overview of the contingency ranking and selection approach.

Section 6 provides a description of the remedial actions methodology.

Section 7 provides an overview of the stochastic power flow methodology.

Section 8 provides an example application of the methodology using the IEEE RTS system.

Section 9 provides a discussion of the conclusions and suggestions for future research.

Finally a concise bibliography is provided.

2. Reliability Assessment – Background Information

One of the major impediments in transmission system reliability is the size of the state space. Considering a large-scale power system, the number of system states is enormous. As an example, a system with n components and each component with two states (up or down), there is a total of 2^n states. When n is 2000, the number of states is more than 10^{600} .

If all the possible states are analyzed one by one to identify the contingencies that contribute to the system unreliability, it requires too much computational effort, which is impractical for a typical power system. As a result, some efforts have been dedicated to the reduction of state space, selection and evaluation of contingencies [1, 5, 9, 11, 12].

2.1 Truncation of the State Space

The state space can be reduced by considering the probabilities of the system states. States that are not likely to occur are omitted. Whether a state represents a system failure that leads to a significant service interruption or that is only a minor violation of the criteria for system success is not taken into account [1].

Given a system with 300 units (FOR=0.05) and 2000 circuits (FOR=0.001), the cumulative probability and number of states are listed in Table 2.1 and 2.2.

Table 2.1. Cumulative probabilities of states as a function of total simultaneous outages m for a system with 300 units (FOR=0.05) and 2000 circuits (FOR=0.001).

| m | 0 | 1 | 2 | 3 | 4 | 5 | 6 |
|-------------------|-----------|-----------|-----------|-----------|-----------|--------|--------|
| $\Pr[N_G \leq m]$ | 2.0753e-7 | 3.4843e-6 | 2.9268e-5 | 1.6406e-4 | 6.9083e-4 | 0.0023 | 0.0065 |
| $\Pr[N_L \leq m]$ | 0.1352 | 0.4059 | 0.6767 | 0.8572 | 0.9474 | 0.9835 | 0.9955 |

The cumulative probability of having a maximum of m units/circuits out simultaneously, i.e., $\Pr(N_G \leq m) / \Pr(N_L \leq m)$ is given by the following recurrence:

$$\Pr(N_G \leq 0) = p_G^{n_G}$$

$$\Pr(N_G \leq m) = \Pr(N_G \leq m-1) + \frac{n_G!}{m!(n_G - m)!} p_G^{(n_G - m)} (1 - p_G)^m, \quad m = 1, 2, \dots, n_G$$

$$\Pr(N_L \leq 0) = p_L^{n_L}$$

$$\Pr(N_L \leq m) = \Pr(N_L \leq m-1) + \frac{n_L!}{m!(n_L - m)!} p_L^{(n_L - m)} (1 - p_L)^m, \quad m = 1, 2, \dots, n_L$$

Table 2.2. Cumulative numbers of states as a function of total simultaneous outages m for a system with 300 units and 2000 circuits.

| m | 0 | 1 | 2 | 3 | 4 | 5 | 6 |
|------------------|---|-------|--------|-------|---------|---------|----------|
| $\#[N_G \leq m]$ | 1 | 301 | 45,151 | 4.5e6 | 3.35e8 | 1.99e10 | 9.827e11 |
| $\#[N_L \leq m]$ | 1 | 2,001 | 2.0e6 | 1.3e9 | 6.66e11 | 2.66e14 | 8.85e16 |

The cumulative number of states having a maximum of m units/circuits out simultaneously, i.e., $\#[N_G \leq m] / \#[N_L \leq m]$ is given by the following recurrence:

$$\#[N_G \leq 0] = 1 \quad \#[N_G \leq m] = \#[N_G \leq m-1] + \frac{n_G!}{m!(n_G - m)!}, \quad m = 1, 2, \dots, n_G$$

$$\#[N_L \leq 0] = 1 \quad \#[N_L \leq m] = \#[N_L \leq m-1] + \frac{n_L!}{m!(n_L - m)!}, \quad m = 1, 2, \dots, n_L$$

Above equations provide guidance for evaluating the probability of truncated state spaces. For example, in case that one truncates the state space to up to seven simultaneous outages, the above equations are used to determine the probability of the truncated state space. As an example consider a system with:

$$n_G = 300, \quad n_L = 2000, \quad p_G = 1 - \text{FOR of units} = 0.95, \quad p_L = 1 - \text{FOR of circuits} = 0.999$$

N_G : number of simultaneous unit outages

N_L : number of simultaneous circuit outages

The probability of the state space that includes seven or more circuit outages is evaluated to be: $\Pr[N_L \geq 7] = 1 - 0.9955 = 0.0045$. This is acceptable but the number of states in the truncated state space is still too large, specifically $8.85e16$. This state space cannot be completely evaluated. For these reasons it is important to develop methodologies that do not evaluate these huge state spaces but rather navigate to identify states that contribute to unreliability. These methods are described next.

2.2 Contingency Selection and Ranking

The impact of outage states on the system reliability is taken into consideration in contingency selection and ranking method. Reduction of the state space is based on the elimination of the states whose impact on the system is small, and the consideration of only those outages that affect system reliability [4]. We refer to these methods as contingency selection and ranking methods.

Several approaches for the contingency selection and ranking have been achieved based on the traditional power flow (TPF) model. These methods are described next.

2.2.1 Performance Index (PI) Method

In this method, a variety of performance indices J , such as circuit current index, voltage index, reactive power index and so on, are defined to measure the normality of a system [4]. When a contingency happens, the system operating conditions change, so do the associated PIs. The

variations of PIs from pre-contingency to post-contingency, i.e., ΔJ , can be considered to indicate the impact of the contingency on system operating conditions. The contingencies are ranked in a descending order of the projected PI changes.

A highly efficient computational method, which is called costate method, has been developed to calculate the changes of performance indices [7,13,15]. The computational burden, as shown in the following procedure, is insignificant.

First, the contingency control variable u is incorporated to system component models, such that

$$u = \begin{cases} 1 & \text{if component is in operation} \\ 0 & \text{if component is outaged} \end{cases}$$

The performance index J is in general a function of u and system states x , i.e., $J = f(x, u)$. The following linearized equation (first order approximation) is used to calculate the value of the performance index after a contingency ($u = 0$), based on the value of PI before contingency ($u = 1$):

$$J_{u=0} = J_{u=1} + \left. \frac{dJ}{du} \right|_{u=1} (u - 1). \quad (2.1)$$

Thus,

$$\Delta J = J_{u=0} - J_{u=1} = - \left. \frac{dJ}{du} \right|_{u=1}, \quad (2.2)$$

where $\frac{dJ}{du}$ is obtained by the costate method:

$$\frac{dJ}{du} = \frac{\partial f(x, u)}{\partial u} - x^T \frac{\partial g(x, u)}{\partial u}, \quad (2.3)$$

$$\text{with } x^T = \frac{\partial f(x, u)}{\partial x} \left(\frac{\partial g(x, u)}{\partial x} \right)^{-1}, \quad (2.4)$$

where $g(x, u) = 0$ is the set of power flow equations.

The above method can handle common mode failures [5]. For example, if a lightning strike happens to two parallel transmission lines, both transmission lines are outaged. By incorporating the same contingency control variables u to the two transmission line models, we can use the same procedure to obtain ΔJ , which is corresponding to this common mode contingency.

The main drawback of PI method is that it is vulnerable to misranking. This is mainly caused by the approximate method used to calculate PIs. As in the costate method, $J_{u=0}$ is obtained by a linear approximation method. Because of the nonlinearities of power system, it will introduce errors to ΔJ . As shown in Figure 2.1, when u varies from 1 to 0, the actual curve of J is nonlinear, the actual ΔJ ($\Delta J = J_{u=0} - J_{u=1}$) is larger than $\Delta J'$ ($\Delta J' = J'_{u=0} - J_{u=1}$), which is

calculated based on linear approximate model. This error may lead to misranking. Especially, when a contingency results in abnormal system conditions, the difference between ΔJ and $\Delta J'$ may be large. Another reason that may result in misranking is the discontinuities of the system model caused by generator reactive limits and regulator tap limits [7].

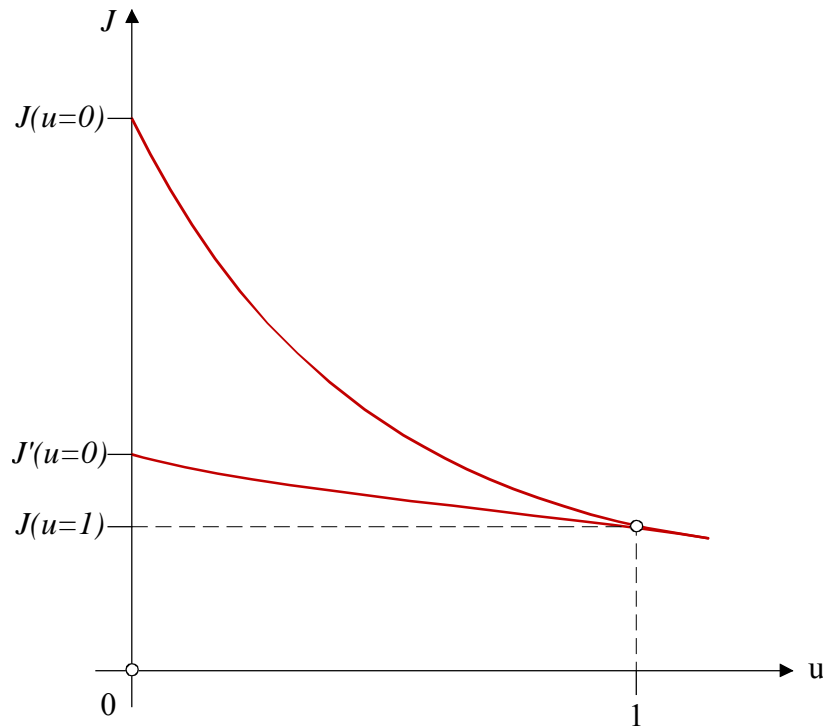


Figure 2.1. Actual performance index curve vs. linearized curve.

2.2.2 Screening Methods

In this class of methods, contingency ranking is based on approximate network solutions, such as Fast Decoupled Power Flow solutions [7, 8]. The method can take care of the nonlinearities to some extent and therefore it is better able to provide more accurate results than that of PI method. However, contingency selection by screening methods is very inefficient because it requires the approximate solution of post contingency states. Therefore, the method is accurate but not efficient.

2.2.3 Hybrid Contingency Selection and Ranking Method [6, 7]

In order to achieve both efficient and accurate contingency selection and ranking, the hybrid scheme combines the PI and screening methods. In hybrid methods, efficiency is achieved by employing the PI method first to quickly identify the contingencies that may have an adverse effect on system reliability. Screening methods are then utilized to the above defined subset of contingencies. The combination of the above two methods can take advantage of the best properties of both methods to achieve efficient and accurate contingency selection.

2.3 Monte Carlo Simulation (MCS)

Previous methods focus on the use of analytical techniques in evaluating contingencies, which represent the system by analytical models and evaluate performance indices from these models using mathematical solutions. Monte Carlo simulation methods, however, estimate the indices by simulating the actual process and random behavior of the system. This method, therefore, treats the problem as a series of experiments instead of studying the analytical models of systems [9].

Monte Carlo simulation consists of randomly sampling system states, testing them for acceptability and aggregating the contribution of loss of load states to the reliability till the coefficients of variation of these indices drop below pre-specified tolerances. The basic approach can be applied for each hour in a year in chronological order (sequential approach) or the hours of the study time can be considered at random (random approach). The simulation of the randomly selected system condition is done with the use of load flows, dispatch algorithms, and pre-selected operating policies. The results of the simulation are distributions of variables of interest (circuit flows, voltage levels, energy curtailment, etc.). These results are used in the computation of appropriate reliability indices [11, 12].

It has been pointed out that the main shortcoming of MCS methods are the enormous amount of experiments needed to run in order to obtain an acceptable level of the accuracy of the performance indices [1]. Due to the required long computational time, MCS methods are not as popular as analytical methods. Several variance reduction techniques [9], such as control variates, importance sampling, stratified sampling and antithetic variates, have been developed to reduce the computation burden, such that a pre specified precision could be achieved with less simulation effort [10].

3. Comprehensive Reliability Assessment Methodology

This section describes the developed methodology for bulk power transmission systems reliability assessment [17]. The overall computational algorithm is illustrated in Figure 3.1, which includes state enumeration, effects analysis, reliability index computations, etc. Note that the methodology provides for an automatic enumeration of outages selected via the contingency selection method. The enumeration is repeated for a number of electric load models. Each selected contingency is subjected to effects analysis. Two options exist: (a) system simulation approach and (b) network solution approach with possible remedial actions. Finally, the results of the effects analysis are processed to provide reliability indices. The basis of the approach and the constituent parts of the methodology are described next.

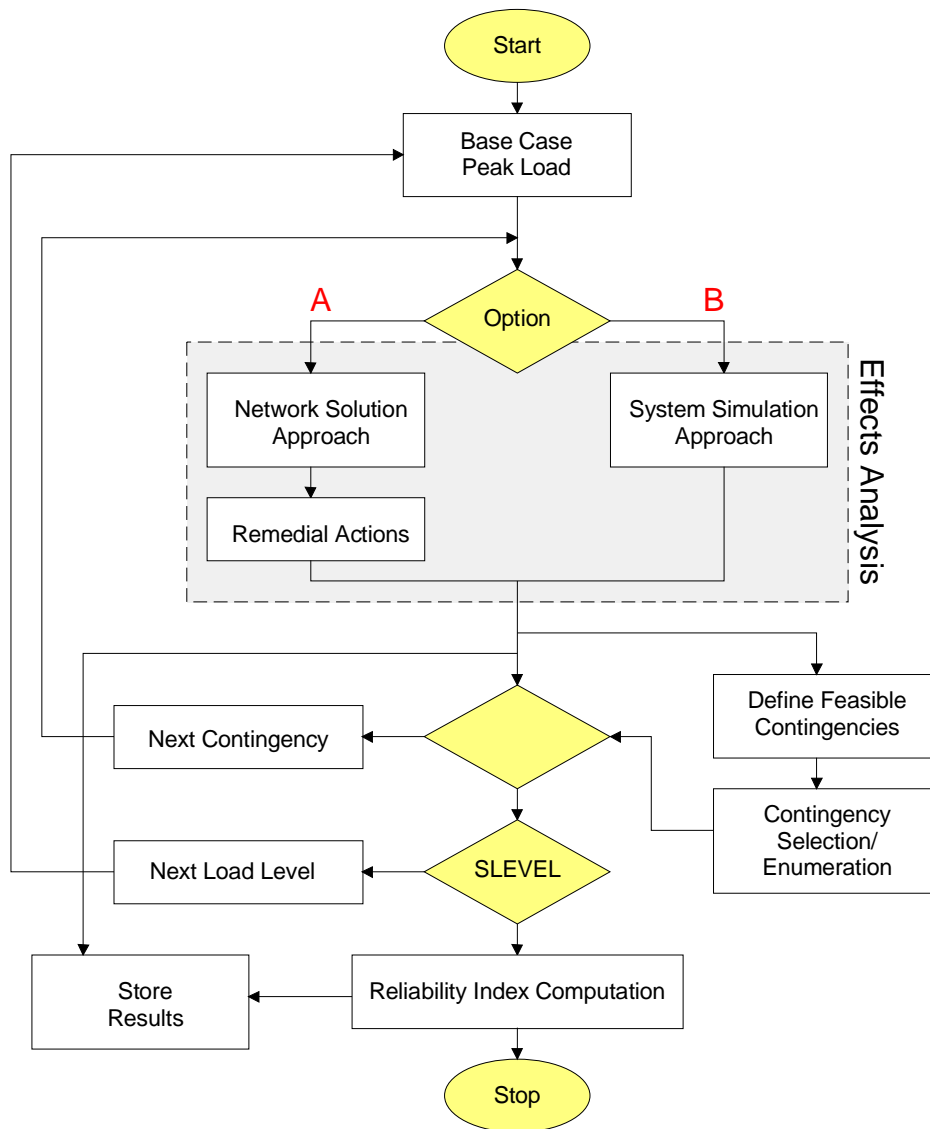


Figure 3.1. Overall computational algorithm for reliability assessment methodology.

3.1 Component and Event Model

The system states (contingencies) and electric load states are generated from a Markov model of system components and electric load levels. Specifically, each component (circuit or unit) is modeled with a two-state Markov model, i.e., the component is either working (up) or failed (down) as shown in Figure 3.2.

Based on the two-state Markov model of each component, a Markov state of a power system is defined by a particular condition where every component is in a given operating state of its own. All the possible states of a system make up the state space [1].

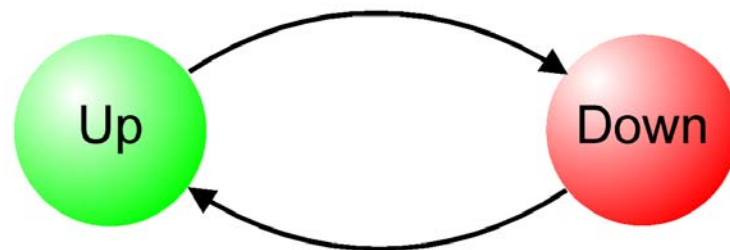


Figure 3.2. Two-state Markov model.

The electric load is modeled as a nonconforming load model. This model relates the bus loads to a small set of independent random variables. Discretization of the independent random variables provides discrete load states that are described with an equivalent Markov model where each load level is characterized with a probability and transition rates to any other load levels. In addition, each bus load is separated into interruptible, firm and critical components and associated with a voltage dependency assumed as follows: for the normal range of the bus voltage, the load is constant; for values below the normal voltage range, the load is dependent upon the voltage with a linear relationship.

3.2 State Enumeration

The state enumeration involves (1) enumeration of contingencies, including both circuit outages and unit outages, and (2) enumeration of electric load levels according to a specified electric load model.

3.2.1 Contingency Enumeration

The objective of contingency enumeration is to identify the contingencies which may lead to unreliability. The enumeration of contingencies is based on the use of multiple contingency ranking schemes. Additional truncation of contingencies is obtained by truncating the depth level of contingencies and by neglecting contingencies with very small probabilities. The depth level is defined with three parameters: (a) Maximum allowable number of simultaneous outages (units or circuits), (b) Maximum allowable number of simultaneous circuit outages and (c) Maximum allowable number of simultaneous circuit outages.

The reasons for the use of multiple contingency ranking schemes are: First, complete and thorough evaluation of all contingencies is impractical. Thus, it is necessary to avoid the evaluation of contingencies that are not likely to affect system reliability. This task is achieved with contingency ranking methods. Second, present state of the art contingency ranking methods do not possess the desired speed and accuracy for reliability analysis.

Generally, contingency-ranking methods may be classified into two categories: (a) Performance Index (PI) methods, and (b) screening methods.

PI methods use the derivative of a performance index (or first order approximation) with respect to an outage to determine the severity of a contingency. In this work the single-phase quadratized power flow (SFQPF) model has been applied towards the development of a contingency selection method using several metrics as performance indices. It is well known that performance index approaches lead to misrankings because of the nonlinearities of the model involved. The quadratized power flow model has milder nonlinearities (by construction) and therefore performs better. The quadratized power flow model will be described later.

Screening methods use approximate network solutions to identify cases causing limit violations. In this approach, contingencies are first analyzed with an approximate model. If the approximate model indicates that the contingency may have severe effects on the system, then the contingency is analyzed to determine its effects on the system. The disadvantage of these methods is the fact that the approximate analysis has to be performed on each contingency. Because of the large number of contingencies, the method is inefficient.

PI methods are typically much faster than screening methods. To take advantage of the best properties of the two approaches, the critical contingencies are selected with a hybrid scheme [7] that separates contingencies into two groups: (a) contingencies with mild nonlinearities and (b) contingencies with potential nonlinearities. The separation is performed with a very simple rule [7]. The first set of contingencies represents the majority and is ranked with PI based methods with multiple PIs. The second set of contingencies is ranked with screening methods. Computational savings are achieved by applying the screening methods only to a small set of contingencies. The details for contingency selection technique can be found in Section 5.

The Wind-Chime enumeration scheme, as shown in Figure 3.3, illustrates the contingency enumeration procedure using the ranking order obtained by the hybrid ranking method. The procedure starts with base case. All the first level contingencies are enumerated and ranked in the decreasing severity order. The second outage level contingencies are obtained from each contingency in the first outage level by having one more component on outage and ranked in the same way. The new outage component should be selected according to certain rule to make sure the obtained contingencies are distinct. This procedure continues until it reaches the predefined depth level or probability criteria of contingencies. In each outage level, contingencies are evaluated in the decreasing severity ranking order. The most severe contingencies are evaluated first. If there are several successive contingencies that are evaluated but have zero contribution to system unreliability, then it is reasonable that the rest contingencies which have lower severity indices need not to be investigated. Figure 3.3 shows these three types of contingencies, they are (1) contingencies that are evaluated and have nonzero contribution to unreliability (2) contingencies that are evaluated but have zero contribution to unreliability (3) contingencies that

are not evaluated.

3.2.2 Electric Load Enumeration

Electric load levels are modeled with a multi-state Markov model. The enumeration of electric load is based on the predefined load levels, i.e., if the load levels change, then the system enters another state.

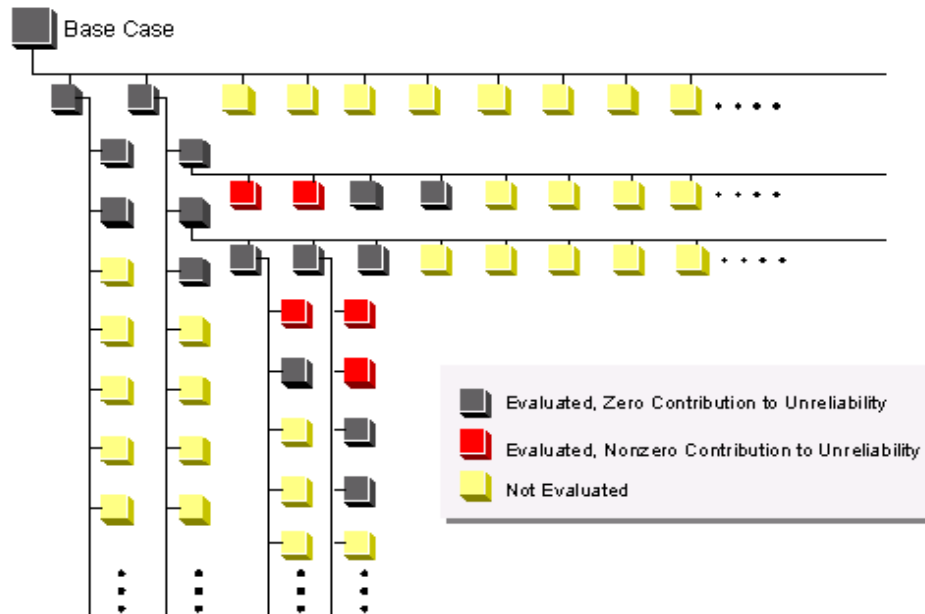


Figure 3.3. Wind-chime enumeration scheme.

3.3 Effects Analysis

Each combination of selected contingency and load level is analyzed to determine the effects on system performance. System performance is measured with a set of pre-specified criteria using the quadratized power flow and remedial actions if necessary. Failure criteria include: (a) circuit overloads, (b) bus under-voltage and over-voltage, (c) curtailment of interruptible load, (d) curtailment of firm load, (e) curtailment of critical load, etc.

As shown in Figure 3.1, in the effects analysis process, two approaches are available: (a) adequacy and (b) security.

3.3.1 Adequacy Approach

In adequacy approach the objective is to determine whether the system is capable of supplying the electric load under the specified contingency without operating constraint violations. For this purpose, the quadratized power flow and the remedial actions module are utilized to determine whether the system is adequate. A concise description of these tools follows.

a) Quadratized Power Flow Model [4, 13]

Quadratized power flow model is set up by applying the Kirchhoff's current law at each bus. The states variables are expressed in Cartesian coordinates. Subsequently, the power flow equations are quadratized, i.e., they are expressed as a set of equations that are linear or quadratic. This formulation is void of trigonometric terms, which makes the power flow equations less complex. The formulation of quadratic power flow provides superior performance in two aspects: (a) faster convergence, (b) ability to model complex load characteristics, and classes of loads such as interruptible load, firm load, critical load, and etc. More details about the quadratized power flow will be described in Section 4.

b) Remedial Actions [17]

Remedial actions greatly affect reliability of the power system operation by providing the means of correcting the abnormal conditions, such as alleviating circuit overloads, abnormal voltages, etc. In the adequacy approach, whenever the inadequacy occurs after certain contingency, the remedial actions without load shedding capability will be applied first. If the operating constraint violations still exist, the remedial actions with load shedding capability are then applied to determine where and how much load shedding will be needed to alleviate emergencies, which is recorded as a system failure. The results of the contingency evaluations are stored and subsequently used by the reliability calculation model to calculate the reliability indices.

A list of system typical remedial actions is given in Table 6.1 in Section 6. The quadratized model and the computation of appropriate remedial actions are also illustrated in Section 6.

3.3.2 Security Approach

The objective of this approach is to determine whether the immediate response of the system will generate potential problems for the system reliability. The simulation approach considers the system conditions during the fault that generates the contingency and consists of an inertial re-dispatch and operating conditions immediately after the contingency and before any controls take effect. The objective is to determine whether cascading failures may occur. This approach encompasses the quasi-transient performance of the system after contingencies.

3.4 Reliability Indices

Reliability indices are computed on the basis of identifying the set of states that satisfy a specific failure criterion and the transition rates from any state inside the set to a state outside the set. Figure 3.4 shows a state space diagram, including the evaluated and not evaluated states (contingencies). A contingency j at certain load level is characterized with a certain probability p_j and transition rates to and from other system states, such as λ_{jk} and λ_{ij} . An event S_r , which contains a set of evaluated states that possess some common features such as system failure states, is identified by retrieving the stored results of effects analysis. Three different classes of reliability indices then can be computed: (a) probability, (b) frequency and (c) duration indices.

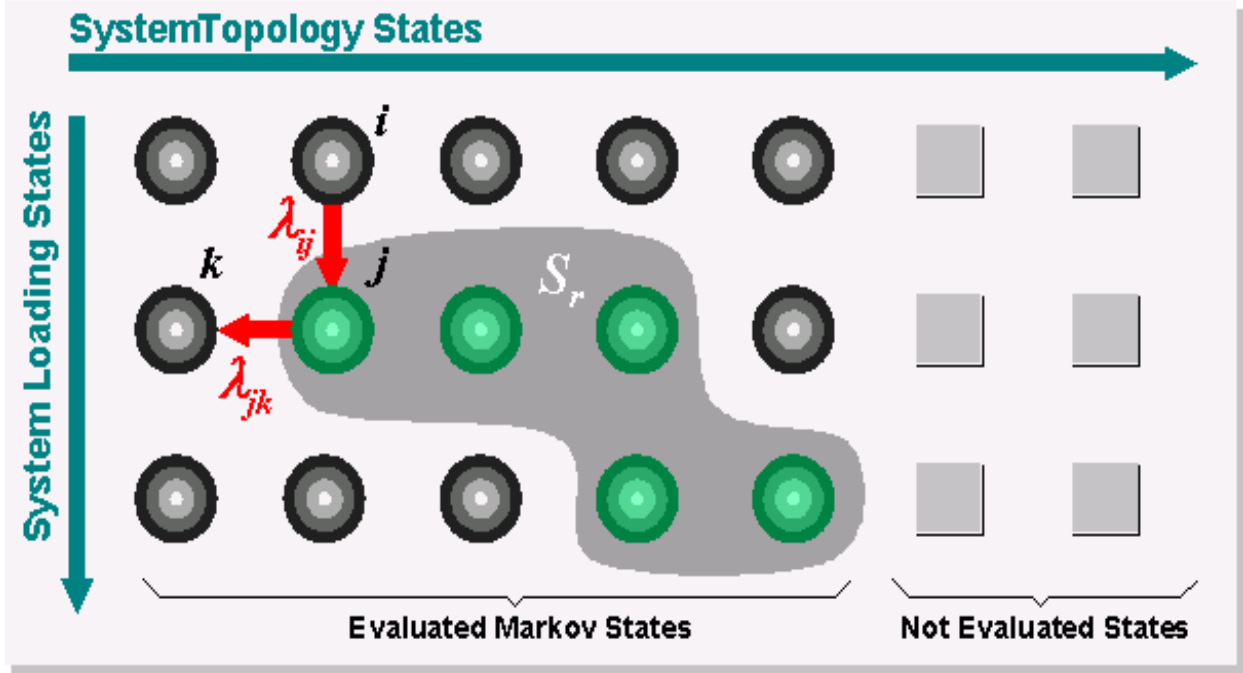


Figure 3.4. State-space diagram.

3.4.1 Probability index

The probability of S_r , $P_r[S_r]$, is obtained by adding all the probabilities p_j , that is:

$$P_r[S_r] = \sum_{j \in S_r} p_j. \quad (3.1)$$

The probabilities p_j , $j \in S_r$, can be added because the events of being in any of the state j are mutually exclusive.

3.4.2 Frequency index

The frequency of S_r , f_{S_r} , is the total of the frequency of leaving a state j for a state i outside S_r , therefore

$$f_{S_r} = \sum_{i \notin S_r} \sum_{j \in S_r} f_{ji} = \sum_{i \notin S_r} \sum_{j \in S_r} p_j \lambda_{ji} = \sum_{j \in S_r} (p_j \sum_{i \notin S_r} \lambda_{ji}), \quad (3.2)$$

where:

λ_{ji} is the transition rate from state j to state i ;

f_{ji} is the frequency of transfer from state j to state i , which is defined as the expected number of direct transfers from j to i per unit time. The relation between f_{ji} and λ_{ji} can be written as $f_{ji} = \lambda_{ji} p_j$.

3.4.3 Duration index

The duration index of S_r , T_{S_r} , can be obtained using the probability index and frequency index given above by the following equation:

$$T_{S_r} = \frac{P_r[S_r]}{f_{S_r}}. \quad (3.3)$$

Considering that not all contingencies are evaluated, we assume the unevaluated contingencies belong to a set N . It is apparent that some of them will be failures and some will be successes. Therefore, it is possible to compute upper and lower bounds [14] on the probability by applying the extreme conditions: (a) all states in N are success, and (b) all states in the set N are failures. As a result,

$$P_r[S_r]^u = \sum_{j \in (S_r + N)} p_j, \quad (3.4)$$

$$P_r[S_r]^l = \sum_{j \in S_r} p_j, \quad (3.5)$$

where $S_r + N$ means the union of the sets S_r and N .

The computation of upper and lower bounds for frequency and duration indices related to the determination of all the transition rates from the failure states to success states. This procedure should be repeated for each frequency index which uses a different failure criterion.

4. Single Phase Quadratized Power Flow Problem

4.1 Introduction

Because of the importance of the power flow model as one of the basic analysis tools in the operations and planning of power systems, many attempts have been made to improve the efficiency and accuracy of power flow solutions. These attempts range from different formulations of the power flow problem to advanced sparsity methods and shortcuts for repeat solutions or even to attempts to obtain a direct non-iterative solution to the problem. In this section a method of reformulating the power flow problem in a way that will improve the efficiency of the solution method is presented. In this context it was observed in the early 70's that expressing the bus voltage phasors in Cartesian coordinates results in a formulation of the power flow problem that is less complex, since trigonometric functions are absent. Going one step further, an improved idea is not only to use Cartesian coordinates for the phasor expressions, but also to "quadratize" the power flow equations, i.e., to express the power flow equations as a set of equations with order no greater than two. It turns out that this can be achieved very easily with the introduction of additional state variables as needed. The advantage of this formulation is that the resulting power flow equations are either linear or quadratic. Application of Newton's method is ideally suitable to quadratic equations. This results in the Quadratized Power Flow (QPF) formulation.

The traditional power flow model consists of the power balance equations at each bus of the system. Power flow equations are expressed in the polar coordinates in terms of the systems states (bus voltage magnitudes and angles). Therefore, trigonometric terms exist in the formulated power flow equations. In addition, induction machine load are very complicated and contain very high-order terms resulting from the complex load model. Consequently, the highest order of the TPF equations is more than two.

Quadratic power flow model, however, is set up based on applying the Kirchhoff's current law at each bus. In addition, the states variables are expressed in Cartesian coordinates. As a result, the power flow equations are quadratized as a set of equations that are linear or quadratic with order no more than two. Also trigonometric terms are absent, which makes the power flow equations less complex. The formulation of quadratic power flow provides superior performance in two aspects: (a) faster convergence, (b) ability to model complex load characteristics, and classes of loads such as interruptible load, critical load, etc.

In general, at a bus, there may be generation, loads (various types of loads), circuits, shunt devices, etc. The general bus of a system is illustrated in Figure 4.1. While the circuits and shunt terms are linear elements, the loads and generation may operate in such a way that imposes nonlinearities. Common loads models are: (a) constant power load, (b) constant impedance load and (c) induction motor load. Common operating modes of generating units are: (a) constant voltage, constant real power operation, (b) constant real power constant power factor operation. The new QPF approach consists of writing the Kirchhoff's current law at each bus of the system. The models of loads and generators are expressed in terms of their terminal current and additional equations in additional state variables that define their operating mode. The additional equations may be nonlinear but of order no higher than two. The resulting set of equations is

consistent, i.e., the number of equations equals the number of unknowns. In addition, the set of equations are linear or quadratic in terms of the state variables. These equations are solved via Newton's method. The proposed model has two advantages: (a) the resulting power flow model is more accurate than usual load models and (b) the convergence characteristics of the proposed model are superior to conventional methods.

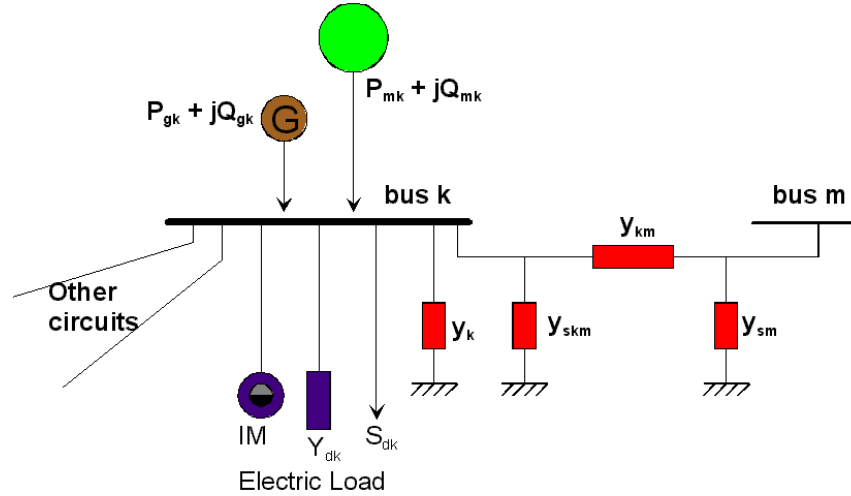


Figure 4.1. General power system bus.

The new formulation of the power flow problem has been applied to a small test system. The performance characteristics of the solution have been compared to those of the traditional power flow problem. The results for a small five-bus system are given in Figure 4.2. Note how fast the new model converges. This is to be expected since the model is quadratic and Newton's method is best suited for quadratic models. We expect that these convergence characteristics carry to large systems.

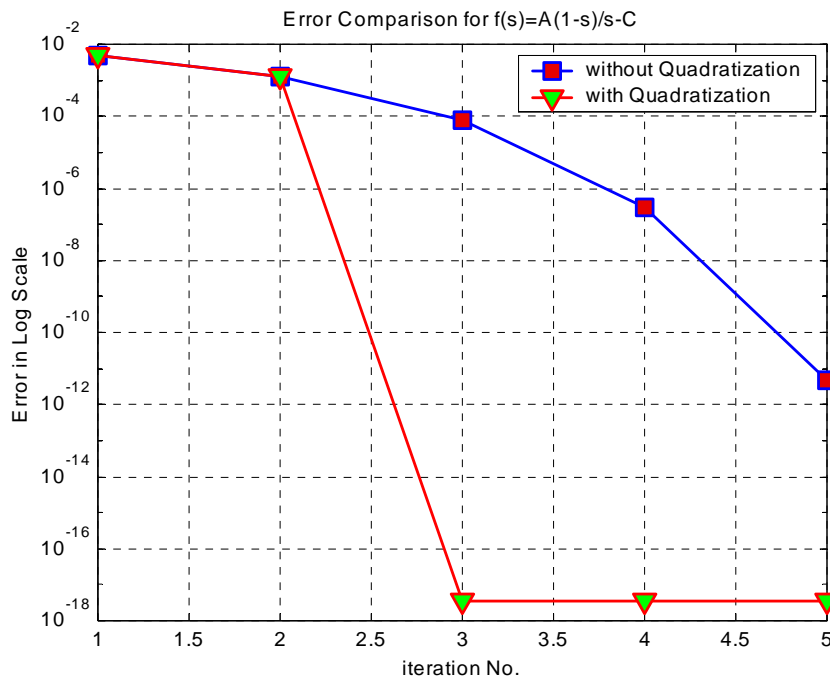


Figure 4.2. Performance comparison of quadratized and traditional power flow method.

4.2 Power Flow Equations using QPF

Consider again a bus of an electric power system as it is illustrated in Figure 4.1. The figure shows a generator, a constant impedance load, a constant power load, an induction motor load and a switched shunt capacitor/reactor load connected to the bus together with a transformed and a circuit (transmission line) to other buses. Each component of the power system illustrated in Figure 4.1 can be modeled with a set of linear and quadratic equations. As an example, the form of the models for a generator, a circuit, a switched shunt capacitor/reactor, a constant impedance load and a constant power load model is described next.

- **Generator Model:** Figure 4.3 illustrates the simplified equivalent circuit model of a single axis generator model. Assume a synchronous generator with admittance $\tilde{y}_{gk} = g_{gk} + jb_{gk}$ and internal emf $\tilde{E}_k = E_{kr} + jE_{ki}$, connected to bus k of voltage $\tilde{V}_k = V_{kr} + jV_{ki}$

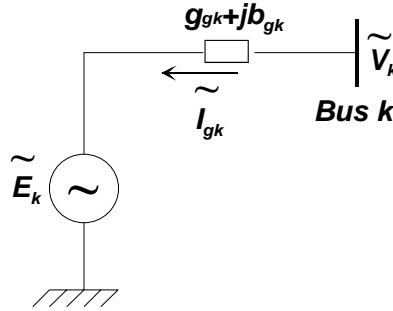


Figure 4.3. Generator connected to bus k.

The electric current of the generator, in the direction from the bus into the generator, is given by the equation:

$$\tilde{I}_{gk} = (g_{gk} + jb_{gk}) \cdot (\tilde{V}_k - \tilde{E}_k), \quad (4.1)$$

where $(g_{gk} + jb_{gk})$ is the generator admittance.

Note here we use the single axis model of the generator for simplicity. The procedure can be applied to the two axes model of the generator as well. This is omitted to avoid the complexity of the two axes model equations.

The state vector for the generator model consists of the terminal voltage \tilde{V}_k and the internal emf \tilde{E}_k . Expressing these quantities in Cartesian coordinates the state vector becomes:

$$x = [V_{kr} \quad V_{ki} \quad E_{kr} \quad E_{ki}]^T, \quad (4.2)$$

where the subscripts "r" and "i" indicate real and imaginary part respectively.

The current equations in Cartesian coordinates are:

$$\begin{aligned}
I_{gkr} &= g_{gk} V_{kr} - g_{gk} E_{kr} - b_{gk} V_{ki} + b_{gk} E_{ki} \\
I_{gki} &= g_{gk} V_{ki} - g_{gk} E_{ki} + b_{gk} V_{kr} - b_{gk} E_{kr}
\end{aligned} \tag{4.3}$$

These expressions will be used in the Kirchoff's voltage law applications when the connectivity constrains of the network are applied. In addition to the two current equations two additional internal equations are needed for the model to be consistent, i.e., the number of equations equals the number of unknown states. There are three control modes for the synchronous generator, i.e., a) Slack mode, b) PQ mode, and c) PV mode. Although the current equations are the same for each mode, the internal equations are the ones that make the model different for each mode. The model of each one of these cases is described next.

Slack mode: In the slack mode, the synchronous generator is controlled to maintain the specified voltage magnitude and zero phase angle. For the slack mode, we have the following equations.

$$\begin{aligned}
I_{gkr} &= g_{gk} V_{kr} - g_{gk} E_{kr} - b_{gk} V_{ki} + b_{gk} E_{ki} \\
I_{gki} &= g_{gk} V_{ki} - g_{gk} E_{ki} + b_{gk} V_{kr} - b_{gk} E_{kr} \\
0.0 &= V_{ki} \\
0.0 &= V_{kr}^2 + V_{ki}^2 - V_{k,specified}^2
\end{aligned} \tag{4.4}$$

Note that the current equations force the phase of the generator terminal voltage to be zero. The last equation forces the magnitude of the generator terminal voltage to be equal to the specified.

PQ mode: In the PQ mode, the synchronous generator is controlled to maintain the specified real and reactive power. For the PQ mode, we have the following equations.

$$\begin{aligned}
I_{gkr} &= g_{gk} V_{kr} - g_{gk} E_{kr} - b_{gk} V_{ki} + b_{gk} E_{ki} \\
I_{gki} &= g_{gk} V_{ki} - g_{gk} E_{ki} + b_{gk} V_{kr} - b_{gk} E_{kr} \\
0.0 &= \frac{P_{k,specified}}{3} + g_{gk} V_{kr}^2 + g_{gk} V_{ki}^2 - g_{gk} V_{kr} E_{kr} - g_{gk} V_{ki} E_{ki} + b_{gk} V_{kr} E_{ki} - b_{gk} V_{ki} E_{kr} \\
0.0 &= \frac{Q_{k,specified}}{3} - b_{gk} V_{kr}^2 - b_{gk} V_{ki}^2 + g_{gk} V_{kr} E_{ki} - g_{gk} V_{ki} E_{kr} + b_{gk} V_{kr} E_{kr} + b_{gk} V_{ki} E_{ki}
\end{aligned} \tag{4.5}$$

Note that the two internal equations impose the requirement that the active and reactive power delivered by the generator equal their specified values.

PV mode: In the PV mode, the synchronous generator is controlled to maintain the specific real power and voltage magnitude. For the PV mode, we have the following equations:

$$\begin{aligned}
I_{gkr} &= g_{gk} V_{kr} - g_{gk} E_{kr} - b_{gk} V_{ki} + b_{gk} E_{ki} \\
I_{gki} &= g_{gk} V_{ki} - g_{gk} E_{ki} + b_{gk} V_{kr} - b_{gk} E_{kr} \\
0.0 &= \frac{P_{k,specified}}{3} + g_{gk} V_{kr}^2 + g_{gk} V_{ki}^2 - g_{gk} V_{kr} E_{kr} - g_{gk} V_{ki} E_{ki} + b_{gk} V_{kr} E_{ki} - b_{gk} V_{ki} E_{kr} \\
0.0 &= V_{kr}^2 + V_{ki}^2 - V_{k,specified}^2
\end{aligned} \tag{4.6}$$

Note that the third equation imposes the requirement that the real power delivered by the generator is equal to the specified real power and the last equation imposes the requirement that the magnitude of the terminal voltage equals the specified value.

In each of the above cases we have an equation that describes the current at the terminal of the generator as a function of state variables and some additional equations expressing the control functions of the generator. All equations are linear or quadratic in terms of the state variables.

- **Circuit Branch Model:** Figure 4.4 illustrates the model of a circuit connecting buses k and m represented with its π -equivalent circuit.

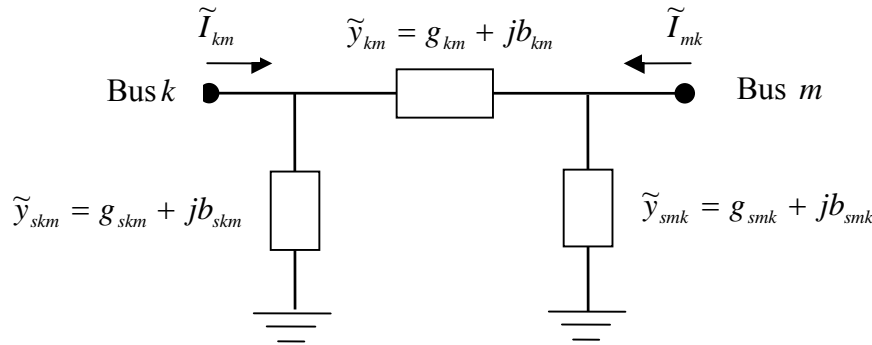


Figure 4.4. π -equivalent of circuit branch.

The state vector for the circuit model consist of the bus voltages \tilde{V}_k and \tilde{V}_m . Expressing these quantities in Cartesian coordinates the state vector becomes:

$$x = [V_{kr} \quad V_{ki} \quad V_{mr} \quad V_{mi}]^T, \quad (4.7)$$

where the subscripts "r" and "i" indicate real and imaginary part respectively.

The circuit model is represented by the following equations:

$$\begin{aligned} I_{kmr} &= (g_{km} + g_{skm})V_{kr} - (b_{km} + b_{skm})V_{ki} - g_{km}V_{mr} + b_{km}V_{mi} \\ I_{kmi} &= (b_{km} + b_{skm})V_{kr} + (g_{km} + g_{skm})V_{ki} - b_{km}V_{mr} - g_{km}V_{mi} \\ I_{mkr} &= -g_{km}V_{kr} + b_{km}V_{ki} + (g_{km} + g_{smk})V_{mr} - (b_{km} + b_{smk})V_{mi} \\ I_{mki} &= -b_{km}V_{kr} - g_{km}V_{ki} + (b_{km} + b_{smk})V_{mr} + (g_{km} + g_{smk})V_{mi} \end{aligned} \quad (4.8)$$

where:

$$\begin{aligned} \tilde{y}_{km} &= g_{km} + jb_{km} && \text{is the circuit series admittance;} \\ \tilde{y}_{skm} &= g_{skm} + jb_{skm} && \text{is the } k \text{ side shunt admittance;} \\ \tilde{y}_{smk} &= g_{smk} + jb_{smk} && \text{is the } m \text{ side shunt admittance;} \\ \tilde{V}_k &&& \text{is the voltage phasor at bus } k ; \\ \tilde{V}_m &&& \text{is the voltage phasor at bus } m . \end{aligned}$$

Note that the equations are linear with respect to the state variables.

- **Switched Shunt Capacitor/Reactor Model:** Figure 4.5 illustrates the model of a switched shunt capacitor/reactor device of impedance $\tilde{y}_{Ck} = g_{Ck} + jb_{Ck}$, connected to bus k .

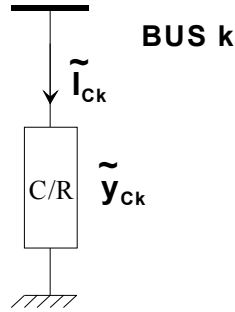


Figure 4.5. Capacitor or reactor at bus k .

The state vector for the shunt capacitor/reactor model consists of the bus voltage \tilde{V}_k . Expressing this voltage in Cartesian coordinates the state vector becomes:

$$x = [V_{kr} \quad V_{ki}]^T, \quad (4.9)$$

where the subscripts "r" and "i" indicate real and imaginary part respectively.

The shunt capacitor/reactor model is represented by the following equations:

$$\begin{aligned} I_{Ckr} &= g_{Ck}V_{kr} - b_{Ck}V_{ki} \\ I_{Cki} &= g_{Ck}V_{ki} + b_{Ck}V_{kr} \end{aligned} \quad (4.10)$$

Note that the equations are linear with respect to the state variables.

- **Constant Impedance Load Model:** Figure 4.6 illustrates the model of a constant impedance load of impedance $\tilde{y}_{Lk} = g_{Lk} + jb_{Lk}$, connected to bus k .

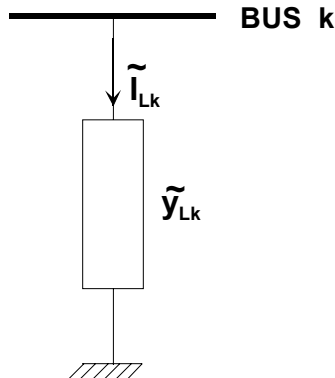


Figure 4.6. Constant impedance load at bus k .

The state vector for the constant impedance load model consists of the bus voltage \tilde{V}_k . Expressing this voltage in Cartesian coordinates the state vector becomes:

$$x = [V_{kr} \quad V_{ki}]^T, \quad (4.11)$$

where the subscripts "r" and "i" indicate real and imaginary part respectively.

The constant impedance load model is represented by the following equations:

$$\begin{aligned} I_{Lkr} &= g_{Lk} V_{kr} - b_{Lk} V_{ki} \\ I_{Lki} &= g_{Lk} V_{ki} + b_{Lk} V_{kr} \end{aligned} \quad (4.12)$$

Note that the equations are linear with respect to the state variables.

- **Constant Power Load Model:** Figure 4.7 illustrates the model of a constant power load, connected to bus k . The constant power load is defined with the total complex power, $S_{dk} = P_{dk} + jQ_{dk}$ that is assumed to be constant, i.e., independent of the voltage magnitude at the bus.

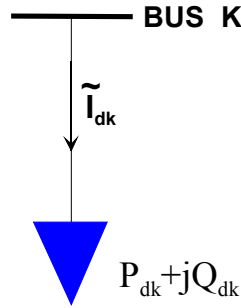


Figure 4.7. Constant power load at bus k .

Define the nominal admittance of the load to be:

$$\tilde{Y}_{dn,k} = \frac{1}{3V_{nk,ph}^2} (P_{dk} - jQ_{dk}) = g_{dn,k} + jb_{dn,k}, \quad (4.13)$$

where $V_{nk,ph}$ is the nominal phase voltage at bus k .

Then the constant power load model can be expressed with the following set of equations.

$$\begin{aligned} I_{dkr} &= g_{dn,k} V_{kr} - b_{dn,k} V_{ki} + u_1 g_{dn,k} V_{kr} - u_1 b_{dn,k} V_{ki} = (1 + u_1) \cdot (g_{dn,k} V_{kr} - b_{dn,k} V_{ki}) \\ I_{dki} &= g_{dn,k} V_{ki} + b_{dn,k} V_{kr} + u_1 g_{dn,k} V_{ki} + u_1 b_{dn,k} V_{kr} = (1 + u_1) \cdot (g_{dn,k} V_{ki} + b_{dn,k} V_{kr}) \\ 0.0 &= u_2 - V_{kr}^2 - V_{ki}^2 \\ 0.0 &= g_{dn,k} u_2 + u_1 u_2 g_{dn,k} - P_{dk} \end{aligned} \quad (4.14)$$

The first two equations are the current equations; the last two are the internal equations of the model. The above equations force the complex power absorbed by the load to be equal to the specified load and constant.

The state vector for the constant impedance load model is:

$$x = [V_{kr} \quad V_{ki} \quad u_1 \quad u_2]^T, \quad (4.15)$$

where the subscripts "r" and "i" indicate real and imaginary part respectively.

Note that the equations are at most quadratic with respect to the state variables.

The examples above show that each component of the system can be represented with an appropriate set of linear or quadratic equations. By expressing the voltage and current phasors with their Cartesian coordinates (i.e., $\tilde{I} = I_r + jI_i$ and $\tilde{V} = V_r + jV_i$) the following general form is obtained for any power system component:

$$\begin{bmatrix} I_r^k \\ I_i^k \\ 0 \end{bmatrix} = y_{eq_real}^k \begin{bmatrix} V_r^k \\ V_i^k \\ y^k \end{bmatrix} + \begin{bmatrix} x^{kT} f_{eq_real1}^k x^k \\ x^{kT} f_{eq_real2}^k x^k \\ \dots \end{bmatrix} - b_{eq_real}^k \quad (4.16)$$

$$\text{where: } x^k = \begin{bmatrix} V_r^k \\ V_i^k \\ y^k \end{bmatrix} \quad (4.17)$$

and $y_{eq_real}^k$, $b_{eq_real}^k$, and $f_{eq_real}^k$ are matrices with appropriate dimensions.

In this section the general quadratic models of five components of an electric power system were discussed, namely, generator, transmission line, switched shunt capacitor/reactor, constant impedance load and constant power load. It is emphasized that this procedure can be applied to any other component, i.e., transformer, variable tap transformer, two axes generator model, etc. The end result will always be a model in the form of the equations (4.16).

4.3 Solution Method

The network solution is obtained with application of Newton's method to a quadratized form of the network equations. The quadratized network equations are generated as follows. Consider the general form of equations for any model of the system (linear or nonlinear), i.e., equation (4.16). Note that this form includes two sets of equation, which are named external equations or current equations and internal equations respectively. The electric currents at the terminals of the component appear only in the external equations. Similarly, the device states consist of two variable sets: external states (i.e., bus voltage $\tilde{V}^k = V_r^k + jV_i^k$) and internal state variables y^k (if any). The set of equations (4.16) is consistent in the sense that the number of external states and the number of internal states equal the number of external and internal equations respectively.

The entire network equations are obtained by application of the connectivity constraints among the system components, i.e., Kirchoff's current law at each system bus. Specifically, Kirchoff's current law applied to all buses of the system yields:

$$\sum_k A^k \tilde{I}^k = 0, \quad (4.18)$$

where $\tilde{I}^k = I_r^k + jI_i^k$ is the device k bus current injections, and A^k is a component incidence matrix with:

$$\{A_{ij}^k\} = \begin{cases} 1, & \text{if bus } j \text{ of device } k \text{ is connected to bus } i \\ 0, & \text{otherwise} \end{cases} \quad (4.19)$$

All the internal equations from all devices should be added to the above equation, yielding the following set of equations:

$$\begin{cases} \sum_k A^k \tilde{I}^k = 0 \\ \text{[internal equations of all devices]} \end{cases} \quad (4.20)$$

Let $\tilde{V} = V_r + jV_i$ be the vector of all bus voltage phasors. Then, the following relationship hold:

$$\tilde{V}^k = (A^k)^T \tilde{V}, \quad (4.21)$$

where \tilde{V}^k is device k bus voltage.

Equations (4.20) can be separated into two sets of real equations by expressing the voltages and currents with their Cartesian coordinates. Then the device currents can be eliminated with the use of equations (4.16). This procedure will yield a set of equations in terms of the voltage variables and the internal device state variables. If all the state variables are represented with the vector x , then the equations can be written in the following form:

$$G(x) = Y_{real}x + \begin{bmatrix} x^T f_1 x \\ x^T f_2 x \\ \dots \end{bmatrix} - B_{real} = 0, \quad (4.22)$$

where x is the vector of all the state variables and Y_{real} , f , B_{real} are matrices with appropriate dimensions. The simultaneous solution of these equations is obtained via Newton's method as described next.

Equation (4.22) is solved using Newton's method. Specifically, the solution is given by the following algorithm:

$$x^{v+1} = x^v - J_G^{-1} \left\{ Y_{real} x^v + \begin{bmatrix} x^{vT} f_1 x^v \\ x^{vT} f_2 x^v \\ \dots \end{bmatrix} - B_{real} \right\} \quad (4.23)$$

where v is the iteration step number; J_G is the Jacobian matrix of the equation (4.22). In particular, the Jacobian matrix takes the following form:

$$J_G = Y_{real} + \begin{bmatrix} x^{vT} (f_1 + f_1^T) \\ x^{vT} (f_2 + f_2^T) \\ \dots \end{bmatrix} \quad (4.24)$$

It is important to note that Newton's method is ideally suited for solution of quadratic equations.

4.4 Numerical Example

The quadratic power flow is demonstrated with an example.

Consider the power system of Figure 4.8. The generator controls the voltage magnitude at bus 1 to the value of 1.0 p.u.

Assume that the electric load at bus 2 is $S_{d2} = 0.85 + j0.36$ p.u. Formulate the traditional power flow problem as well as the quadratized power flow problem. Solve both problems starting from flat start, i.e., the voltage at bus 2 equal to 1.0 p.u. Record the mismatch at each iteration and tabulate the results.

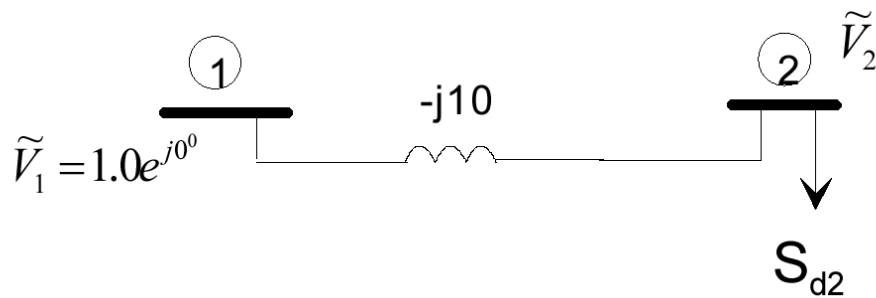


Figure 4.8. A simplified two-bus example power system.

Solution:

a) The traditional power flow problem for this system is defined with the following equations:

$$\begin{aligned} g_1(x) &= 10.0V_2 \sin \delta_2 + 0.85 = 0.0 \\ g_2(x) &= 10.0V_2^2 - 10.0V_2 \cos \delta_2 + 0.36 = 0.0 \end{aligned} \quad (4.25)$$

The iterative solution algorithm is:

$$x^{v+1} = x^v - J_g^{-1}(x^v)g(x^v), \quad (4.26)$$

where:

$$x = \begin{bmatrix} \delta_2 \\ V_2 \end{bmatrix}, \quad g(x^v) = \begin{bmatrix} g_1(x^v) \\ g_2(x^v) \end{bmatrix}, \quad J_g(x) = \begin{bmatrix} 10.0V_2 \cos \delta_2 & 10.0 \sin \delta_2 \\ 10.0V_2 \sin \delta_2 & 20.0V_2 - 10.0 \cos \delta_2 \end{bmatrix}.$$

b) The quadratized power flow problem for this system is defined with the following equations:

$$\begin{aligned} -j10.0(\tilde{V}_2 - 1.0) + (1 + u_1)(0.85 - j0.36)\tilde{V}_2 &= 0.0 \\ 0.85u_2 + 0.85u_1u_2 - 0.85 &= 0.0 \\ u_2 - V_2^2 &= 0.0 \end{aligned} \quad (4.27)$$

Note that the first equation is complex while the second and third are real. Upon expressing the complex voltage for bus 2 with its Cartesian coordinates and conversion of the complex equation into two real equations yields:

$$\begin{aligned} G_1(y) &= -6.36V_{2r} + 0.85V_{2i} - 0.36V_{2r}u_1 + 0.85V_{2i}u_1 + 6.0 = 0.0 \\ G_2(y) &= 0.85V_{2r} + 6.36V_{2i} + 0.85V_{2r}u_1 + 0.36V_{2i}u_1 = 0.0 \\ G_3(y) &= 0.85u_2 + 0.85u_1u_2 - 0.85 = 0.0 \\ G_4(y) &= u_2 - V_{2r}^2 - V_{2i}^2 = 0.0 \end{aligned} \quad (4.28)$$

Note that the above equations are quadratic and include four unknowns. The iterative solution algorithm is:

$$y^{v+1} = y^v - J_G^{-1}(y^v)G(y^v), \quad (4.29)$$

where:

$$y = \begin{bmatrix} V_{2r} \\ V_{2i} \\ u_1 \\ u_2 \end{bmatrix}, \quad G(y^v) = \begin{bmatrix} G_1(y) \\ G_2(y) \\ G_3(y) \\ G_4(y) \end{bmatrix}, \quad J_G(y) = \begin{bmatrix} -6.36 - 0.36u_1 & 0.85 + 0.85u_1 & -0.36V_{2r} + 0.85V_{2i} & 0 \\ 0.85 + 0.85u_1 & 6.36 + 0.36u_1 & 0.85V_{2r} + 0.36V_{2i} & 0 \\ 0 & 0 & 0.85u_2 & 0.85 + 0.85u_1 \\ -2V_{2r} & -2V_{2i} & 0 & 1.0 \end{bmatrix}.$$

The iterations for both methods start from the same initial guess: $\tilde{V}_2 = 1.0e^{j0}$. The first three iterations of the algorithm are summarized in Table 4.1. To minimize the data, the table reports the solution at each iteration as well as the following norm:

$$\|g\| = \sqrt{\frac{1}{N} \sum_i g_i^2(x)}$$

Table 4.3. Comparison of traditional and quadratized power flow convergence properties.

| Iteration | Newton-Rapston | | Quadratized Power Flow | |
|-----------|------------------------|-------------------------|------------------------|--------------------------|
| | V | $\ g\ $ | V | $\ g\ $ |
| 0 | $1.0e^{j0^0}$ | 0.6525 | $1.0e^{j0^0}$ | 0.4615 |
| 1 | $0.964e^{-j4.870^0}$ | 0.4049×10^{-1} | $0.95894e^{-j5.129^0}$ | 0.7367×10^{-2} |
| 2 | $0.95854e^{-j5.086^0}$ | 0.2879×10^{-3} | $0.95850e^{-j5.088^0}$ | 0.5816×10^{-5} |
| 3 | $0.95850e^{-j5.088^0}$ | 0.15×10^{-7} | $0.95850e^{-j5.088^0}$ | 0.7997×10^{-11} |

It is important to observe in this example that the convergence characteristics of the quadratized power flow are superior to those of the traditional power flow method. Specifically, the norm of mismatches of the quadratized power flow is consistently lower than that of the traditional method. For example, at the second iteration, the norm of mismatches of the quadratized power flow is two orders of magnitude lower than that of the traditional method. The quadratized power flow formulation appears to be more complicated than the usual formulation in terms of the polar form of voltages. However, the advantage of the quadratized power flow formulation is the improved convergence characteristics that lead to an overall algorithm that is more efficient than the traditional formulation. This property carries to large scale systems.

5. Advanced Contingency Selection

5.1 Security Assessment

Security assessment is defined as the real time analysis procedures by which the security of the system is measured (assessed). Security assessment procedures are classified into steady state and dynamic depending on whether the transients following the disturbance are neglected or not. Most of transmission line and transformer outages cause a rather fast rerouting of power flow in such a way that the transients following the disturbance are not of great consequence. The same is true for generating unit outages when the unit is small compared to the system or operating at low power points prior to the event. These cases represent the majority of outage events. Cases of major generation unit outages or major tie lines may cause transients with major effects on security. In this case, the transients must be studied and their effect on security must be assessed. This process is called dynamic security assessment.

In general, considering the power system as a nonlinear dynamic system, we can say that the steady state security assessment should evaluate if after a contingency (or a number of contingencies) occurs there will be a new equilibrium state for the post-contingency system and how secure this state is. The dynamic security assessment will, in addition to that, also show if there will in fact be a transient trajectory in the state space from the original pre-contingency equilibrium point to the post-contingency equilibrium point (thus, if the system will actually reach that equilibrium point) and what will be the security level of the system during this transition. It is therefore possible, for some severe disturbances, that even if a post-contingency equilibrium point exists the system may not be able to reach it, because there is no transient path from the one equilibrium to the other one. Or the final equilibrium state may be reached and may be a secure state, however, some of the transient states the system went through during the transition may have not be acceptably secure. This can only be investigated using transient analysis. However, in this report we are interested only in steady state or static security assessment. The purpose of this part of the project is simply to use security assessment techniques for contingency screening and ranking (not analysis) in order to reduce the size of the space of system states, to the few ones that worth to be further analyzed from the system reliability point of view. Dynamic security assessment is therefore beyond the scope of this report.

Steady state security assessment, i.e., assessment of the effects of equipment outages on system security, requires the analysis of the post-contingency steady state conditions. In other words, steady state security assessment involves the analysis of the steady state post-contingency conditions for any foreseeable and probable outage. Since the number of such contingencies may be extremely large for practical systems, the basic problems in static security assessment are: (a) identification of contingencies which may cause system problems or adversely affect security (contingency selection) and (b) techniques for contingency simulation to assess the effects of the contingency. These problems will be discussed next.

5.2 Contingency Ranking/Selection

Contingency analysis is necessary to determine the level of security and/or reliability of a given system following a disturbance (contingency). Because of the large number of possible contingencies, this analysis can be extremely costly from the computational point of view. Fortunately for practical power systems, only a small number of contingencies are potentially critical to system security and/or reliability. If these contingencies can be identified, then only these contingencies should be analyzed to determine their effect. The problem of identifying the critical contingencies is known as contingency ranking. That is, contingencies are ranked in terms of their severity

Contingency ranking methods can be divided into two categories: Performance index (PI) methods and screening methods based on approximate power flow solutions. In the first case, the contingency ranking is facilitated by the use of performance indices which provide a measure of system “normality”. These methods are computationally simple and efficient, however, they are prone to misranking. On the other hand the methods based on approximate power flow solutions are in generally less efficient and require more computation; their accuracy depends on the level of approximation used. In this study we are interested only in PI methods and we use them to evaluate the system state after certain disturbances, therefore, estimate the severity of each disturbance. The more sever disturbances are to be further analyzed using reliability analysis methods.

Several different performance indices can be defined and used, depending on then network quantities that are considered more important for the specific study. Some of the most commonly used indices are listed below:

- **Current Based Loading Index:**

$$J_C = \sum_j w_j \left(\frac{I_j}{I_{N,j}} \right)^{2n} \quad (5.1)$$

- I_j : current magnitude in circuit j ;
- $I_{N,j}$: current rating of circuit j ;
- w_j : appropriate circuit weight, $0 < w_j \leq 1$;
- n : integer parameter defining the exponent.

- **Apparent Power Flow Based Loading Index:**

$$J_T = \sum_j w_j \left(\frac{T_j}{T_{N,j}} \right)^{2n} \quad (5.2)$$

- T_j : apparent power flow in circuit j ;
- $T_{N,j}$: apparent power flow rating of circuit j ;
- w_j : appropriate circuit weight, $0 < w_j \leq 1$;
- n : integer parameter defining the exponent.

- **Active Power Flow Based Loading Index:**

$$J_P = \sum_j w_j \left(\frac{P_j}{P_{N,j}} \right)^{2n} \quad (5.3)$$

- P_j : active power flow in circuit j ;
- $P_{N,j}$: current rating of circuit j ;
- w_j : appropriate circuit weight, $0 < w_j \leq 1$;
- n : integer parameter defining the exponent.

- **Voltage Index:**

$$J_V = \sum_k w_k \left(\frac{V_k - V_{k,mean}}{V_{k,step}} \right)^{2n} \quad (5.4)$$

- V_k : voltage magnitude at bus k ;
- $V_{k,mean}$: nominal voltage value (typically 1.0 p.u.) ;

It is in general the mean value in the desired range, i.e., $\frac{1}{2}(V_k^{\max} + V_k^{\min})$.

- $V_{k,step}$: voltage deviation tolerance (i.e., $\frac{1}{2}(V_k^{\max} - V_k^{\min})$);
- w_k : appropriate bus weight $0 < w_k \leq 1$;
- n : integer parameter defining the exponent.

- **Generation Reactive Power Index:**

$$J_Q = \sum_{j=1}^L w_j \left(\frac{Q_j - Q_{j,mean}}{Q_{j,step}} \right)^{2n} \quad (5.5)$$

- w_j : real number representing generator weight $0 < w_j \leq 1$;
- $Q_{j,mean}$: real number representing the expected generated reactive power value;
This is the mean value is the allowable range for each generator, i.e.,
 $\frac{1}{2}(Q_j^{\max} + Q_j^{\min})$.
- $Q_{j,step}$: reactive power deviation tolerance;
This is half of the allowable range, i.e., $\frac{1}{2}(Q_j^{\max} - Q_j^{\min})$;
- Q_j : reactive power generated by unit j ;
- n : integer parameter defining the exponent.

Note that the quantities inside the parenthesis express normalized circuit power flow, circuit current, voltage magnitude and generator reactive power respectively. The normalization is with respect to equipment capability or allowable limits. Thus, values of the quantities in the

parenthesis in the range (-1.0 to -1.0) indicate normal operation while values outside this range indicate abnormal operation. When these quantities are raised to the $2n$ power, they will produce a large number for abnormal conditions and a very small number for normal conditions. Specifically, large values of the performance indices J_C , J_T , J_P indicate that one or more circuits are overloaded. Similarly, large values of the performance index J_V indicate that one or more voltage magnitudes are outside the permissible range for voltage magnitude. Large values of the performance index J_Q indicate that one or more generating unit produces reactive power outside its limits. A contingency will cause a change in system operating conditions which will be accompanied by a change in the performance indices J_C , J_T , J_P or J_Q .

The security indices provide a quantitative way to access the security of the system. Contingencies that may impact system security can be recognized by the change of the performance indices. Thus in order to rank contingencies on the basis of their impact on security, we can use the changes in the performance indices due to the contingency. In general, the exact change of the performance indices J_C , J_T , J_P or J_Q due to a contingency can be computed by first obtaining the system post contingency solution (power flow solution) and then computing the performance index by direct substitution. This procedure is computationally demanding and negates the objectives of a contingency ranking algorithm. Specifically, the objective of contingency ranking is to compute the approximate change of the security indices due to a set of postulated contingencies with a highly efficient computational method. Such methods were introduced in the late 70's.

In this work the Quadratized Power Flow (QPF) model has been applied towards the development of a contingency selection method using as metric performance indices. It is well known that performance index approaches lead to misrankings because of the nonlinearities of the model involved. The idea here is to use the quadratized power flow model that is expected to have milder nonlinearities and therefore should performed better. This is indeed the case. In addition, the quadratized power flow model is better suited to use current based ratings of circuits as opposed to power based ratings of circuits. It is pointed out that most capacity limitations of circuits are thermal limitations, i.e., electric current limitations. Thus using current limits, results in a more realistic approach.

The described approach has been applied to contingency selection using a variety of performance indices, circuit current index, voltage index, reactive power index, etc. In this report we present the methodology of the new method for some of these performance indices.

The contingency selection is based on the computation of the performance index change due to a contingency and subsequent ranking of the contingencies on the basis of the change. Mathematically one can view the outage of a circuit as a reduction of the admittance of the circuit to zero. We introduce a new control variable, the outage control variable, u_c , as illustrated in Figure 5.1. Note that the contingency control variable, u_c , has the following property:

$$u_c = \begin{cases} 1.0, & \text{if the component is in operation} \\ 0.0, & \text{if the component is outaged} \end{cases} \quad (5.6)$$

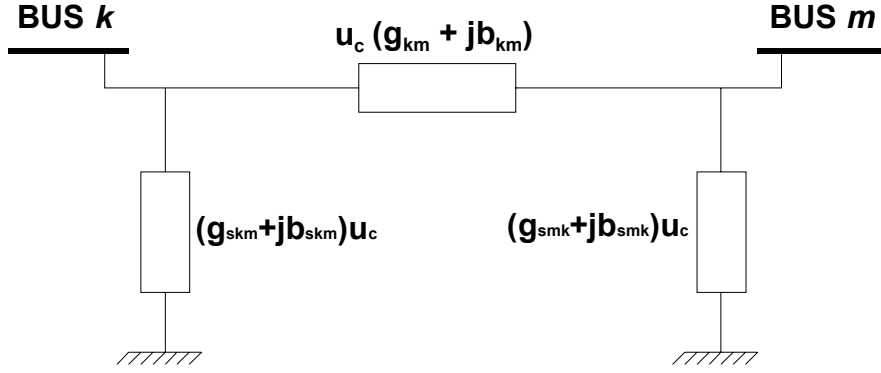


Figure 5.1. Definition of the contingency control variable u_c .

The current flow in the circuit km is now a function of the contingency control variable, u_c .

$$\begin{aligned} I_{kmr} &= [(g_{km} + g_{skm})V_{kr} - (b_{km} + b_{skm})V_{ki} - g_{km}V_{mr} + b_{km}V_{mi}] \cdot u_c = I_{kmr}^0 \cdot u_c \\ I_{kmi} &= [(b_{km} + b_{skm})V_{kr} + (g_{km} + g_{skm})V_{ki} - b_{km}V_{mr} - g_{km}V_{mi}] \cdot u_c = I_{kmi}^0 \cdot u_c \end{aligned} \quad (5.7)$$

where

- V_{kr} is the real part of the voltage at bus k ;
- V_{ki} is the imaginary part of the voltage at bus k ;
- V_{mr} is the real part of the voltage at bus m ;
- V_{mi} is the imaginary part of the voltage at bus m ;

and

- I_{kmr}^0 is the real part of the base case current value from bus k to bus m ;
- I_{kmi}^0 is the imaginary part of the base case current value from bus k to bus m .

Similarly, consider the outage of a generating unit. Following the outage, the system will experience a generation deficiency which will result in frequency decrease. The outage will be also followed by transient. At the same time, the output of other generators will increase accordingly to their inertia initially. The net interchange (power import export) will also change. In the post contingency steady state the output of the remaining units will be increased by the action of the AGC and the net interchange will return to its scheduled value. The change of the remaining generating unit outputs at the steady state is determined by economic factors. In other words, the lost generation will be made up by increasing the output of the remaining generators according to their economic participation factors. This is shown in Figure 5.2. Specifically, considering the outage of unit i , we introduce again a contingency control variable u_c which is defined as follows:

$$P_{gi} = u_c P_{gi}^0 \quad (5.8)$$

where

- P_{gi}^0 is the precontingency output of the generating unit i ;
- P_{gi} is the generating unit i output.

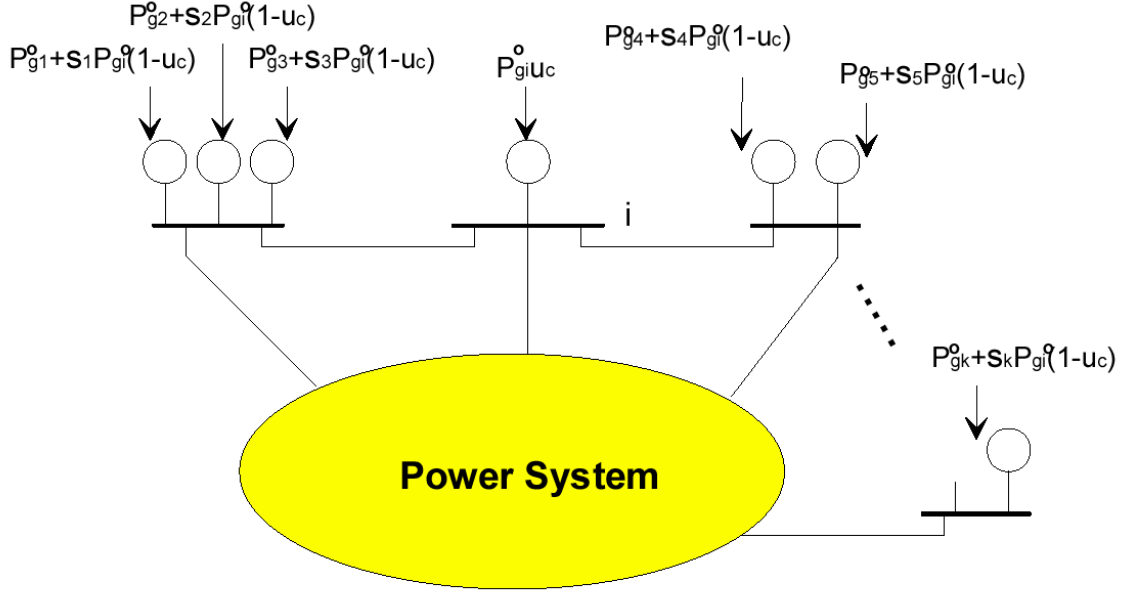


Figure 5.2. Illustration of a unit outage model with the contingency control variable u_c .

Note again that

$$u_c = \begin{cases} 1.0, & \text{if the unit is in operation} \\ 0.0, & \text{if the unit is outaged} \end{cases} \quad (5.9)$$

The generation deficiency P_{gi}^0 caused by the outage of this unit is absorbed by the other units. Consider the generating unit j . The output of this unit will be controlled by the automatic generation control loop to the value:

$$P_{gj} = P_{gj}^0 + (1 - u_c) \sigma_j P_{gi}^0, \quad (5.10)$$

where σ_j is the unit economic participation factor. Note again that the generating unit outputs are expressed as a function of the contingency control variable. The reactive power deficiency will also be allocated the same way.

It should be noted that the use of the contingency control variable also provides a very simple and efficient way of modeling common mode contingencies (outages). Common mode contingencies are defined as contingencies that take place together. In the general case this may be a very low probability event, however in certain specific cases this is not necessarily true. In the case of a double transmission line for example (parallel lines on the same pole), an event (e.g. a tree fall, or a lightning strike) can cause the outage of both lines at the same time instead of just one. This is a common mode outage and can be modeled with one outage control variables as illustrated in Figure 5.3.

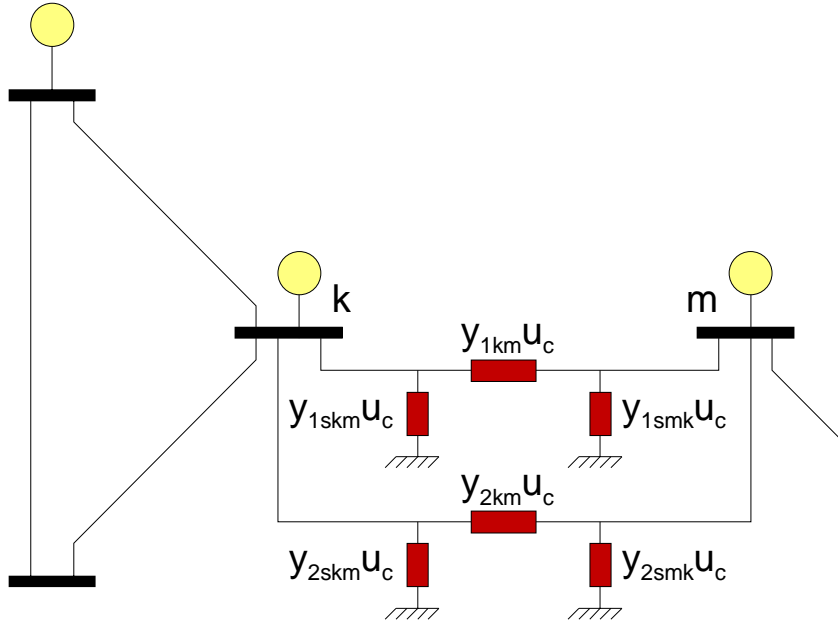


Figure 5.3. Illustration of a common mode line outage model with the contingency control variable u_c .

In summary, any circuit or generating unit outage can be modeled with a control variable, the contingency control variable. Using these control variables, the power flow equations can be written as a function of the control variables. Specifically, the quadratic power flow equations are written in the usual compact form:

$$G(x, u) = 0.0 \quad (5.11)$$

where u is a vector of all contingency variables. The contingency control variable, u_c , completely defines a contingency. $u_c = 1$ defines the precontingency system and $u_c = 0$ defines the post-contingency system. The security indices are in general complicated functions of the contingency control variables. Let J be anyone of the performance indices discussed earlier. Linearization of the performance index around the precontingency condition ($u_c = 1$) yields:

$$J(u_c) \cong J(u_c = 1) + \frac{dJ}{du_c}(u_c - 1.0). \quad (5.12)$$

The first order change of the security index ΔJ due to a contingency is given by:

$$\Delta J = J(u_c = 0) - J(u_c = 1) = -\frac{dJ}{du_c}. \quad (5.13)$$

The above equation provides the basis of contingency ranking algorithms: The first order approximation of the effect of a contingency on security indices is determined by the derivative of the security index with respect to the contingency control variable.

Thus, the central computational problem in contingency ranking is the computation of the sensitivities $\frac{dJ}{du_c}$. For this purpose, observe that, in general, the performance index is a function of the system state, x , and the contingency control variables u .

$$J = f(x, u). \quad (5.14)$$

On the other hand, the state of the system must obey the power flow equations:

$$G(x, u) = 0. \quad (5.15)$$

The costate method (previously developed by the authors) is applied to perform sensitivity analysis of the system state with respect to the control variable:

$$\frac{dJ}{du_c} = \frac{df}{du_c} = \frac{\partial J}{\partial u_c} - \hat{x}^T \left[\frac{\partial G(x, u)}{\partial u_c} \right], \quad (5.16)$$

where

$$\hat{x}^T = - \left[\frac{\partial J(x, u)}{\partial x} \right] \left[\frac{\partial G(x, u)}{\partial x} \right]^{-1} \text{ is the costate vector.} \quad (5.17)$$

Note that the costate is precomputed at the present operating condition and remains invariant for all contingencies. Thus for each contingency we have to only compute the partial derivatives of the power flow equation $G(x, u)$ with respect to the contingency control variable. This vector has only few nonzero entries and therefore the computations are extremely fast.

5.3 Examples of Detailed Performance Index Sensitivity Calculations

Some examples of the calculation of the first order sensitivity of a performance index using the quadratic power flow formulation are presented in this section. The current based loading index and the voltage index will be used in order to illustrate the computation of the sensitivities with respect to the outage control variable for both a transmission line and a generator outage.

5.3.1 Current based loading index

- *Computation of the costate vector \hat{x}^T*

The costate vector depends only on the current state of the system and it is independent of the contingency. Therefore, its value is constant for any circuit outage and any generator outage.

$$\hat{x}^T = \left[\frac{\partial J_c}{\partial x} \right] \cdot \left[\frac{\partial G(x, u)}{\partial x} \right]^{-1} \quad (5.18)$$

$\left[\frac{\partial G(x, u)}{\partial x} \right]$ is the Jacobian matrix of the system and it is already computed for the solution of the base case.

$$\frac{\partial J_c}{\partial x} = 2n \cdot \sum_{k=1}^N \sum_{m \in S(k)} \left[\frac{w_{km}}{(I_{N,km})^2} \cdot \left(\frac{|I_{km}^0|}{(I_{N,km})} \right)^{2n-2} \cdot \left(I_{kmr}^0 \cdot \frac{\partial I_{kmr}}{\partial x} + I_{kmi}^0 \cdot \frac{\partial I_{kmi}}{\partial x} \right) \right] \quad (5.19)$$

$$\frac{\partial I_{kmr}}{\partial x} = [0 \quad \dots \quad 0 \quad (g_{km} + g_{skm}) \quad -(b_{km} + b_{skm}) \quad 0 \quad \dots \quad 0 \quad -g_{km} \quad b_{km} \quad 0 \quad \dots \quad 0] \quad (5.20)$$

$$\frac{\partial I_{kmi}}{\partial x} = [0 \quad \dots \quad 0 \quad (b_{km} + b_{skm}) \quad (g_{km} + g_{skm}) \quad 0 \quad \dots \quad 0 \quad -b_{km} \quad -g_{km} \quad 0 \quad \dots \quad 0] \quad (5.21)$$

\downarrow \downarrow \downarrow \downarrow
 index of index of index of index of
 V_{kr} in x V_{ki} in x V_{mr} in x V_{mi} in x

Circuit outage between buses i and j .

- Computation of $\frac{\partial J_c}{\partial u_{ij}}$

$$\frac{\partial J_1}{\partial u_{ij}} = 2n \cdot w_{ij} \cdot \left(\frac{|I_{ij}^0|}{(I_{N,ij})} \right)^{2n} + 2n \cdot w_{ji} \cdot \left(\frac{|I_{ji}^0|}{(I_{N,ji})} \right)^{2n} = 2n \cdot w_{ij} \cdot \left(\frac{|I_{ij}^0|^{2n} + |I_{ji}^0|^{2n}}{(I_{N,ij})^{2n}} \right) \quad (5.22)$$

for $w_{ij} = w_{ji}$ and $I_{N,ij} = I_{N,ji}$.

- Computation of $\frac{\partial G(x, u)}{\partial u_{ij}}$

$$\frac{\partial G(x, u)}{\partial u_{ij}} = \begin{bmatrix} 0 \\ \dots \\ 0 \\ I_{ijr}^0 \\ I_{iji}^0 \\ 0 \\ \dots \\ 0 \\ I_{jir}^0 \\ I_{jii}^0 \\ 0 \\ \dots \\ 0 \end{bmatrix} \quad \left. \begin{array}{l} \\ \\ \end{array} \right\} \begin{array}{l} \text{Position of QPF Equations for bus } i \\ \text{Position of QPF Equations for bus } j \end{array} \quad (5.23)$$

Outage of generating unit i .

- Computation of $\frac{\partial J_c}{\partial u_i}$

$$\frac{\partial J_c}{\partial u_i} = 0 \tag{5.24}$$

- Computation of $\frac{\partial G(x, u)}{\partial u_i}$

PQ Controlled Generator:

$$\frac{\partial G(x, u)}{\partial u_i} = \begin{bmatrix} 0 \\ \dots \\ 0 \\ \frac{P_{i,spec}^0}{3} \\ \frac{Q_{i,spec}^0}{3} \\ 0 \\ \dots \\ 0 \\ -\sigma_1 \cdot \frac{P_{i,spec}^0}{3} \\ -\sigma_1 \cdot \frac{Q_{i,spec}^0}{3} \\ 0 \\ \dots \\ 0 \\ -\sigma_j \cdot \frac{P_{i,spec}^0}{3} \\ -\sigma_j \cdot \frac{Q_{i,spec}^0}{3} \\ 0 \\ \dots \\ 0 \\ -\sigma_k \cdot \frac{P_{i,spec}^0}{3} \\ 0 \\ \dots \\ 0 \end{bmatrix} \tag{5.25}$$

} Position of QPF internal equations for generator i

Position of QPF first internal equation for all PQ or PV controlled generators

Position of QPF second internal equation for all PQ controlled generators

σ_j is the unit economic participation factor.

PV Controlled Generator:

$$\frac{\partial G(x,u)}{\partial u_i} = \begin{bmatrix} 0 \\ \dots \\ 0 \\ \frac{P_{i,spec}^0}{3} \\ 0 \\ 0 \\ \dots \\ 0 \\ -\sigma_1 \cdot \frac{P_{i,spec}^0}{3} \\ -\sigma_1 \cdot \frac{a_i P_{i,spec}^0}{3} \\ 0 \\ \dots \\ 0 \\ -\sigma_j \cdot \frac{P_{i,spec}^0}{3} \\ -\sigma_j \cdot \frac{a_i P_{i,spec}^0}{3} \\ 0 \\ \dots \\ 0 \\ -\sigma_k \cdot \frac{P_{i,spec}^0}{3} \\ 0 \\ \dots \\ 0 \end{bmatrix} \quad (5.26)$$

} Position of QPF internal equations for generator i
 Position of QPF first internal equation for all PQ or PV controlled generators
 Position of QPF second internal equation for all PQ controlled generators

σ_j is the unit economic participation factor.

a_i is the ratio $\frac{Q_i^0}{P_{i,spec}^0}$ for the outaged PV controlled unit, with Q_i^0 the reactive production of the unit at base case.

Slack Generator:

$$\frac{\partial G(x, u)}{\partial u_i} = \begin{bmatrix} 0 \\ \dots \\ 0 \\ -\sigma_1 \cdot \frac{P_{i,spec}^0}{3} \\ -\sigma_1 \cdot \frac{a_i P_{i,spec}^0}{3} \\ 0 \\ \dots \\ 0 \\ -\sigma_j \cdot \frac{P_{i,spec}^0}{3} \\ -\sigma_j \cdot \frac{a_i P_{i,spec}^0}{3} \\ 0 \\ \dots \\ 0 \\ -\sigma_k \cdot \frac{P_{i,spec}^0}{3} \\ 0 \\ \dots \\ 0 \end{bmatrix} \quad (5.27)$$

Position of QPF first internal equation for all PQ or PV controlled generators
 Position of QPF second internal equation for all PQ controlled generators

σ_j is the unit economic participation factor.

a_i is the ratio $\frac{Q_i^0}{P_{i,spec}^0}$ for the outaged PV controlled unit, with Q_i^0 the reactive production of the unit at base case.

5.3.2 Voltage index

- *Computation of the costate vector \hat{x}^T*

The costate vector depends only on the current state of the system and it is independent of the contingency. Therefore, its value is constant for any circuit outage and any generator outage:

$$\hat{x}^T = \left[\frac{\partial J_v}{\partial x} \right] \left[\frac{\partial G(x, u)}{\partial x} \right]^{-1} \quad (5.28)$$

$\left[\frac{\partial G(x, u)}{\partial x} \right]$ is the Jacobian matrix of the system and it is already computed for the solution of the base case.

$$\frac{\partial J_V}{\partial x} = 2n \cdot \sum_{k=1}^N \frac{w_k}{V_{k,step}} \cdot \left(\frac{|V_k|^0 - V_{k,mean}}{V_{k,step}} \right)^{2n-1} \cdot \frac{1}{|V_k|^0} \cdot (V_{kr}^0 e_i^T + V_{ki}^0 e_{i+1}^T) \quad (5.29)$$

where e_i is the column vector all elements of which are zero, except for a “1” in the i -th position. The index i corresponds to the position of the state variable V_{kr} in the state vector.

Circuit outage between buses i and j .

- Computation of $\frac{\partial J_V}{\partial u_{ij}}$

$$\frac{\partial J_V}{\partial u_{ij}} = 0 \quad (5.30)$$

- Computation of $\frac{\partial G(x, u)}{\partial u_{ij}}$

$$\frac{\partial G(x, u)}{\partial u_{ij}} = \begin{bmatrix} 0 \\ \dots \\ 0 \\ I_{ijr}^0 \\ I_{iji}^0 \\ 0 \\ \dots \\ 0 \\ I_{jir}^0 \\ I_{jii}^0 \\ 0 \\ \dots \\ 0 \end{bmatrix} \left. \begin{array}{l} \} \\ \\ \} \end{array} \right\} \begin{array}{l} \text{Position of QPF Equations for bus } i \\ \\ \text{Position of QPF Equations for bus } j \end{array} \quad (5.31)$$

Outage of generating unit i .

- Computation of $\frac{\partial J_V}{\partial u_i}$

$$\frac{\partial J_V}{\partial u_i} = 0 \quad (5.32)$$

- Computation of $\frac{\partial G(x, u)}{\partial u_i}$

PQ Controlled Generator:

$$\frac{\partial G(x, u)}{\partial u_i} = \begin{bmatrix} 0 \\ \dots \\ 0 \\ \frac{P_{i,spec}^0}{3} \\ \frac{Q_{i,spec}^0}{3} \\ 0 \\ \dots \\ 0 \\ -\sigma_1 \cdot \frac{P_{i,spec}^0}{3} \\ -\sigma_1 \cdot \frac{Q_{i,spec}^0}{3} \\ 0 \\ \dots \\ 0 \\ -\sigma_j \cdot \frac{P_{i,spec}^0}{3} \\ -\sigma_j \cdot \frac{Q_{i,spec}^0}{3} \\ 0 \\ \dots \\ 0 \\ -\sigma_k \cdot \frac{P_{i,spec}^0}{3} \\ 0 \\ \dots \\ 0 \end{bmatrix} \quad \begin{array}{l} \left. \begin{array}{l} \frac{P_{i,spec}^0}{3} \\ \frac{Q_{i,spec}^0}{3} \end{array} \right\} \text{Position of QPF internal equations for generator } i \\ \\ \begin{array}{l} \leftarrow \text{Position of QPF first internal equation for all PQ or PV} \\ \text{controlled generators} \\ \leftarrow \text{Position of QPF second internal equation for all PQ} \\ \text{controlled generators} \end{array} \end{array} \quad (5.33)$$

σ_j is the unit economic participation factor.

PV Controlled Generator:

$$\frac{\partial G(x,u)}{\partial u_i} = \begin{bmatrix} 0 \\ \dots \\ 0 \\ \frac{P_{i,spec}^0}{3} \\ 0 \\ 0 \\ \dots \\ 0 \\ -\sigma_1 \cdot \frac{P_{i,spec}^0}{3} \\ -\sigma_1 \cdot \frac{a_i P_{i,spec}^0}{3} \\ 0 \\ \dots \\ 0 \\ -\sigma_j \cdot \frac{P_{i,spec}^0}{3} \\ -\sigma_j \cdot \frac{a_i P_{i,spec}^0}{3} \\ 0 \\ \dots \\ 0 \\ -\sigma_k \cdot \frac{P_{i,spec}^0}{3} \\ 0 \\ \dots \\ 0 \end{bmatrix} \tag{5.34}$$

} Position of QPF internal equations for generator i
 Position of QPF first internal equation for all PQ or PV controlled generators
 Position of QPF second internal equation for all PQ controlled generators

σ_j is the unit economic participation factor.

a_i is the ratio $\frac{Q_i^0}{P_{i,spec}^0}$ for the outaged PV controlled unit, with Q_i^0 the reactive production of the unit at base case.

Slack Generator:

$$\frac{\partial G(x, u)}{\partial u_i} = \begin{bmatrix} 0 \\ \dots \\ 0 \\ -\sigma_1 \cdot \frac{P_{i,spec}^0}{3} \\ -\sigma_1 \cdot \frac{a_i P_{i,spec}^0}{3} \\ 0 \\ \dots \\ 0 \\ -\sigma_j \cdot \frac{P_{i,spec}^0}{3} \\ -\sigma_j \cdot \frac{a_i P_{i,spec}^0}{3} \\ 0 \\ \dots \\ 0 \\ -\sigma_k \cdot \frac{P_{i,spec}^0}{3} \\ 0 \\ \dots \\ 0 \end{bmatrix} \quad (5.35)$$

Position of QPF first internal equation for all PQ or PV controlled generators

Position of QPF second internal equation for all PQ controlled generators

σ_j is the unit economic participation factor.

a_i is the ratio $\frac{Q_i^0}{P_{i,spec}^0}$ for the outaged PV controlled unit, with Q_i^0 the reactive production of the unit at base case.

5.4 Improvements in Performance Index Contingency Ranking Methods

Performance index contingency ranking methods are very efficient and fast, however, they are susceptible to misrankings, mainly due to the highly nonlinear nature of the power flow equations. In this report, besides from transforming the power flow problem using the QPF formulation, several techniques are investigated to achieve less misranking.

In order to reduce the error introduced by the approximation in PI method, one approach is to include higher order terms to reduce the error. Another method is to do the proper control variable transformation such that the resulting $J - u$ curve has less nonlinearity. Both methods based on the quadratic power flow model are described below:

5.4.1 QPF Sensitivity Method [13]

The described approach has been applied to contingency selection using a variety of performance indices, circuit current index, voltage index, reactive power index, etc. In this report we present the methodology and comparison of the new method for one of these performance indices.

In this method, instead of linearizing the performance indices directly, the system states of the QPF model are linearized with respect to the control variable, the performance index J is then calculated as following:

$$J = J(x^0 + \frac{dx}{du}(u-1), u), \quad (5.36)$$

where

- x^0 : present operating condition ;
- x : system state of the QPF problem;
- u : control variable.

The utilization of the linearized system states in calculating the system performance index provides the higher order terms in Taylor's series. The unique potential of this method has been proven in the simulation of an example power system given in [13]. Three indices, the quasi-linearized indices by the QPF sensitivity method, the linearized indices based on TPF, and the original index, have been computed and compared. The QPF sensitivity method provides the traces of indices with curvature, which can follow the highly nonlinear variations of the original indices to some extent. While the TPF method provides only the straight line. Therefore, the QPF higher order sensitivity method is superior to the PI method based on TPF.

The contingency selection is based on the computation of the performance index change due to a contingency and subsequent ranking of the contingencies on the basis of the change. Mathematically one can view the outage of a circuit as a reduction of the admittance of the circuit to zero. We use again the outage control variable, u_c , as illustrated in Figures 5.1 and 5.2. Consider the performance index, J . The change of the performance index due to the contingency is:

$$\Delta J = J\left(x^0 + \frac{dx}{du_c}(u_c - 1), u_c\right) - J(x^0, u_c = 1.0) \quad (5.37)$$

where x^0 is the present operating condition. The sensitivity of the state with respect to the control variable can be easily computed as:

$$\frac{dx}{du_c} = -\left[\frac{\partial G(x, u)}{\partial x}\right]^{-1} \left[\frac{\partial G(x, u)}{\partial u_c}\right] \quad (5.38)$$

Note that $\frac{\partial G(x, u)}{\partial x}$ is the Jacobian of the system and therefore it is precomputed at the present operating condition and remains invariant for all contingencies. Thus for each contingency we have to only compute the partial derivatives of the power flow equation $G(x, u)$ with respect to

the contingency control variable. This vector has only few nonzero entries and therefore the computations are extremely fast. It should also be noted that $\frac{dx}{du_c}$ is a vector of the same size as the state vector each element of which is the derivative of the corresponding state with respect to the control variable. Once the new state is computed via this linear approximation, the calculation of the new value of the performance index is a straightforward operation.

The concept of the approach is presented graphically in Figures 5.4 and 5.5 based on results obtained from the application of the method to a test system. The first order analysis curve represents the classical linear curve after performing the linearization of the index with respect to the contingency control variable. The higher order analysis curve is the state linearization curve with respect to the contingency control variable.

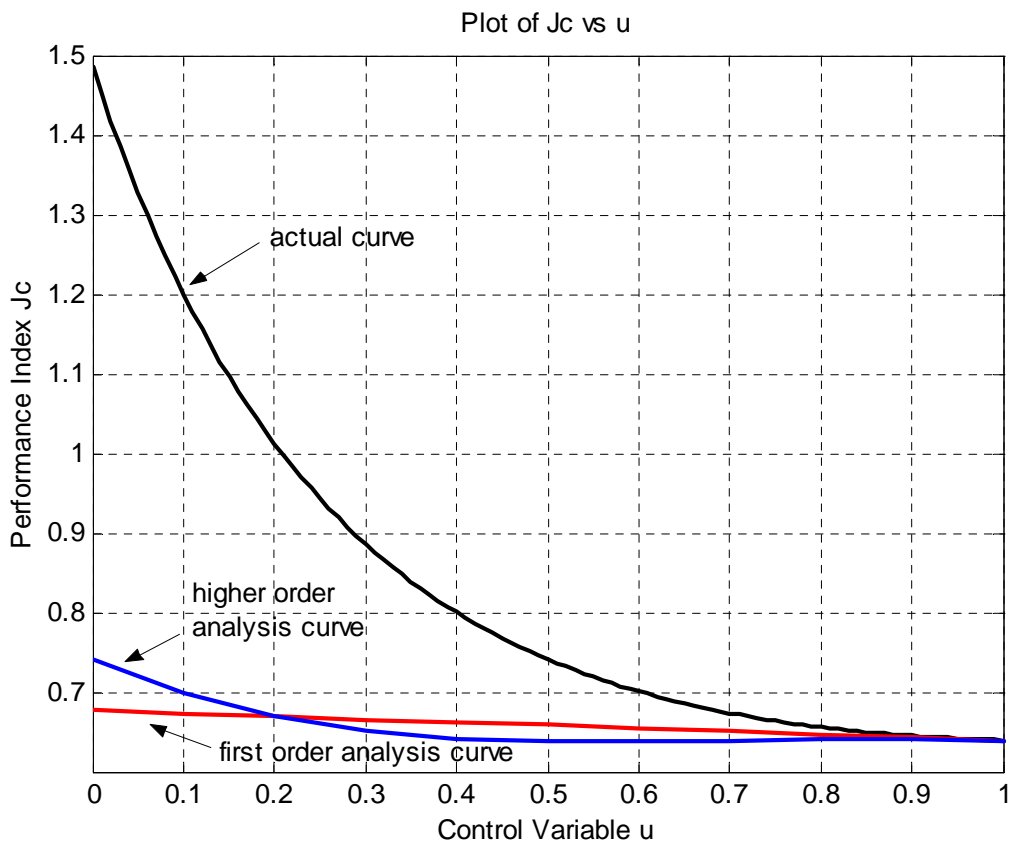


Figure 5.4. Plots of circuit-loading index vs. the contingency control variable u_c .

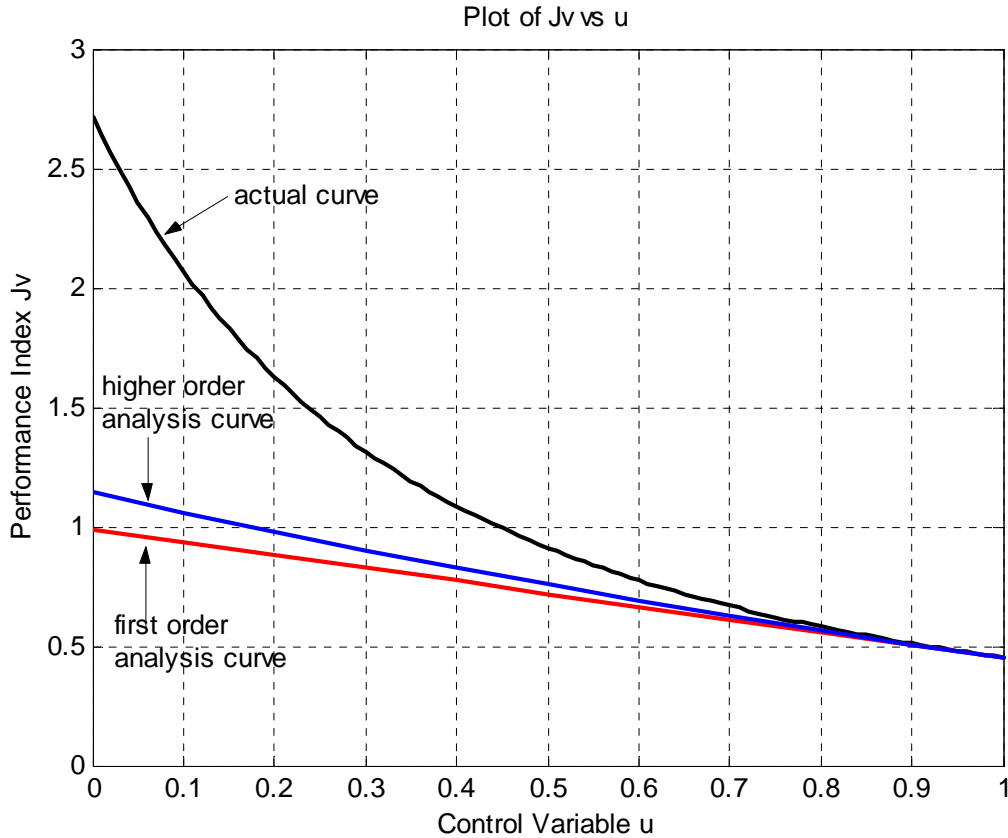


Figure 5.5. Plots of voltage index vs. the contingency control variable u_c .

The method has been applied to a small power system and compared to the traditional contingency selection algorithms (based on the traditional power flow formulation) [13]. The results for both methods are shown in Tables 1 and 2. Note that the proposed method predicts much better the changes of the performance index due to the outage (Table 5.1). Note also that the proposed method provides the correct ranking of the outages, as compared to the traditional method which results in severe misrankings for this system (Table 5.2).

Table 5.1. Performance index change computed directly, with the traditional method and with the proposed method.

| Contingency | Before Contingency | After Contingency | | | | | |
|-------------|--------------------|-------------------|---------|------------------------|---------|------------------------|---------|
| | Original Index | Original Index | | Linearized Index (TPF) | | Linearized Index (QPF) | |
| | | Value | Change | Value | Change | Value | Change |
| u_{c12} | 0.30392 | 0.30395 | 0.00003 | 0.30394 | 0.00002 | 0.30394 | 0.00002 |
| u_{c13} | 0.3039 | 5.6357 | 5.3318 | 0.1917 | -0.1122 | 0.5403 | 0.2364 |
| u_{c14} | 0.3039 | 4.9665 | 4.6626 | 0.4910 | 0.1871 | 0.9684 | 0.6645 |
| u_{c24} | 0.3039 | 2.7788 | 2.4749 | 0.3046 | 0.0007 | 0.3284 | 0.0245 |
| u_{c34} | 0.3039 | 0.2921 | -0.0118 | 0.2977 | -0.0062 | 0.2994 | -0.0045 |

Table 5.2. Ranking results.

| Contingency | Ranking | | | | |
|--------------------------|-----------|-----------|-----------|-----------|-----------|
| | u_{c12} | u_{c13} | u_{c14} | u_{c24} | u_{c34} |
| Original Index | 4 | 1 | 2 | 3 | Improved |
| Linearized Index (Pbase) | 2 | improved | 1 | Improved | Improved |
| Linearized Index (TPF) | 3 | improved | 1 | 2 | Improved |
| Linearized Index (QPF) | 4 | 2 | 1 | 3 | Improved |

Some additional results from the small test system illustrated in Figure 5.6 are presented in Tables 5.3 and 5.4.

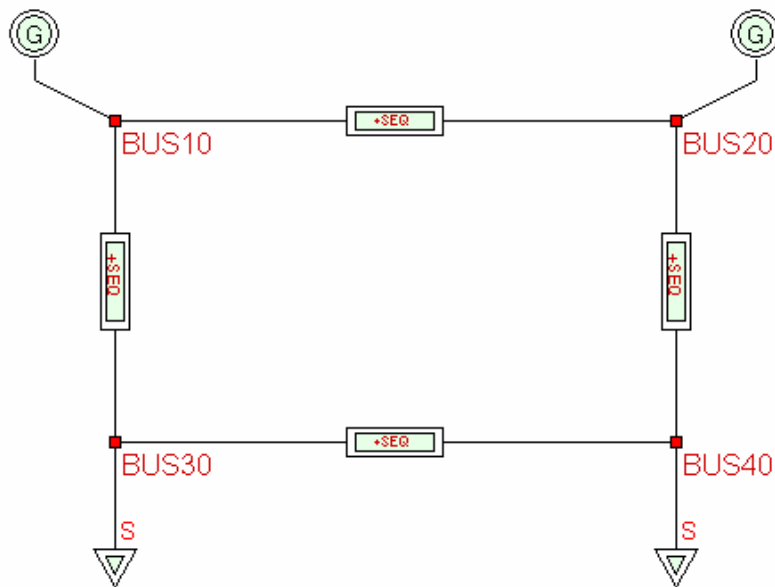


Figure 5.6. Test system used for contingency ranking evaluation.

Table 5.3. Performance index change and ranking results for the circuit loading index.

| Outaged Line | $J(u=1)$ | $J(u=0)$ | Actual ΔJ | Nonlinear Approach Ranking | $\Delta J = -dJ/du$ | Proposed Index Linearization Ranking | State Linearization Analysis ΔJ | Proposed State Linearization Ranking |
|--------------|----------|----------|-------------------|----------------------------|---------------------|--------------------------------------|---|--------------------------------------|
| 10_30 | 8.84401 | | | 1 | 24.87533 | 1 | 51.93819 | 1 |
| 20_40 | 8.84401 | 18800.67 | 18791.83 | 2 | 19.98223 | 2 | 41.22497 | 2 |
| 30_40 | 8.84401 | 12.28402 | 3.44001 | 3 | -0.0082 | 4 | 0.01342 | 3 |
| 10_20 | 8.84401 | 8.99846 | 0.15445 | 4 | -0.00059 | 3 | -0.00316 | 4 |

Table 5.4. Performance index change and ranking results for the voltage index.

| Outaged Line | $J(u=1)$ | $J(u=0)$ | Actual ΔJ | Nonlinear Approach Ranking | $\Delta J = -dJ/du$ | Proposed Index Linearization Ranking | State Linearization Analysis ΔJ | Proposed State Linearization Ranking |
|--------------|----------|----------|-------------------|----------------------------|---------------------|--------------------------------------|---|--------------------------------------|
| 10_30 | 0.27091 | | | 1 | -0.06029 | 4 | 1.92924 | 1 |
| 20_40 | 0.27091 | 22.24559 | 21.97468 | 2 | 0.1814 | 1 | 0.97924 | 2 |
| 10_20 | 0.27091 | 0.31572 | 0.04481 | 3 | 0.0029 | 2 | 0.00311 | 3 |
| 30_40 | 0.27091 | 0.25285 | -0.01806 | 4 | -0.00861 | 3 | -0.00737 | 4 |

Finally some preliminary results from the IEEE 24-Bus Reliability Test System, depicted in Figure 5.7, are presented in Table 5.5.

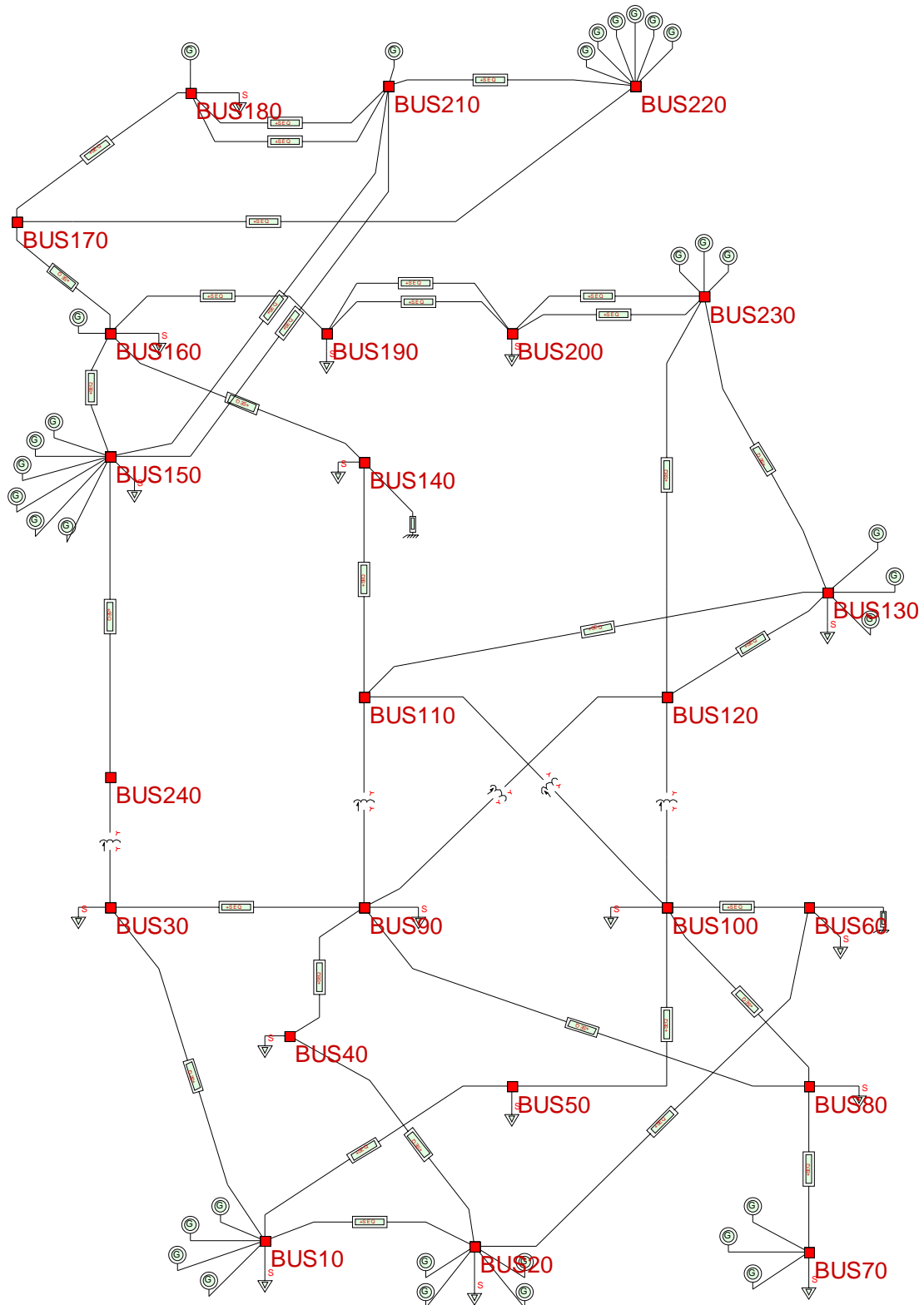


Figure 5.7. The IEEE 24-bus reliability test system.

Table 5.5. Performance index change and ranking results for the voltage index for the IEEE 24-bus reliability test system.

| Outaged Branch | $J(u=1)$ | $J(u=0)$ | Actual ΔJ | Nonlinear Approach Ranking | $\Delta J = -dJ/du$ | Proposed Index Linearization Ranking | State Linearization Analysis ΔJ | Proposed State Linearization Ranking |
|----------------|----------|----------|-------------------|----------------------------|---------------------|--------------------------------------|---|--------------------------------------|
| 60_100 C | 25.41 | 3306.22 | 3280.81 | 1 | -243.87 | 39 | 120.99 | 1 |
| 20_60 | 25.41 | 133.82 | 108.41 | 2 | 30.72 | 1 | 49.99 | 2 |
| 100_110 T | 25.41 | 63.10 | 37.69 | 3 | 16.73 | 2 | 24.95 | 3 |
| 150_240 | 25.41 | 58.58 | 33.17 | 4 | 0.00 | 19 | 1.65 | 8 |
| 50_100 | 25.41 | 55.57 | 30.16 | 5 | 7.48 | 5 | 8.68 | 6 |
| 100_120 T | 25.41 | 50.63 | 25.22 | 6 | 12.98 | 3 | 19.67 | 4 |
| 80_100 | 25.41 | 48.74 | 23.33 | 7 | 10.20 | 4 | 12.24 | 5 |
| 10_50 | 25.41 | 39.40 | 13.98 | 8 | 4.12 | 6 | 4.55 | 7 |
| 240_30 T | 25.41 | 37.04 | 11.63 | 9 | -1.33 | 31 | -0.90 | 32 |
| 110_140 | 25.41 | 30.62 | 5.21 | 10 | 1.08 | 7 | 1.18 | 9 |
| 30_90 | 25.41 | 28.41 | 3.00 | 11 | 0.88 | 8 | 1.10 | 10 |

5.4.2 Reducing the nonlinearity of the variations of performance indices

In the formulation of QPF model, the control variable transformation is introduced to reduce the nonlinearity of the changes of performance indices. As shown in Figure 5.8, the curve, which represents the relation between a performance index and a control variable, is generally nonlinear due to the inherent nonlinearity of power systems.

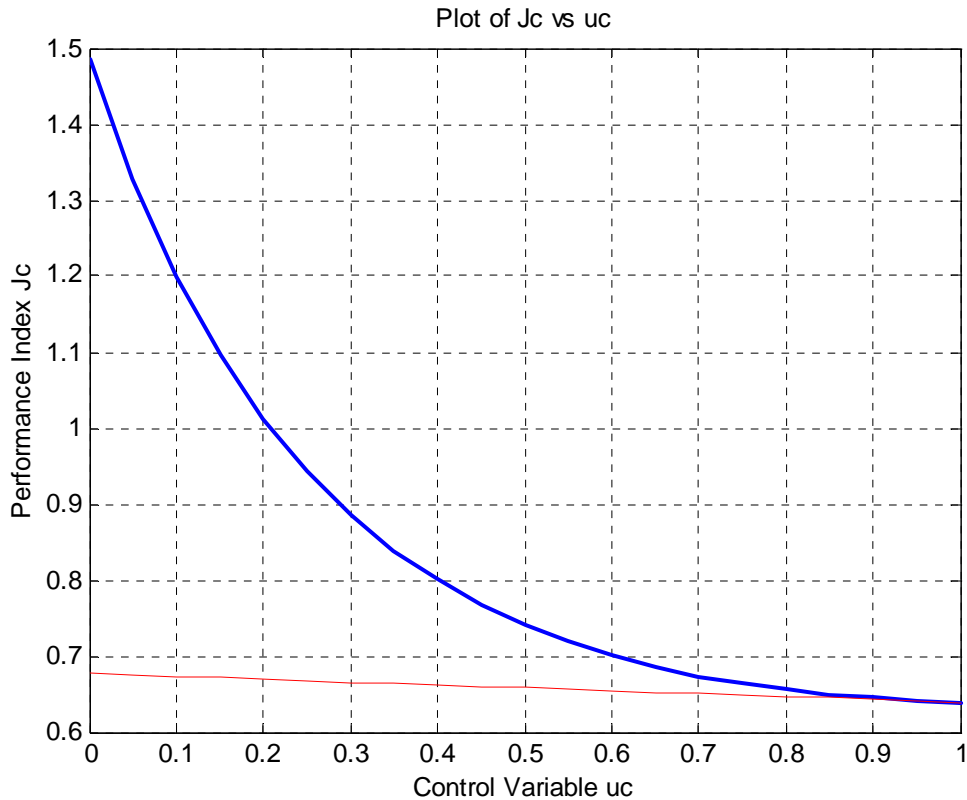


Figure 5.8. Nonlinear curve of current based loading performance index with respect to a circuit outage control variable.

If proper control variable transformation is applied, such that the curve of the performance index via the new control variable is more close to a straight line, then the prediction of post-

contingency performance index based on the new curve can provide more accurate information by the linearized model. A basic restriction is that the values of the original and transformed control variables (and therefore the performance index values) at the end points should be the same, i.e., zero and one. The proper control variable transformation is still being investigated.

The general concept of the approach is graphically presented in Figures 5.9 and 5.10. Some preliminary results and some more details of the approach can be found in [15].

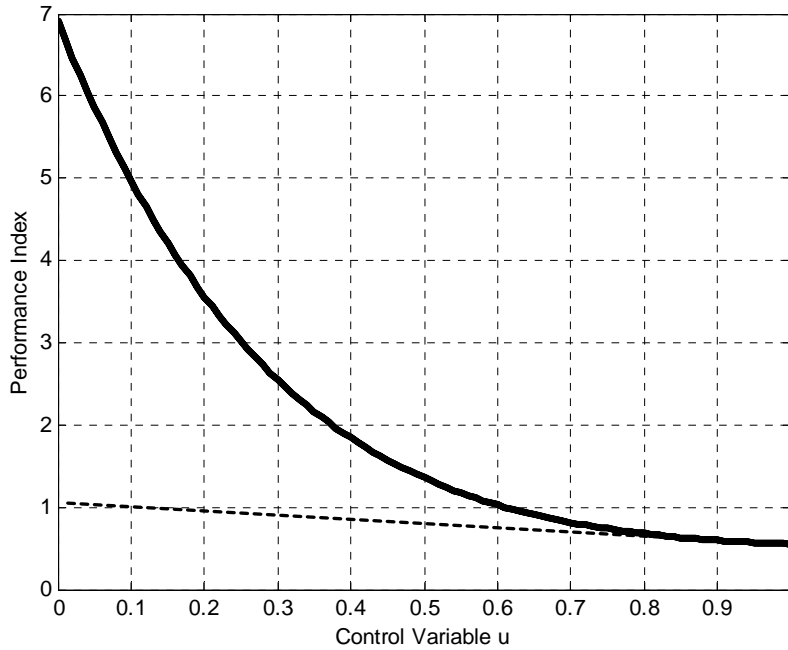


Figure 5.9. Nonlinear curve of original performance index with respect to a circuit outage control variable u and first order approach line.

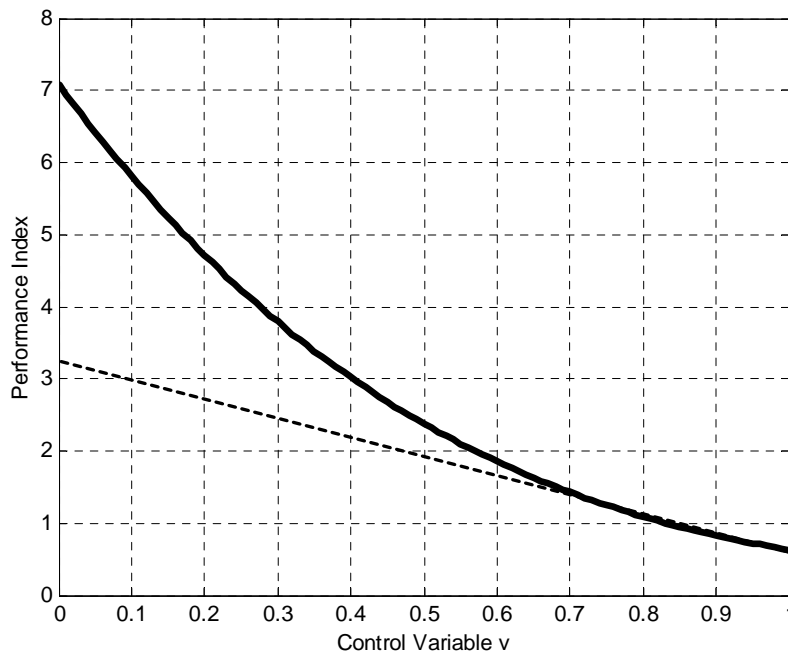


Figure 5.10. Nonlinear curve of transformed performance index with respect to a transformed circuit outage control variable v and first order approach line.

6. Remedial Actions

This section presents the methodology for remedial action computations using the quadratized power flow model. Remedial actions (RAs) provide the means of correcting the abnormal conditions, such as circuit overloads, abnormal voltages, etc. These abnormal conditions usually result from scheduled or random events, especially the system contingencies.

A list of system typical remedial actions is given in Table 6.1. The table provides an indication of the relative cost associated with each remedial action. According to the cost, the remedial actions can be divided into three levels, i.e., low, moderate and high cost levels. From the viewpoint of power system economic operation, the low cost remedial actions should be considered first in the case of abnormal conditions, if they cannot improve the situation to the required level, the moderate and even high cost remedial actions are then applied.

Remedial actions greatly affect reliability and to a lesser degree economics of the power system operation. Different mathematical problems can be defined to address the problem depending on the objectives of remedial actions, such as minimum control actions, minimum deviation from economic operation, etc.

Table 6.1. List of possible remedial actions.

| | Remedial Action | Associate Cost |
|----|----------------------------|-----------------------|
| 1 | Shunt Capacitor Switching | Low |
| 2 | Shunt Reactor Switching | Low |
| 3 | Phase Shifter Adjustment | Low |
| 4 | MVAR Generation Adjustment | Low |
| 5 | Generation Bus Voltage | Low |
| 6 | Transformer Taps | Low |
| 7 | FACTS Controls | Low |
| 8 | Load Transfer | Low |
| 9 | MW Generation Adjustments | Moderate |
| 10 | Area Interchange | High |
| 11 | Interruptible Load | High |
| 12 | Firm Load | High |
| 13 | Critical Load | High |

6.1 Quadratized Remedial Action Models

The quadratized remedial action models are illustrated in this section in an effort to analyze the effect of remedial actions on the power system reliability. The control variable u is integrated to each remedial action model to represent the availability and magnitude of these control actions.

6.1.1. Shunt Capacitor/Reactor Switching

Figure 6.1 shows a shunt switched capacitor/reactor model that is connected at a bus k . The switched capacitor/reactor model is characterized with admittance $\tilde{y}_{k,\max}$ and control variable

u_{SCR} .

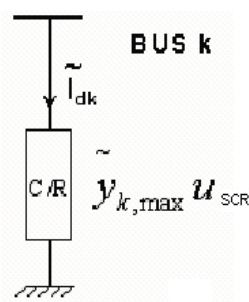


Figure 6.1. Shunt capacitor or reactor at bus k .

The control variable u_{SCR} is defined as:

$$u_{SCR} = \frac{i}{n}, \quad i = 0, 1, \dots, n,$$

where n is the number of switched steps.

The quadratized model in standard form is given as:

$$\tilde{I}_{dk} = \tilde{y}_{k,\max} u_{SCR} \tilde{V}_k \quad (6.1)$$

6.1.2. Regulating Transformer--- Phase Shift / Transformer Tap Adjustment

Figure 6.2 illustrates a regulating transformer connected to buses k and m . The transformer model is characterized with series admittance $2\tilde{y}_s$, shunt admittance \tilde{y}_s , phase shift α and tap setting t . This model assumes that the tap is on the k bus side. The transformer can work in two modes: (1) Variable Tap with Fixed Phase Shift and (2) Variable Phase Shift with Fixed Tap. In these two modes, the regulating transformer can regulate the voltage magnitude or real power through adjusting the tap setting t or phase shift α .

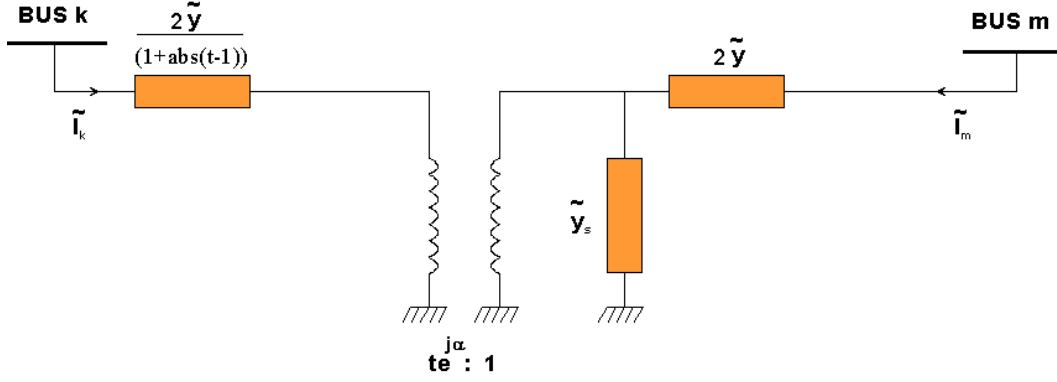


Figure 6.2. Regulating transformer model (Tap side = bus k).

(1) Transformer Tap Adjustment

In this case, the transformer tap varies to control the voltage magnitude on one end of the transformer. It is assumed that m side voltage magnitude is controlled to a specified value $V_{m,specified}$. The primal equations for this model are:

$$\begin{aligned}
 \tilde{I}_k &= 2\tilde{y}T_1(\tilde{V}_k - te^{j\alpha}\tilde{E}_m) \\
 \tilde{I}_m &= 2\tilde{y}(\tilde{V}_m - \tilde{E}_m) \\
 0 &= (\tilde{y}_s + 2\tilde{y} + 2\tilde{y}T_1t^2)\tilde{E}_m - 2\tilde{y}T_1te^{-j\alpha}\tilde{V}_k - 2\tilde{y}\tilde{V}_m \\
 0 &= |\tilde{V}_m| - V_{m,specified}
 \end{aligned} \tag{6.2}$$

where

$$T_1 = \frac{1}{1 + abs(t-1)},$$

t is tap of the transformer,
 α is phase shift angle.

Since the tap is variable, this model contains terms that are not quadratic, such as T_1 . In order to develop quadratized equations, the following variables are introduced to handle the non-quadratic terms.

$$\begin{aligned}
 x_1 &= abs(t-1) \\
 x_2 &= T_1 = \frac{1}{1+x_1} \\
 x_3 &= x_2t \\
 x_4 &= x_3t
 \end{aligned} \tag{6.2}$$

Substituting the above variables to the primal equations, the quadratized model is then obtained:

$$\begin{aligned}
\tilde{I}_k &= 2\tilde{y}(x_2\tilde{V}_k - x_3e^{j\alpha}\tilde{E}_m) \\
\tilde{I}_m &= 2\tilde{y}(\tilde{V}_m - \tilde{E}_m) \\
0 &= (\tilde{y}_s + 2\tilde{y} + 2\tilde{y}x_4)\tilde{E}_m - 2\tilde{y}x_3e^{-j\alpha}\tilde{V}_k - 2\tilde{y}\tilde{V}_m \\
0 &= V_{mr}^2 + V_{mi}^2 - V_{m,specified}^2 \\
0 &= x_1^2 - t^2 + 2t - 1 \\
0 &= x_2 + x_2x_1 - 1 \\
0 &= x_3 - x_2t \\
0 &= x_4 - x_3t \\
0 &= x_1 - x_5^2 \\
t_{\min} &\leq t \leq t_{\max}
\end{aligned} \tag{6.3}$$

Introducing the control variable u_{TT} to the transformer tap adjustment model, above equations are modified as follows:

$$\begin{aligned}
\tilde{I}_k &= 2\tilde{y}(x_2\tilde{V}_k - x_3e^{j\alpha}\tilde{E}_m) \\
\tilde{I}_m &= 2\tilde{y}(\tilde{V}_m - \tilde{E}_m) \\
0 &= (\tilde{y}_s + 2\tilde{y} + 2\tilde{y}x_4)\tilde{E}_m - 2\tilde{y}x_3e^{-j\alpha}\tilde{V}_k - 2\tilde{y}\tilde{V}_m \\
0 &= V_{mr}^2 + V_{mi}^2 - (V_{m,specified} + u_{TT})^2 \\
0 &= x_1^2 - t^2 + 2t - 1 \\
0 &= x_2 + x_2x_1 - 1 \\
0 &= x_3 - x_2t \\
0 &= x_4 - x_3t \\
0 &= x_1 - x_5^2
\end{aligned} \tag{6.4}$$

where

$$\begin{aligned}
t_{\min} &\leq t \leq t_{\max} \\
V_{m,\min} - V_{m,specified} &\leq u_{TT} \leq V_{m,\max} - V_{m,specified}
\end{aligned}$$

Note:

- (1) The last equation $0 = x_1 - x_5^2$ is to make sure that $x_1 \geq 0$, x_5 can take any real value.
- (2) This model imposes limits to the state variable t , i.e., $t_{\min} \leq t \leq t_{\max}$. The limits are observed as following:
 - (a) If t is within limits, the above model is used
 - (b) If t is outside limits, t should be set to the nearest limit and the model should switch to that of Fixed Tap and Phase Shift.

(2) Phase Shift Adjustment

In this case, the phase shift α is variable. It varies to control the real power on one end of the transformer. It is assumed that the real power on m bus side is controlled to be a specified value $P_{m,specified}$. The primal equations for this model are:

$$\begin{aligned}
\tilde{I}_k &= 2\tilde{y}T_1(\tilde{V}_k - te^{j\alpha}\tilde{E}_m) \\
\tilde{I}_m &= 2\tilde{y}(\tilde{V}_m - \tilde{E}_m) \\
0 &= (\tilde{y}_s + 2\tilde{y} + 2\tilde{y}T_1t^2)\tilde{E}_m - 2\tilde{y}T_1te^{-j\alpha}\tilde{V}_k - 2\tilde{y}\tilde{V}_m \\
0 &= \text{Re}\{\tilde{V}_m \tilde{I}_m^*\} + \frac{P_{m,\text{specified}}}{3}
\end{aligned} \tag{6.5}$$

where

$$T_1 = \frac{1}{1 + \text{abs}(t-1)}.$$

In this case, two state variables x_1 and x_2 are introduced to handle the non quadratized term $e^{j\alpha}$:

$$x_1 + jx_2 = e^{j\alpha}, \quad \alpha_{\min} \leq \alpha \leq \alpha_{\max}$$

where

$$\begin{aligned}
x_1 &= \cos \alpha \\
x_2 &= \sin \alpha. \\
x_1^2 + x_2^2 &= 1
\end{aligned}$$

Substitute above state variables to the primal equations, the quadratized model can be obtained:

$$\begin{aligned}
\tilde{I}_k &= 2\tilde{y}T_1(\tilde{V}_k - t(x_1 + jx_2)\tilde{E}_m) \\
\tilde{I}_m &= 2\tilde{y}(\tilde{V}_m - \tilde{E}_m) \\
0 &= (\tilde{y}_s + 2\tilde{y} + 2\tilde{y}T_1t^2)\tilde{E}_m - 2\tilde{y}T_1t(x_1 - jx_2)\tilde{V}_k - 2\tilde{y}\tilde{V}_m \\
0 &= 2g(V_{mr}^2 + V_{mi}^2 - V_{mr}E_{mr} - V_{mi}E_{mi}) + 2b(V_{mr}E_{mi} - V_{mi}E_{mr}) + \frac{P_{m,\text{specified}}}{3} \\
0 &= x_1^2 + x_2^2 - 1
\end{aligned} \tag{6.6}$$

where

$$\begin{aligned}
T_1 &= \frac{1}{1 + \text{abs}(t-1)}, \\
x_1 + jx_2 &= e^{j\alpha}, \alpha_{\min} \leq \alpha \leq \alpha_{\max}, \\
\tilde{y} &= g + jb.
\end{aligned}$$

Introducing the control variable u_{ps} to the phase shift adjustment model, above equations are modified as follows:

$$\begin{aligned}
\tilde{I}_k &= 2\tilde{y}T_1(\tilde{V}_k - t(x_1 + jx_2)\tilde{E}_m) \\
\tilde{I}_m &= 2\tilde{y}(\tilde{V}_m - \tilde{E}_m) \\
0 &= (\tilde{y}_s + 2\tilde{y} + 2\tilde{y}T_1t^2)\tilde{E}_m - 2\tilde{y}T_1t(x_1 - jx_2)\tilde{V}_k - 2\tilde{y}\tilde{V}_m \\
0 &= 2g(V_{mr}^2 + V_{mi}^2 - V_{mr}E_{mr} - V_{mi}E_{mi}) + 2b(V_{mr}E_{mi} - V_{mi}E_{mr}) - \frac{P_{m,specified} + u_{PS}}{3} \\
0 &= x_1^2 + x_2^2 - 1
\end{aligned} \tag{6.7}$$

where

$$\begin{aligned}
T_1 &= \frac{1}{1 + abs(t-1)}, \\
x_1 + jx_2 &= e^{j\alpha}, \alpha_{\min} \leq \alpha \leq \alpha_{\max}, \\
\tilde{y} &= g + jb, \\
P_{m,\min} - P_{m,specified} &\leq u_{PS} \leq P_{m,\max} - P_{m,specified}.
\end{aligned}$$

Note that this model imposes limits to phase shift α . The limits are observed as follows:

- (1) If α is within limits, the above model is used.
- (2) If α is outside limits, α should be set to the nearest limit and the model should switch to that of Fixed Tap and Phase Shift.

6.1.3. MVAR Generation / Bus Voltage Adjustments

Since bus voltage adjustment is very sensitive, usually it is achieved by the MVAR generation adjustment. Figure 6.3 shows a generator connected at bus k. The generator is characterized with a current injection from the bus k to the generator, i.e., \tilde{I}_k . The total complex power generation is $P_k + jQ_k$.

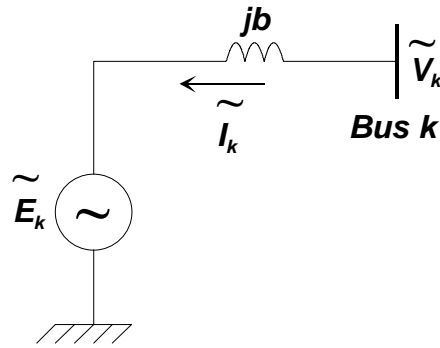


Figure 6.3. Generator connected to bus k.

The current equation from bus k to the generator is:

$$\tilde{I}_k = jb(\tilde{V}_k - \tilde{E}_k) \tag{6.8}$$

There are three control modes for the synchronous generator, i.e., a) Slack mode, b) PQ mode, and c) PV mode. MVAR generation adjustment is only related with the PQ mode:

PQ mode

In the PQ mode, the synchronous generator is controlled to maintain the specified real and reactive power. For the PQ mode, we have the following real and imaginary equations:

$$\begin{aligned}
 I_{kr} &= -bV_{ki} + bE_{ki} \\
 I_{ki} &= bV_{kr} - bE_{kr} \\
 0.0 &= bV_{kr}E_{ki} - bV_{ki}E_{kr} + \frac{P_{k,specified}}{3} \\
 0.0 &= -bV_{kr}^2 + bV_{kr}E_{kr} - bV_{ki}^2 + bV_{ki}E_{ki} + \frac{Q_{k,specified}}{3}
 \end{aligned} \tag{6.9}$$

Introducing the control variable u_{MVAR_PQ} to the MVAR generation adjustment, above equations are modified as follows:

$$\begin{aligned}
 I_{kr} &= -bV_{ki} + bE_{ki} \\
 I_{ki} &= bV_{kr} - bE_{kr} \\
 0.0 &= bV_{kr}E_{ki} - bV_{ki}E_{kr} + \frac{P_{k,specified}}{3} \\
 0.0 &= -bV_{kr}^2 + bV_{kr}E_{kr} - bV_{ki}^2 + bV_{ki}E_{ki} + \frac{Q_{k,specified} + u_{MVAR_PQ}}{3}
 \end{aligned} \tag{6.10}$$

where

u_{MVAR_PQ} : reactive power change

The constraints of u_{MVAR_PQ} are derived below:

$$Q_{\min} \leq Q_{k,specified} + u_{MVAR_PQ} \leq Q_{\max}$$

then

$$Q_{\min} - Q_{k,specified} \leq u_{MVAR_PQ} \leq Q_{\max} - Q_{k,specified}$$

6.1.4. Load Transfer

Figure 6.4 illustrates the load transfer. Assuming that originally the total load at bus m is S_{dm} and the total load at bus k is S_{dk} , which both are constant power loads:

$$\begin{aligned}
 S_{dm} &= P_{dm} + jQ_{dm} \\
 S_{dk} &= P_{dk} + jQ_{dk}
 \end{aligned}$$

The constant power load model can be expressed with the following set of equations.

For load at bus m, define the nominal admittance of the load to be:

$$\tilde{Y}_{dn,m} = \frac{1}{V_m^2} (P_{dm} - jQ_{dm}) = g_{dn,m} + jb_{dn,m} \quad (6.11)$$

$$\begin{aligned} \tilde{I}_{dm} &= \tilde{Y}_{dn,m} \tilde{V}_m (1 + a_1) \\ 0 &= g_{dn,m} a_2 (1 + a_1) - P_{dm} \\ 0 &= a_2 - V_m^2 \end{aligned} \quad (6.12)$$

For load at bus k, define the nominal admittance of the load to be:

$$\tilde{Y}_{dn,k} = \frac{1}{V_k^2} (P_{dk} - jQ_{dk}) = g_{dn,k} + jb_{dn,k} \quad (6.13)$$

$$\begin{aligned} I_{dk} &= Y_{dn,k} V_k (1 + a_3) \\ 0 &= g_{dn,k} a_4 (1 + a_3) - P_{dk} \\ 0 &= a_4 - V_k^2 \end{aligned} \quad (6.14)$$

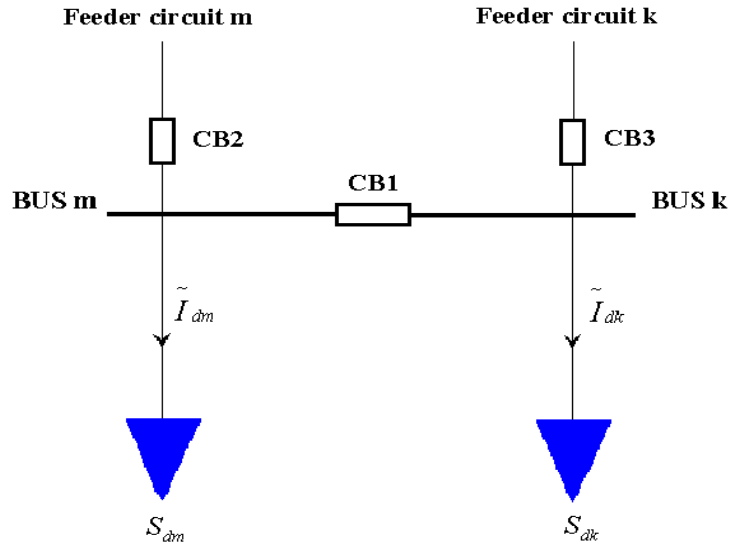


Figure 6.4. Load transfer.

If any disturbance occurs to bus m or feeder circuit m, some or all of S_{dm} can be transferred to bus k through the operation of circuit breaker CB1 and CB2. Similarly, if any disturbance occurs to bus k or feeder circuit k, some or all of S_{dk} can be transferred to bus m through the operation of circuit breaker CB1 and CB3. The control variable u_{LT} is introduced to represent the transferred load. The load models at bus m and k are modified as follow:

For load at bus m :

$$\begin{aligned}
I_{dm} &= Y_{dn,m} V_m (1 + a_1) \\
0 &= g_{dn,m} a_2 (1 + a_1) - (P_{dm} - u_{LT}) \\
0 &= a_2 - V_m^2
\end{aligned} \tag{6.15}$$

For load at bus k :

$$\begin{aligned}
I_{dk} &= Y_{dn,k} V_k (1 + a_3) \\
0 &= g_{dn,k} a_4 (1 + a_3) - (P_{dk} + u_{LT}) \\
0 &= a_4 - V_k^2
\end{aligned} \tag{6.16}$$

where $P_{dm} - u_{LT} \geq 0$ and $P_{dk} + u_{LT} \geq 0$.

The constraint of u_{LT} is derived as:

$$-P_{dk} \leq u_{LT} \leq P_{dm}.$$

6.1.5. MW generation adjustments

Among the three control modes for the synchronous generator, i.e., a) Slack mode, b) PQ mode, and c) PV mode, MW generation adjustment is related with both PV and PQ modes:

PQ mode

In the PQ mode, the synchronous generator is controlled to maintain the specified real and reactive power. For the PQ mode, we have the following real and imaginary equations.

$$\begin{aligned}
I_{kr} &= -bV_{ki} + bE_{ki} \\
I_{ki} &= bV_{kr} - bE_{kr} \\
0.0 &= bV_{kr} E_{ki} - bV_{ki} E_{kr} + \frac{P_{k,specified}}{3} \\
0.0 &= -bV_{kr}^2 + bV_{kr} E_{kr} - bV_{ki}^2 + bV_{ki} E_{ki} + \frac{Q_{k,specified}}{3}
\end{aligned} \tag{6.17}$$

Introducing the control variable u_{MW_PQ} to the MW generation adjustment, the above equations are modified as follows:

$$\begin{aligned}
I_{kr} &= -bV_{ki} + bE_{ki} \\
I_{ki} &= bV_{kr} - bE_{kr} \\
0.0 &= bV_{kr} E_{ki} - bV_{ki} E_{kr} + \frac{P_{k,specified} + u_{MW_PQ}}{3} \\
0.0 &= -bV_{kr}^2 + bV_{kr} E_{kr} - bV_{ki}^2 + bV_{ki} E_{ki} + \frac{Q_{k,specified}}{3}
\end{aligned} \tag{6.18}$$

where

u_{MW_PQ} : active power change.

The constraints for u_{MW_PQ} is derived below:

$$P_{\min} \leq P_{k,specified} + u_{MW_PQ} \leq P_{\max}$$

then

$$P_{\min} - P_{k,specified} \leq u_{MW_PQ} \leq P_{\max} - P_{k,specified}$$

PV mode

In the PV mode, the synchronous generator is controlled to maintain the specified real power and voltage magnitude. For the PV mode, we have the following real and imaginary equations.

$$\begin{aligned} I_{kr} &= -bV_{ki} + bE_{ki} \\ I_{ki} &= bV_{kr} - bE_{kr} \\ 0.0 &= bV_{kr}E_{ki} - bV_{ki}E_{kr} + \frac{P_{k,specified}}{3} \\ 0.0 &= V_{kr}^2 + V_{ki}^2 - V_{k,specified}^2 \end{aligned} \quad (6.19)$$

Introducing the control variable u_{MW_PV} to the MW generation adjustment, the above equations are modified as follows:

$$\begin{aligned} I_{kr} &= -bV_{ki} + bE_{ki} \\ I_{ki} &= bV_{kr} - bE_{kr} \\ 0.0 &= bV_{kr}E_{ki} - bV_{ki}E_{kr} + \frac{P_{k,specified} + u_{MW_PV}}{3} \\ 0.0 &= V_{kr}^2 + V_{ki}^2 - V_{k,specified}^2 \end{aligned} \quad (6.20)$$

where

u_{MW_PV} : active power change.

The constraints for u_{MW_PV} is derived below:

$$P_{\min} \leq P_{k,specified} + u_{MW_PV} \leq P_{\max}$$

then

$$P_{\min} - P_{k,specified} \leq u_{MW_PV} \leq P_{\max} - P_{k,specified}$$

6.1.6. Interruptible / Firm / Critical Loads

The constant power load is used as an example to illustrate the remedial action model of shedding loads. The constant power load is defined with the total complex power that is assumed to be constant, i.e., independent of the voltage at the bus. Figure 6.5 shows the constant power interruptible load S_{dki} , firm load S_{dkf} and critical load S_{dkc} that are connected at a bus k.

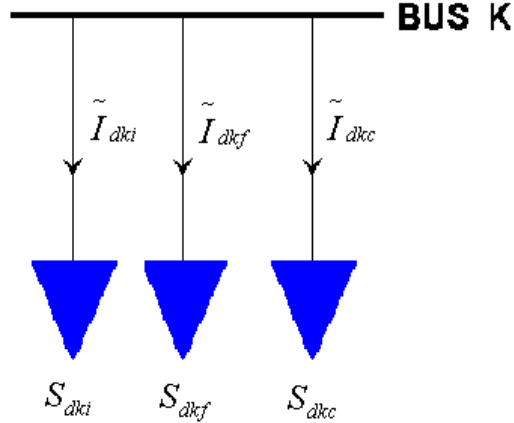


Figure 6.5. Constant power critical load at bus k.

$$S_{dki} = P_{dki} + jQ_{dki}$$

$$S_{dkf} = P_{dkf} + jQ_{dkf}$$

$$S_{dkc} = P_{dkc} + jQ_{dkc}$$

Define the nominal admittance of the loads to be

$$\text{Interruptible load: } \tilde{Y}_{dn,ki} = \frac{1}{V_{nk}^2} (P_{dki} - jQ_{dki}) = g_{dn,ki} + jb_{dn,ki}$$

$$\text{Firm load: } \tilde{Y}_{dn,kf} = \frac{1}{V_{nk}^2} (P_{dkf} - jQ_{dkf}) = g_{dn,kf} + jb_{dn,kf}$$

$$\text{Critical load: } \tilde{Y}_{dn,kc} = \frac{1}{V_{nk}^2} (P_{dkc} - jQ_{dkc}) = g_{dn,kc} + jb_{dn,kc}$$

where V_{nk} is the nominal voltage at bus k.

The constant power load model can be expressed with the following set of equations.

Interruptible load:

$$\begin{aligned} \tilde{I}_{dki} &= \tilde{Y}_{dn,ki} \tilde{V}_k (1 + a_5) \\ 0 &= g_{dn,ki} a_6 (1 + a_5) - P_{dki} \\ 0 &= a_6 - V_k^2 \end{aligned} \tag{6.21}$$

Firm load:

$$\begin{aligned}
\tilde{I}_{dkf} &= \tilde{Y}_{dn,kf} \tilde{V}_k (1 + a_7) \\
0 &= g_{dn,kf} a_8 (1 + a_7) - P_{dkf} \\
0 &= a_8 - V_k^2
\end{aligned} \tag{6.22}$$

Critical load:

$$\begin{aligned}
\tilde{I}_{dkc} &= \tilde{Y}_{dn,kc} \tilde{V}_k (1 + a_9) \\
0 &= g_{dn,kc} a_{10} (1 + a_9) - P_{dkc} \\
0 &= a_{10} - V_k^2
\end{aligned} \tag{6.23}$$

Introducing the control variable, u_{IL} , u_{FL} and u_{CL} related to the interruptible, firm and critical Load model separately, the load models at bus k are expressed as:

Interruptible load:

$$\begin{aligned}
\tilde{I}_{dki} &= \tilde{Y}_{dn,ki} \tilde{V}_k (1 + a_5) \\
0 &= g_{dn,ki} a_6 (1 + a_5) - (P_{dki} + u_{IL}) \\
0 &= a_6 - V_k^2
\end{aligned} \tag{6.24}$$

Firm load:

$$\begin{aligned}
\tilde{I}_{dkf} &= \tilde{Y}_{dn,kf} \tilde{V}_k (1 + a_7) \\
0 &= g_{dn,kf} a_8 (1 + a_7) - (P_{dkf} + u_{FL}) \\
0 &= a_8 - V_k^2
\end{aligned} \tag{6.25}$$

Critical load:

$$\begin{aligned}
\tilde{I}_{dkc} &= \tilde{Y}_{dn,kc} \tilde{V}_k (1 + a_9) \\
0 &= g_{dn,kc} a_{10} (1 + a_9) - (P_{dkc} + u_{CL}) \\
0 &= a_{10} - V_k^2
\end{aligned} \tag{6.26}$$

Constraints for u_{IL} , u_{FL} and u_{CL} are given:

$$\begin{aligned}
- P_{dki} &\leq u_{IL} \leq 0 \\
- P_{dkf} &\leq u_{FL} \leq 0 \\
- P_{dkc} &\leq u_{CL} \leq 0
\end{aligned}$$

6.2 Remedial Action Computation Methodology

The remedial action computation methodology for the purpose of alleviating the abnormal conditions is addressed next based on the derived quadratized remedial action models.

6.2.1 Problem Formulation

Remedial actions are computed via an optimization problem that is formulated as an optimization model as follows:

$$\text{Min } f(x,u) \quad (6.27)$$

$$\text{s.t. } g(x,u) = 0 \quad (6.28)$$

$$h_{l \min} \leq h_l(x,u) \leq h_{l \max} \quad (6.29)$$

$$u_{pi \min} \leq u_{pi} \leq u_{pi \max} \quad (6.30)$$

where

p : remedial action type as listed in Table 6.1;

i : remedial action device number;

u_{pi} : control variable of remedial action with type p and device i ;

u : vector of control variables;

x : system state vector;

$h_l(x,u)$: operating constraint expression;

$h_{l \min}$: operating constraint lower bound;

$h_{l \max}$: operating constraint upper bound;

$u_{pi \min}$: remedial action control variable lower bound;

$u_{pi \max}$: remedial action control variable upper bound;

Eq. (6.27): objective functions, such as minimum remedial actions and etc;

Eq. (6.28): quadratized power flow equation;

Eq. (6.29): operating constraints.

6.2.2 Nondivergent Optimal Power Flow Approach

In this section, a special optimal power flow model, i.e., the nondivergent optimal power flow approach is utilized to solve the optimization problem formulated above, which combines the quadratized power flow model, remedial actions and optimal power flow algorithm in one unified approach. The new model also leads to a non-divergent power flow algorithm.

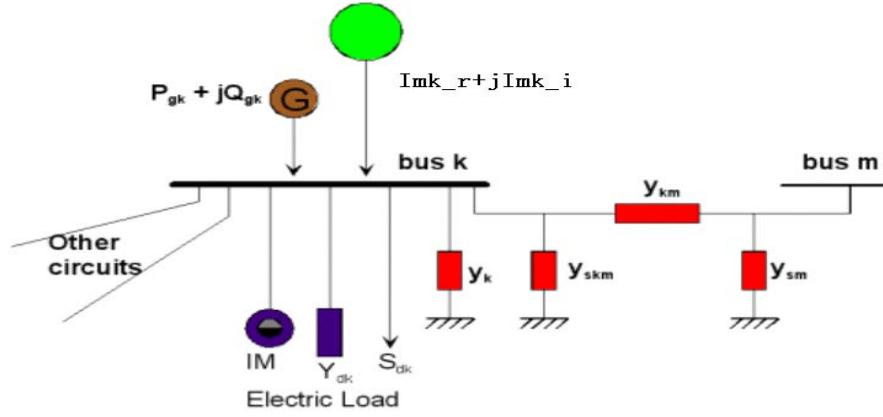


Figure 6.6 Illustration of a general bus k of an electric power system with a fictitious current source.

Consider an electric power system comprising n buses. Let the state of the system be represented with the vector x . Let the vector u represent the control variables of available remedial actions. Assuming a given operating state x^0 and settings of controls u^0 . Further, consider bus k as is illustrated in Figure 6.6. Unless x^0 and u^0 represent a power flow solution, there will be a current mismatch at bus k equal to $I_{mk_r}^0 + jI_{mk_i}^0$. Now place a fictitious current source at bus k , the output of it is $I_{mk_r}^0 + jI_{mk_i}^0$. In this case, x^0 and u^0 represent the present operating condition of the system. The actual operating condition of the system can be obtained by gradually reducing the output of the fictitious current sources at each bus to zero and computing the system variables x and u which will make the mismatch $dI_{mk_r} + jdI_{mk_i}$ equal to zero. This transition can be achieved along a trajectory which maintains feasibility and optimality with respect to a postulated objective. Mathematically, by modifying the objective function (6.1), this procedure is formulated as follows:

$$\text{Min } f(x, u) + \mu \sum_k (|dI_{mk_r}| + |dI_{mk_i}|) \quad (6.31)$$

$$\text{s.t. } g(x, u) = 0 \quad (6.32)$$

$$h_{l\min} \leq h_l(x, u) \leq h_{l\max} \quad (6.33)$$

$$u_{pi\min} \leq u_{pi} \leq u_{pi\max} \quad (6.34)$$

The last term of the objective function is a penalty function weighted with μ , which tends to reduce the fictitious mismatches to zero, thus reaching feasibility.

The defined optimization problem is a large-scale problem. The size of this problem can be drastically reduced with simple transformations. That is, the incremental mismatch variables can be substituted with one control variable v as follow:

$$dI_{mk_r} = I_{mk_r}^0 v \quad k = 1, 2, \dots, n$$

$$dI_{mk_i} = I_{mk_i}^0 v \quad k = 1, 2, \dots, n$$

where the variable v represents the normalized change of the mismatch variables ($0 \leq v \leq 1$). This transformation replaces all the mismatch variables (a total of $2n$) with a single variable v . So the above formulation becomes:

$$\text{Min} \quad f(x, u) + \mu \sum_k (|I_{mk_r}^0| + |I_{mk_i}^0|)v \quad (6.35)$$

$$\text{s.t.} \quad g(x, u) = 0 \quad (6.36)$$

$$h_{l\min} \leq h_l(x, u) \leq h_{l\max} \quad (6.37)$$

$$u_{pi\min} \leq u_{pi} \leq u_{pi\max} \quad (6.38)$$

Under the initial condition, the variable v is 1. The decreasing step size of the variable v is controlled so that at each step, the number of failed operating constrains is relative small and appropriate remedial actions can be applied. In this way, a feasibility and optimality transition with respect to the objective function can be achieved until v finally reaches zero.

6.2.3 Solution Methodology

The solution method for the above problem is iterative and includes two steps in each iteration: (a) linearization of objective function and operating constraints, (b) solution of the resulting linear programming.

Linearization of the optimization problem requires the computation of sensitivities of the objective function and operating constraints with respect to each control variable u_{pi} . For this purpose the costate method is employed. The resulting general expression of the sensitivity of a quantity f with respect to a control variable u_{pi} is:

$$\frac{df}{du_{pi}} = \frac{\partial f}{\partial u_{pi}} - \hat{x}^T \frac{\partial g}{\partial u_{pi}} \quad (6.13)$$

$$\hat{x}^T = \frac{\partial f}{\partial x} J^{-1} \quad (6.14)$$

where

f : quantity of interest (objective function or operating constraints)

u_{pi} : control parameter of interest (u_{pi} or v)

g : quadratized power flow equations

J : Jacobian matrix

\hat{x}^T : costate vector

Linearization of the quantity f with respect to u_{pi} involves the computation of $\frac{\partial f}{\partial u}$, $\frac{\partial g}{\partial u}$ and \hat{x}^T .

The computation of $\frac{\partial f}{\partial u}$ and $\frac{\partial g}{\partial u}$ is straightforward. With respect to the computation of costate vector \hat{x}^T , the Jacobian matrix J is a matrix that is available from the last iteration of the

quadratic power flow solution. $\frac{\partial f}{\partial u}$ is a computable vector at the present operating condition. The costate vector \hat{x}^T needs to be computed only once and then it is used for computing the sensitivities for all control variables. Based on the above analysis, the linearization procedure by the costate method is efficient.

The linearization procedure results in an optimization problem of the linear programming variety. The simplex method or interior point method [16] can then be used to solve this problem. The application of this remedial computation method on Reliability Test System is described in [17].

To increase efficiency, the size of the linear program is decreased (model reduction). The model reduction methodology developed is based on sensitivity information and does not affect the solution. A brief description of the method is as follows: based on the sensitivity values, the remedial action which is most effective to correct a failed constraint is identified. Next the remedial actions which have sensitivities below a predetermined cutoff value (typically 0.1 of maximum sensitivity) are flagged as ineffective to correct the failed constraints. The procedure is repeated for all failed constraints. Then the remedial actions which are ineffective for all failed constraints are eliminated from the model. It should be emphasized that the model reduction procedure does not affect the accuracy of the final result.

7. Probabilistic Power Flow

7.1 Introduction

The reliability analysis method presented in this report requires also enumeration of various load levels. An alternative to electric load level enumeration is the use of stochastic power flows. Specifically, stochastic power flows provide the procedure to consider the variation of the electric load within one power flow solution. This approach is very attractive for reliability analysis. It offers two advantages: (a) better modeling the effects of electric load variation and (b) better overall efficiency since it eliminates the evaluation of many power flows that scan the various load levels. An improved stochastic power flow methodology has been developed and described in this section.

The operation of a power system is determined to a great extent by the load demand it has to satisfy. The use of traditional load flow analysis to simulate the system operation is based on the assumption that the system loading at each bus is precisely known. That is, the electric load and additionally the generating unit outputs are deterministically known quantities. This can be considered quite accurate when on-line measurements are used for real time analysis; however for off-line analysis for planning or reliability studies this is not true. Therefore, an important issue in reliability studies is the inherent uncertainty in the knowledge of the electric load demand. The demand is in general unknown and stochastic in nature and therefore the power system operation has to be studied and planned based on estimates of this demand and taking into consideration the probabilistic nature of the load. This issue can be handled either by performing several studies under various loading levels or by directly treating the stochastic nature of the load. This is performed using the stochastic load flow analysis, also referred to as probabilistic power flow analysis. Probabilistic power flow is a term that refers to power flow analysis methods that directly treat the uncertainty of electric load and generation.

A brief review of the research on probabilistic power flow analysis can be found in [19] and [21-23]. This work extends the ideas presented in [18], [19] and [20] to a quadratized power flow AC network model. More specifically, a comprehensive model for probabilistic power flow is proposed for the purpose of evaluating the statistics of bus voltage magnitudes and circuit current and apparent power flows, given the statistics of the loads. The proposed method is based on the quadratized power flow model and a non-conforming electric load model. The stochastic electric load model is accurately represented with a few independent stochastic processes, $[\nu]$. The statistics of the quantities under study are computed from their linearized models with respect to the independent load variables $[\nu]$, around the expected value of the non-conforming load. Major operating practices such as economic dispatch and congestion management are also taken into consideration.

7.2 Problem Statement and Solution Approach

Consider an electric power system consisting of the power grid (a network of interconnected transmission lines) and generating units, as illustrated in Fig. 7.1. Given the probabilistic load

model, it is desired to calculate the statistics of the voltage magnitude at each bus and of the current magnitude and power flow at each system branch.

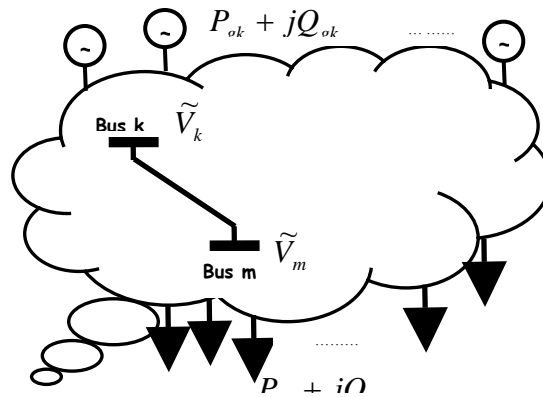


Figure 7.1. Schematic illustration of an electric power system.

More specifically it is desired to compute the statistics of the current magnitude I_{km} (or the apparent power flow T_{km}) of any circuit connecting buses k and m , or the voltage magnitude at any bus k , V_k . Major operating practices such as economic dispatch and congestion management should be accounted for in the evaluation of these statistics.

The proposed solution methodology consists of the following steps. First, a non-conforming probabilistic load model is assumed. The load model is described with a small set of independent random variables (typically 2 or 3). This model realistically captures the stochastic nature of the load, and the strong correlation of electric loads at each bus. The total increase or decrease in the required system generation is a dependant random variable. In fact it depends on the independent load random variables via an economic dispatch operation. The output of each generating unit is expressed as a function of the total generation change using linearization assuming the computed values of the participation factors of each unit at the base case operating point. Therefore the statistics (probability distribution functions) of the total generation of generation buses are computed.

Second, circuit currents, circuit power flows and bus voltage magnitudes are expressed as linear combinations of the defined random variables. The appropriate coefficients are the sensitivities of each quantity with respect to the corresponding random variable and can be simply and efficiently computed using the costate method. This linearized relationship allows the computation of the statistics of circuit currents, circuit power flows and bus voltage magnitudes.

The proposed approach and methodology is validated with an independent method based on Monte Carlo simulation. Specifically, the same problem is also solved via Monte Carlo simulations in which each random sample is fully solved, thus incorporating nonlinearities resulting from the AC power flow equations and major operating practices such as economic dispatch and possibly congestion management. Both the linearization solution and the Monte Carlo approach are based on the Single Phase Quadratic Power Flow model.

7.3 Proposed Model Description

Models of the various components of the system are presented in this section. Based on the approach described in the previous section, three main subsystems need to be modeled: (1) The electric load, (2) the generation system and (3) the transmission network.

7.3.1 Electric Load Stochastic Model

The typical load model is a conforming electric load model, i.e., a specific bus load is a percent of the total system load. Statistically, this means that the bus loads are correlated one hundred percent. This practice fails to represent the fact that the actual loads are not fully correlated. For a more realistic representation of the electric load, it is necessary to represent the bus electric load as a nonconforming load. For this purpose a nonconforming electric load model is proposed in terms of n independent and zero mean random variables. These random variables can follow any distribution, provided that they have zero mean. For example, uniform or Gaussian distributions can be assumed. The load at any system bus k can be expressed as

$$P_{dk} = P_{dk}^0 + \sum_{i=1}^n p_{dk}^i \cdot v_i, \quad (7.1)$$

where

P_{dk} : Active power demand (load) at bus k ,

P_{dk}^0 : Base case load value at bus k ,

v_i : i^{th} random variable from the set of independent zero mean load random variables,

p_{dk}^i : Participation coefficient for the i^{th} random variable v_i .

Note that the base case load value is the expected value (mean value) of the load at the specific bus. Note also that the bus load is defined to be a dependent random variable by virtue of expressing it as a linear combination of the v_i 's.

The presented non-conforming load model assumes correlation between the various bus loads. However, the bus loads are not fully correlated, as it would be the case in a conventional conforming load model. This depicts a more realistic situation. If $v_i = 0$ for $i = 2, \dots, n$ then the above model becomes a simple conforming load. The load variations at every bus have the exact same statistics, imposed by the single random variable v_1 . If $n \geq 2$ then the above model becomes a non-conforming load model.

An additional assumption made in the load model is that the load at each bus k maintains a constant power factor; therefore the reactive power consumption at bus k is proportional to the active power consumption, which is a constant of proportionality a_k depending on the power factor:

$$Q_{dk} = a_k \cdot P_{dk}, \quad (7.2)$$

where:

Q_{dk} : Reactive power consumption (load) at bus k ,

P_{dk} : Active power consumption (load) at bus k ,

a_k : Proportionality constant.

More specifically, if the load at bus k has a power factor pf_k , then $a_k = \tan(\cos^{-1}(pf_k))$. Q_{dk} is therefore another dependent random variable depending linearly on v_i 's.

If the number of individual loads in the system is L , then we can represent the entire system active loading as a L -dimensional vector \vec{P}_d :

$$\vec{P}_d = \vec{P}_d^0 + \sum_{i=1}^n (v_i \cdot \vec{p}_d^i), \quad (7.3)$$

where:

\vec{P}_d : L -dimensional active load vector, $\vec{P}_d = [P_{dk}]$,

\vec{P}_d^0 : L -dimensional base case load vector, $\vec{P}_d^0 = [P_{dk}^0]$,

v_i : i^{th} random variable from the set of independent zero mean Gaussian distributed rv's,

\vec{p}_d^i : L -dimensional vector of participation coefficients of the i^{th} random variable v_i , $\vec{p}_d^i = [p_{dk}^i]$

Equations (7.3) can be rewritten in a more compact matrix form as:

$$\vec{P}_d = \vec{P}_d^0 + \vec{v} \cdot \vec{P}_d, \quad (7.4)$$

where:

\vec{P}_d : L -dimensional active load vector, $\vec{P}_d = [P_{dk}]$,

\vec{P}_d^0 : L -dimensional base case load vector, $\vec{P}_d^0 = [P_{dk}^0]$,

\vec{v} : n -dimensional vector of independent zero mean Gaussian distributed rv's v_i 's, $\vec{v} = [v_i]$,

\vec{P}_d : $n \times L$ matrix of participation coefficients, $\vec{P}_d = [p_{dk}^i]$, $i = 1, \dots, n$ and $k = 1, \dots, L$.

Based on the constant power factor assumption the reactive loading of the system can be represented as an L -dimensional vector \vec{Q}_d , so that

$$\vec{Q}_d = A \cdot \vec{P}_d, \quad (7.5)$$

where:

\vec{Q}_d : L -dimensional reactive load vector,

\vec{P}_d : L -dimensional active load vector,

A : $L \times L$ diagonal matrix of constants of proportionality, $A = \text{diag}(a_k)$ $k = 1, \dots, L$.

7.3.2 Probabilistic Generation Model

I. Introduction

The probabilistic nature of the load imposes variations to the total generation required by the system. This is mainly due to the variation of the demand, and to a lesser degree on changes in transmission losses. Therefore, the variations in transmission losses due to the load fluctuations are also another factor that needs to be considered. In order to deal with the random load variation from the generation viewpoint the following different approaches can be considered.

- a) The generation of each unit can be considered constant at its base case value. Therefore, the slack bus picks up all the required generation variation, in order to compensate for the load changes and the changes in losses. This approach is very simplified and quite unrealistic.
- b) The total change in load demand can be calculated as the sum of the change at each bus. Therefore, based on equation (7.4), for example, this is the sum of the L elements of the vector $\bar{v} \cdot \bar{P}_d$. Alternative and in more detail we can write:

$$\Delta P_d = \sum_{k=1}^L \sum_{i=1}^n P_{dk}^i \cdot v_i \quad (7.6)$$

using the quantities as defined in equation (7.1).

This is a sum of random variables, thus it is also a random variable, but dependent on v_i 's. Since the total change can be either positive or negative, we can define two such new random variables, called w^+ and w^- , one for load increase and one for load decrease. However, for any sample realization of the independent random variables, only one of these two variables is nonzero, since we can have either an increase in the demand compared to the expected demand or a decrease. Ignoring the changes in losses, this can be assumed the total generation change that needs to be dispatched between the units. This can be done, by assuming that each unit is dispatched an amount of the total change (increase or decrease) proportional to its participation factor, computed at the base case. The participation factor of each unit can be computed as a by-product of an economic dispatch algorithm at base case, for either increase or decrease in generation. For units operating in PQ mode, constant power factor operation is assumed. The advantage of this case is that there is an explicit and exact linear relation between the independent random variables v_i and the dependent random variables of the total generation change. More specifically it holds that:

$$w^+ - w^- = \sum_{k=1}^L \sum_{i=1}^n P_{dk}^i \cdot v_i \quad (7.7)$$

with $w^+, w^- \geq 0$ and $w^+ \cdot w^- = 0$.

However, the disadvantage is that this model ignores the dispatch of changes in losses, and therefore it is assumed that the slack bus is picking up all the losses.

- c) The total change in generation is considered to be the load change plus the change in losses. This is to be dispatched among the units of the system. The dispatch is performed assuming linearization and using the participation factors of each unit computed by an economic dispatch at base case. Again the units operating in PQ mode are assumed to work with constant power factor. This approach is very similar to the previous one, however, it assumes the changes in demand as well as the consequent changes in the losses. We can assume again two new dependent random variables for the required increase or decrease in generation, say w^+ and w^- respectively. Again, for any sample realization of the independent random variables, only one of these two variables is nonzero, since we can have either an increase in the demand compared to the expected demand or a decrease. Assuming that the losses can be expressed as a percentage of the load we can write:

$$\frac{w^+}{\gamma^+} - \frac{w^-}{\gamma^-} = \sum_{k=1}^L \sum_{i=1}^n p_{dk}^i \cdot v_i \quad (7.8)$$

with $w^+, w^- \geq 0$ and $w^+ \cdot w^- = 0$. Furthermore, $\gamma^+, \gamma^- \geq 1$.

This model includes the losses in the dispatch, however, it is more difficult to find a relation between the independent and the dependent random variables. This will be the model that will be mostly used in the rest of the work. Note that for $\gamma^+ = 1$ or $\gamma^- = 1$ we get the approach described in (b). This is the approach that will be used from now on in this report.

- d) The full economic dispatch problem is considered. In the two previous cases, a linearized generation dispatch was assumed based on participation factors. In this approach the full economic dispatch model is assumed. This provides the more accurate results, however, it seems to be impractical for theoretical probabilistic studies, because of its complexity. Furthermore, since an attempt to approach the probabilistic power flow problem via linearization is made, the previous approach is considered more than accurate, and no need to incorporate an economic dispatch algorithm is necessary. In addition, such a method would not result in significant improvement, since linearization would be applied to the problem anyway. Nevertheless, this method can be used in a Monte Carlo simulation approach, where all the nonlinearities are included in the calculations. Therefore, we will address the generation dispatch problem using full scale economic dispatch for validation purposes in a Monte Carlo approach.

II. Mathematical Details

In this section some more mathematical details on the generation model are presented, for the approaches discussed in the previous section.

a) *Deterministic generation model - Slack bus picks all variations*

If it is assumed that the slack bus will pick all the load variations then no additional random variables are introduced and no additional equations are necessary. A new load flow will adjust the output of the slack bus so that there is a total power balance in the system. Furthermore, the same assumption will hold for the linearization procedure and the computed values of the sensitivities will implicitly have the information that the slack bus takes all the variations. We can assume that this method will provide some valid first approximation.

b) Probabilistic generation model - Load demand is dispatched linearly, slack bus picks variations in losses

Based on the nonconforming load model described in section 2 the electric load at each system bus is given by equations (7.1) and (7.2). The generation of each unit is adjusted to the load changes based on its participation factor. For units on PQ operation mode a constant power factor assumption is made. The total change in generation that is to be dispatched among the units is set equal to the total change in load, thus by equation (7.6) we have:

$$\Delta P_g = \sum_{k=1}^L \sum_{i=1}^n P_{dk}^i \cdot v_i \quad (7.9)$$

This quantity is a random variable (not independent though since it depends on the v_i 's) and it can get either a positive or negative values. To distinguish between the two cases we assume two different rv's one for each case, therefore we have w^+ and w^- . The distinction is necessary since we will assume a linearized unit dispatch and the participation factors for increase and decrease in load are in general different for each unit, especially if for example a unit is operating close to its limits or at its limits. At each time one of w^+ or w^- is nonzero, therefore it holds that:

$$w^+ \cdot w^- = 0 \quad (7.10)$$

and in addition:

$$w^+, w^- \geq 0 \quad (7.11)$$

Thus the active power generation of each unit k is given by:

$$P_{gk} = P_{gk}^0 + p_{gk}^+ w^+ - p_{gk}^- w^- \quad (7.12)$$

where:

P_{gk} : The new active power production of unit k ;

P_{gk}^0 : The base case active power production of unit k ;

p_{gk}^+ : The participation factor of unit k for a total demand increase;

p_{gk}^- : The participation factor of unit k for a total demand decrease;

w^+ : The dependent random variable of total demand increase;
 w^- : The dependent random variable of total demand decrease.

In addition we can write equation (7.7) as:

$$w^+ - w^- = \sum_{k=1}^L \sum_{i=1}^n p_{dk}^i \cdot v_i \quad (7.13)$$

since (7.10) holds and this introduces a linear relation between the independent and the dependent random variables. This relation can be simplified by combining the coefficients corresponding to the same random variables.

$$w^+ - w^- = \sum_{i=1}^n \theta_i \cdot v_i \quad (7.14)$$

where $\theta_i = \sum_{k=1}^L p_{dk}^i$, L being the total number of loads.

For the generated reactive power of units operating in PQ mode, we assume that the power factor is constant, therefore the change in their reactive production is proportional to the change the active power production so that the power factor is kept constant.

The additional losses (or the decrease in losses) introduced by the load change are assumed to be picked up by the slack bus. Thus the slack bus picks up some additional load and all the additional losses. This is quite unrealistic, however, it can be considered as a valid assumption.

c) Probabilistic generation model - Load demand and losses are dispatched linearly

In this approach the same concepts as in the previous one apply, with the exception that losses are also considered in the generation dispatch. Based on the nonconforming load model described in section 2 the electric load at each system bus is given by equations (7.1) and (7.2). Therefore, the total change in generation is now given by:

$$\frac{w^+}{\gamma^+} - \frac{w^-}{\gamma^-} = \sum_{k=1}^L \sum_{i=1}^n p_{dk}^i \cdot v_i = \sum_{i=1}^n \theta_i \cdot v_i \quad (7.15)$$

where $\theta_i = \sum_{k=1}^L p_{dk}^i$, L being the total number of loads, and $\gamma^+, \gamma^- \geq 1$.

The generation of each unit is adjusted to the load and losses changes based on its participation factor. Therefore the active power generation of each unit is given by:

$$P_{gk} = P_{gk}^0 + p_{gk}^+ w^+ - p_{gk}^- w^- \quad (7.16)$$

where:

P_{gk} : The new active power production of unit k ;

P_{gk}^0 : The base case active power production of unit k ;

p_{gk}^+ : The participation factor of unit k for a net total demand increase;

p_{gk}^- : The participation factor of unit k for a net total demand decrease;

w^+ : The dependent random variable of net total demand increase (load + losses);

w^- : The dependent random variable of net total demand decrease (load + losses).

Note that in every case one of either w^+ or w^- will be zero, since the demand will either increase or decrease. Therefore:

$$w^+ w^- = 0. \quad (7.17)$$

w^+ and w^- are random variables that depend on the independent random variables v_i 's and the relation between them is rather complicated, since w^+ and w^- also include changes in system losses. Equation (7.15) does not practically provide this relation since the parameters γ^+ and γ^- are unknown.

For the generated reactive power of units operating in PQ mode, we assume that the power factor is constant, therefore the change in their reactive production is proportional to the change the active power production so that the power factor is kept constant.

In order to simply identify a relation between w^+ , w^- and v_i 's (γ^+ and γ^- in equation 7.15 are unknown) let's assume for a moment that there is a fictitious generator located at bus *fict.*. In this case it holds from the power balance equation that:

$$P_{g,fict.} = \sum_{lines(fict.)} P_{line} + \sum_{loads(fict.)} P_{load} - \sum_{gen(fict.)} P_{gen}, \quad (7.18)$$

where:

$P_{g,fict.}$: The power produced by the fictitious generator;

P_{line} : The line flow for each line connected to the fictitious generator bus;

P_{load} : The demand of each load connected to the fictitious generator bus;

P_{gen} : The active power production of each generator connected to the fictitious generator bus;

$lines(fict.)$: The set of lines connected to the fictitious generator bus;

$loads(fict.)$: The set of loads connected to the fictitious generator bus;

$gen(fict.)$: The set of generators connected to the fictitious generator bus.

Equation (7.18) can be linearized with respect to the random variables introduced in the problem. The loads are by definition linear functions of the introduced independent

random variables. The line flows and the generator outputs can also be expressed as linearized functions of the rv's, using the costate method. The method for doing that will be presented in the following sections. However, it should be mentioned that it is preferable to assume a fictitious generator at a bus that does not have any other generators connected, or even at a bus without any loads, since this will simplify the problem considerably. For now let's assume that $P_{g,fict.}$ can be written as:

$$P_{g,fict.} = \sum_{i=1}^n a_i v_i + b^+ w^+ + b^- w^- \quad (7.19)$$

where:

$P_{g,fict.}$: The power produced by the fictitious generator;

v_i : i^{th} random variable from the set of independent zero mean Gaussian distributed rv's;

w^+ : The dependent random variable of net total demand increase (load + losses);

w^- : The dependent random variable of net total demand decrease (load + losses),

and $a_i = \frac{dP_{g,fict.}}{dv_i}$, $b^+ = \frac{dP_{g,fict.}}{dw^+}$, $b^- = \frac{dP_{g,fict.}}{dw^-}$.

However, since $P_{g,fict.}$ is in fact produced by a fictitious generator we want it to be equal to zero. Therefore, setting $P_{g,fict.} = 0$ we get the desired relation between the independent random variables v_i 's and the dependent w^+ and w^- :

$$0 = \sum_{i=1}^n a_i v_i + b^+ w^+ + b^- w^- . \quad (7.20)$$

7.3.3 Transmission System Model

The network quantities (circuit currents, power flows or bus voltages) are also treated as random variables that depend on the stochastic load variables, v_i 's. Linear dependence is assumed for small deviations around a base case operating point, and therefore the circuit currents and flows as well as the bus voltages are linearized with respect to the probabilistic control variables. The derived linear functions are used for the calculation of the statistical properties of each quantity.

More specifically, a network quantity F (i.e., a line current, power flow or a bus voltage) is expressed as a linear combination of the load random variables as:

$$F = F^0 + \sum_{i=1}^n (c_i \Delta v_i), \quad (7.21)$$

where

F^0 : Base case value of F ;

c_i : Linearization coefficient of quantity F with respect to v_i .

Based on equation (7.21) and since v_i 's are independent random variables the statistics of the quantity F can be derived from the statistics of the load random variables by simply performing a series of convolutions on the probability density functions of v_i 's.

The values of the linearization coefficients are obtained by calculating the corresponding sensitivities from the network equations. This is done using the costate method described in the Appendix. It should be noted that the network quantities are linearized only with respect to the probabilistic load variables, not with respect to the system state variables. Therefore, full AC system model is used to model the power system under study and no approximations or simplifications are made. Each system component is modeled using the quadratized power flow model, which is a full scale AC model that incorporates all the nonlinearities. Then the quadratic power flow equations of the system are constructed and solved at base case. The linearization coefficients are computed around the base case operating point taking into account the system of quadratic power flow equations.

7.4 Example Results

This section presents example results obtained with the proposed methodologies.

7.4.1 System Description

The proposed method has been applied to the IEEE 24-Bus Reliability Test System (RTS-24), illustrated in Figure 7.2. The system is assumed to be operating at peak loading at base case, the detailed system data for each system component can be found in [24]. The nonconforming load model consists of two zero mean stochastic load variables namely v_1 and v_2 . Therefore, each bus load is expressed as a linear function of these two random variables, i.e.,

$$P_{dk} = P_{dk}^0 + p_{dk}^1 \cdot v_1 + p_{dk}^2 \cdot v_2 \quad (7.22)$$

where

P_{dk} : Active power demand (load) at bus k ;

P_{dk}^0 : Base case load value at bus k ;

p_{dk}^1 : Participation coefficient for the first random variable;

p_{dk}^2 : Participation coefficient for the second random variable.

The random load variables are assumed to be uniformly distributed in the interval $[-1.0, 1.0]$ or normally distributed with zero mean and variance of 0.1.

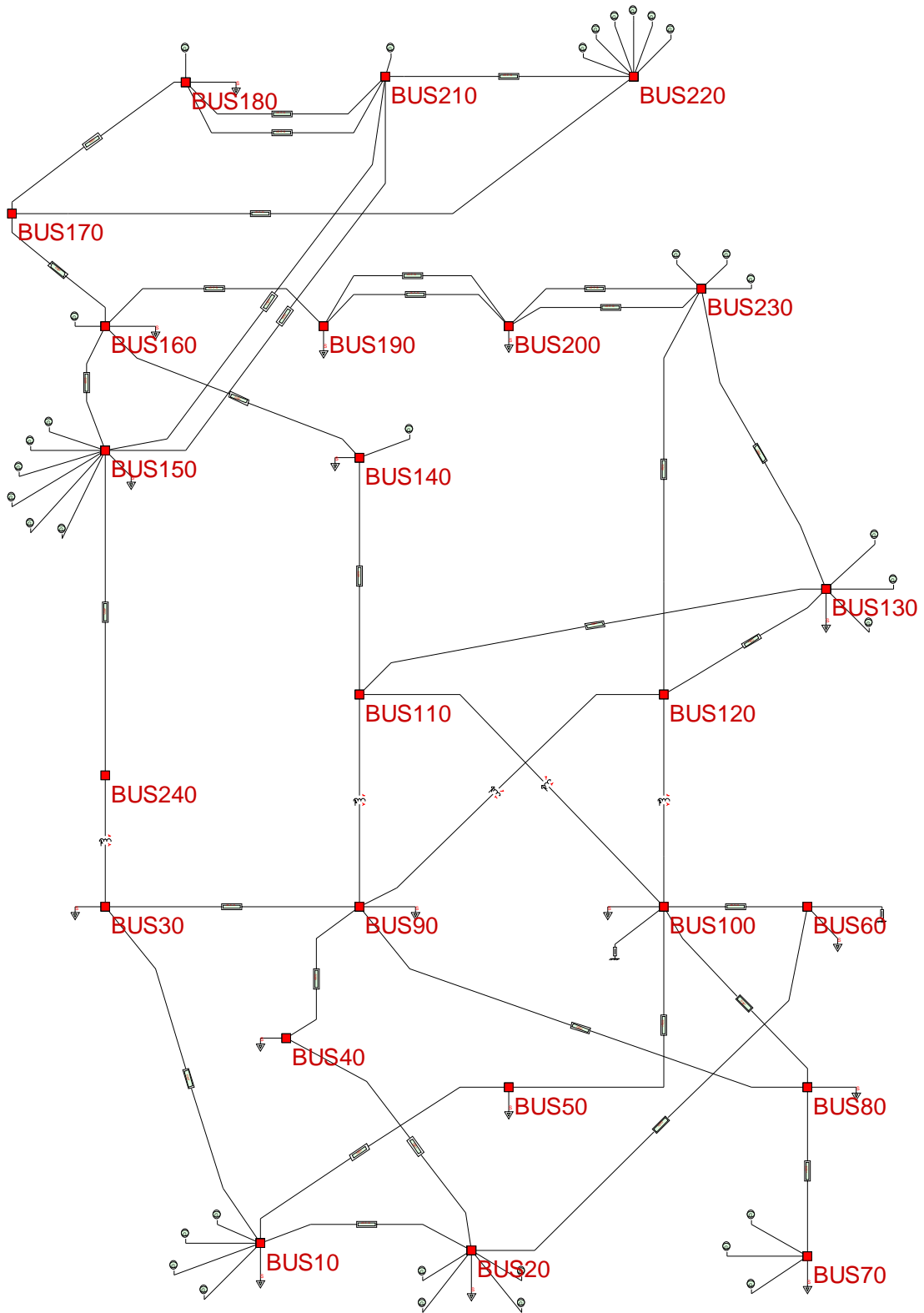


Figure 7.2. The IEEE 24-bus reliability test system.

7.4.2 Numerical Results

Initially the base case is solved and network quantities under study are linearized with respect to the two random variables, around the base case operating point. Subsequently their distributions are calculated using these linearized expressions. The results are also validated via Monte Carlo simulations. Ten thousand trials are simulated in order to obtain an adequate level of accuracy. Some typical results assuming Gaussian distribution are presented in Figures 7.3 through 7.6. Tables 7.1 and 7.2 show a comparison of the mean value and the standard deviation for several network quantities, as calculated using the proposed approach and using the Monte Carlo simulation results. Note a very close agreement between the results.

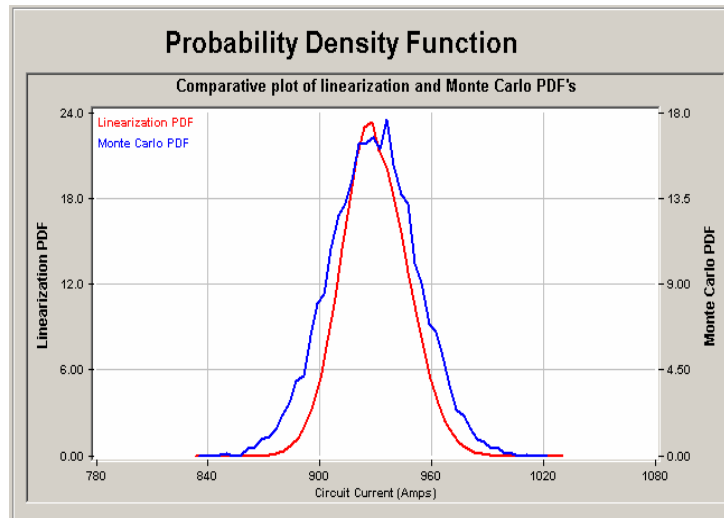


Figure 7.3. Comparison of proposed method and Monte Carlo simulation results; probability density function of circuit 140-160 current assuming Gaussian distributions.

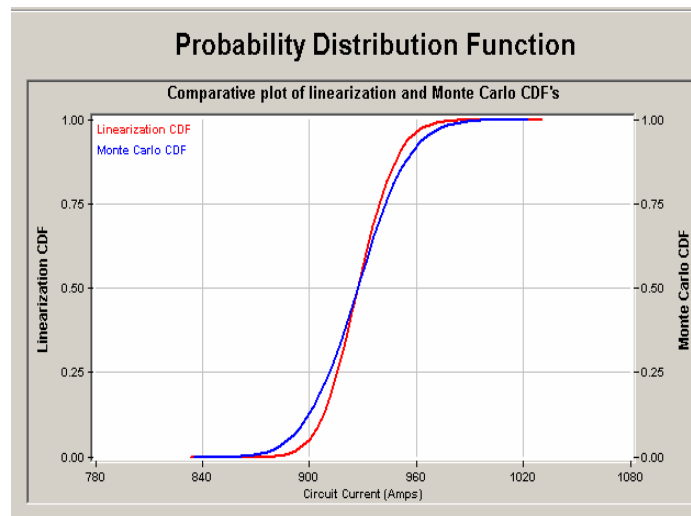


Figure 7.4. Comparison of proposed method and Monte Carlo simulation results; cumulative probability function of circuit 140-160 current assuming Gaussian distributions.

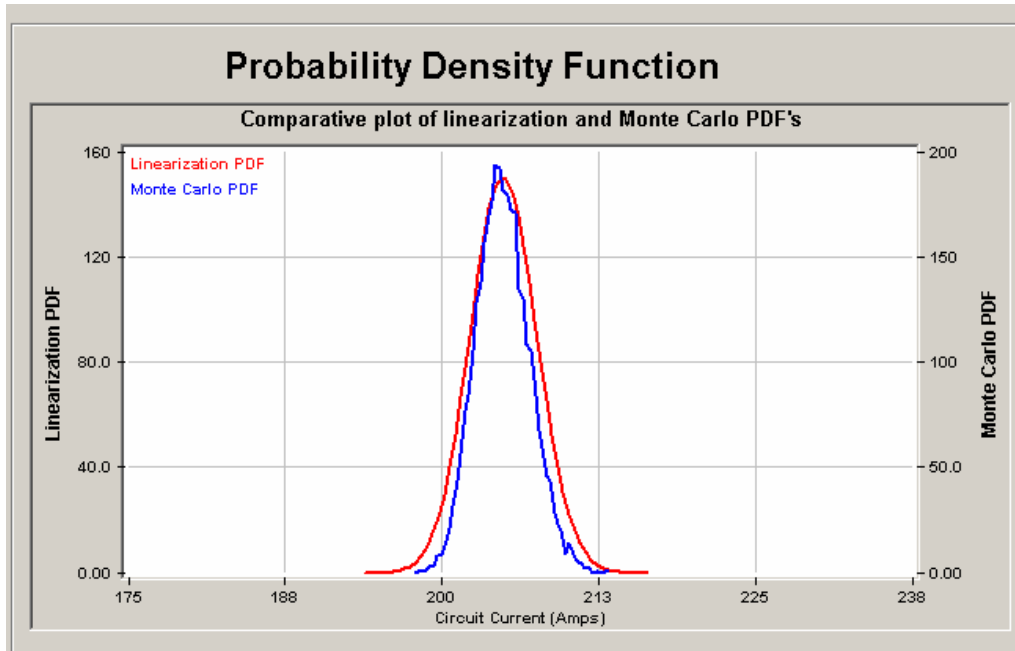


Figure 7.5. Comparison of proposed method and Monte Carlo simulation results; probability density function of circuit 10-20 current assuming Gaussian distributions.

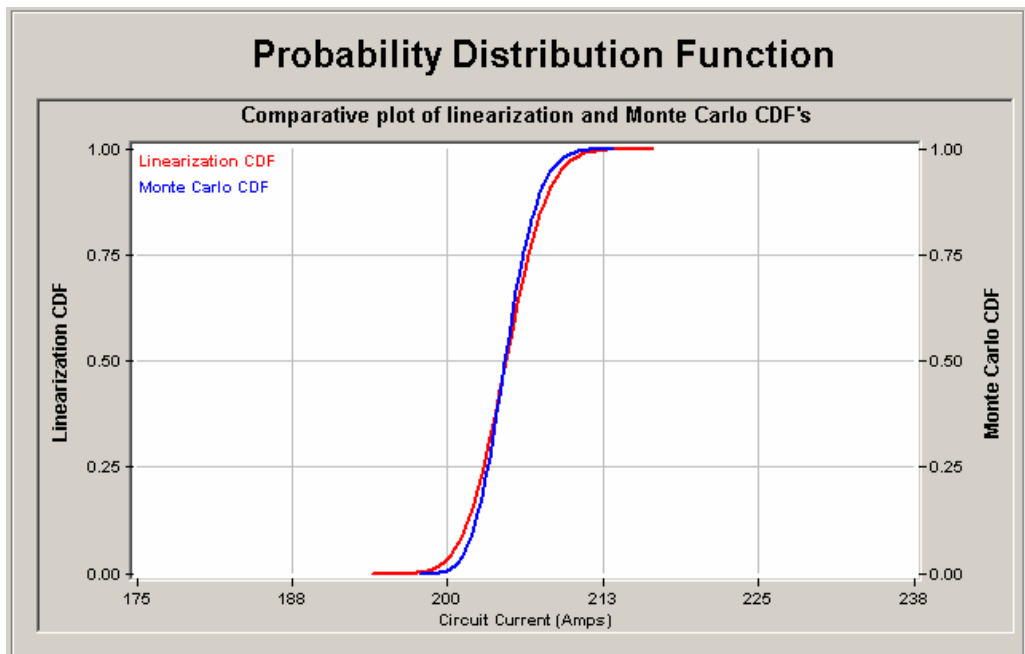


Figure 7.6. Comparison of proposed method and Monte Carlo simulation results; cumulative probability function of circuit 10-20 current assuming Gaussian distributions.

Table 7.1. Comparison of proposed method and Monte Carlo simulation results for voltage magnitude assuming Gaussian distribution.

| Bus | Proposed Method | | Monte Carlo | |
|-----|-----------------|----------------|-------------|----------------|
| | Mean (kV) | Std. Dev. (kV) | Mean (kV) | Std. Dev. (kV) |
| 40 | 135.09 | 0.29 | 135.06 | 0.24 |
| 50 | 137.30 | 0.32 | 137.26 | 0.26 |
| 100 | 140.18 | 0.38 | 140.13 | 0.32 |
| 110 | 237.22 | 0.37 | 237.18 | 0.35 |
| 190 | 229.54 | 0.07 | 229.55 | 0.07 |
| 200 | 231.01 | 0.04 | 231.02 | 0.05 |

Table 7.2. Comparison of proposed method and Monte Carlo simulation results for circuit currents assuming Gaussian distribution.

| Circuit | Proposed Method | | Monte Carlo | |
|---------|-----------------|---------------|-------------|---------------|
| | Mean (A) | Std. Dev. (A) | Mean (A) | Std. Dev. (A) |
| 10-20 | 204.87 | 2.15 | 204.79 | 2.12 |
| 20-40 | 179.02 | 13.16 | 180.72 | 8.96 |
| 10-30 | 50.37 | 3.47 | 49.98 | 5.51 |
| 60-100 | 1434.60 | 4.90 | 1433.72 | 4.86 |
| 140-160 | 929.22 | 17.51 | 928.42 | 23.64 |
| 150-160 | 284.79 | 27.52 | 280.02 | 27.79 |

Figures 7.7 through 7.10 present results of the same system assuming uniform distribution in the interval [-1.0,1.0] for the load random variables. Table 7.3 also shows a comparison of the mean values and the standard deviations, for uniform distributions. Note again the close agreement between the results.

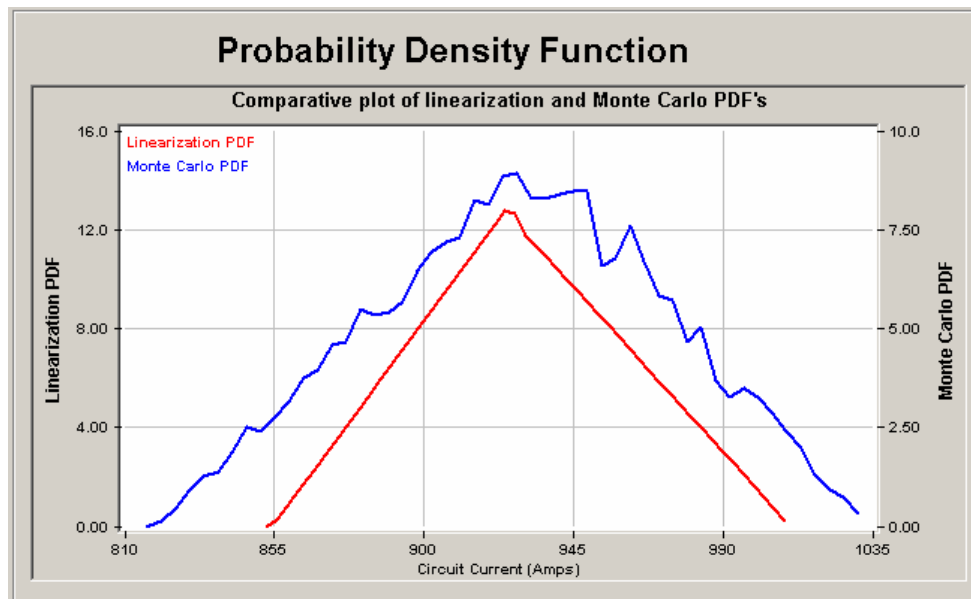


Figure 7.7. Comparison of proposed method and Monte Carlo simulation results; probability density function of circuit 140-160 current assuming uniform distributions.

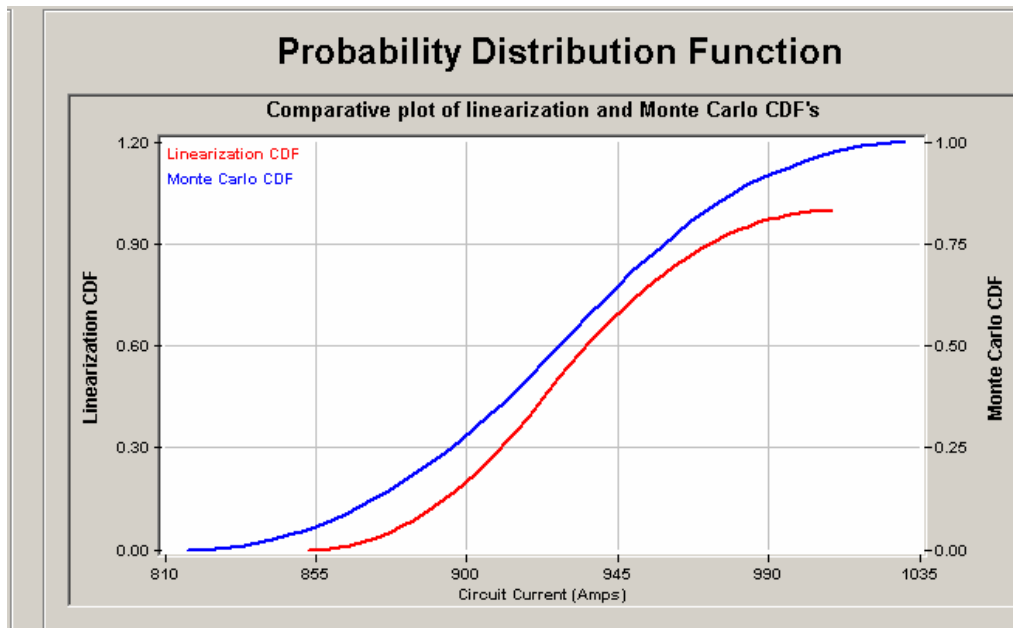


Figure 7.8. Comparison of proposed method and Monte Carlo simulation results; cumulative probability function of circuit 140-160 current assuming uniform distributions.

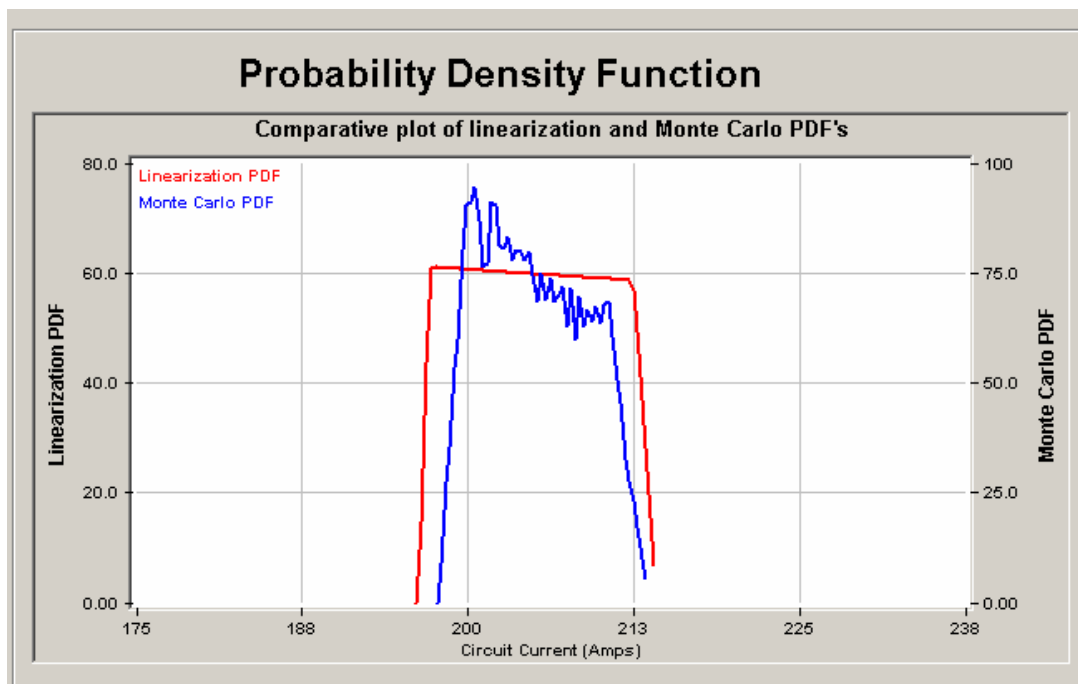


Figure 7.9. Comparison of proposed method and Monte Carlo simulation results; probability density function of circuit 10-20 current assuming uniform distributions.

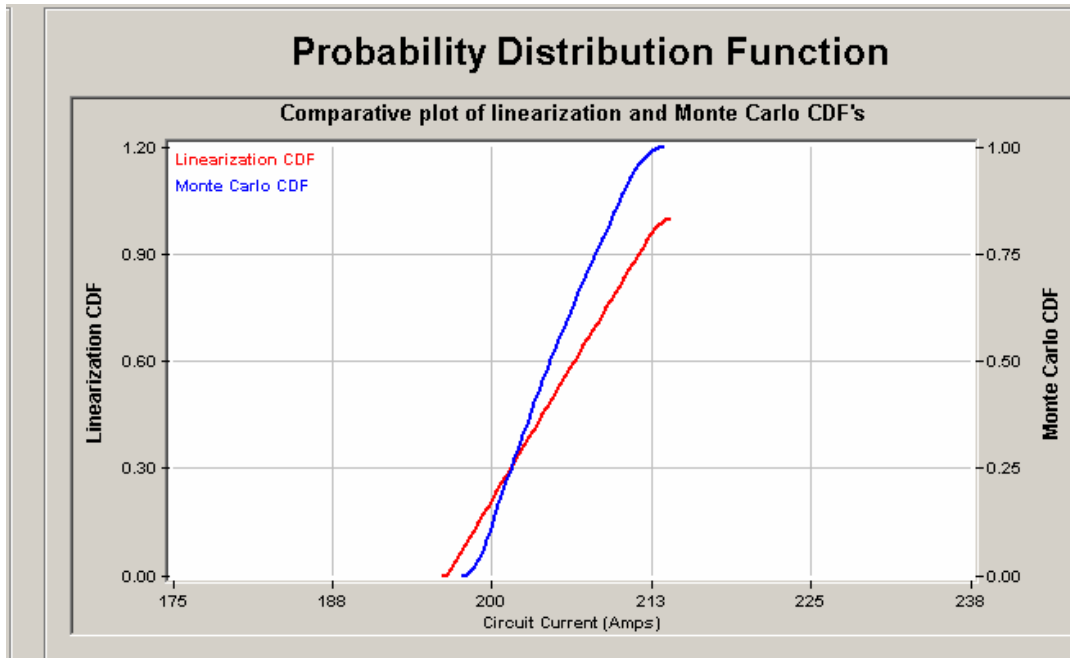


Figure 7.10. Comparison of proposed method and Monte Carlo simulation results; cumulative probability function of circuit 10-20 current assuming uniform distributions.

Table 7.3. Comparison of proposed method and Monte Carlo simulation results for circuit currents assuming uniform distribution.

| Circuit | Proposed Method | | Monte Carlo | |
|---------|-----------------|---------------|-------------|---------------|
| | Mean (A) | Std. Dev. (A) | Mean (A) | Std. Dev. (A) |
| 10-20 | 204.90 | 4.83 | 204.94 | 3.91 |
| 10-30 | 50.86 | 6.32 | 50.61 | 10.28 |
| 60-100 | 1435.39 | 8.92 | 1435.11 | 9.07 |
| 150-160 | 287.74 | 50.15 | 280.81 | 51.54 |

7.5 Stochastic Power Flow via Multi-Point-Linearization

The proposed stochastic load flow methodology can be further developed and improved. Examples of areas that need to be addressed are: (a) congestion management, and (b) effects of possible contingencies. Both of these issues can be addressed with multiple linearizations. Specifically, the non-conforming load can be sectionalized into a small number of segments, for example five. Then a linearized system model is constructed around the expected value of the electric load of each load segment. The proposed methodology of this paper will be applied to each of these models and the results will be combined. Note that at each expected value of a load segment, congestion management can be applied, as well as the effect of possible contingencies can be accounted. Other operating practices can be easily incorporated, as well.

In the previous section, the linearized model was computed around the expected value of the electric load. This approach is not very accurate because the validity of the linearized model is confined within a small neighborhood of the electric load model around the linearization point. To further improve on the accuracy of the proposed method the non-conforming load model (described in section 7.3) can be sectionalized into a small number of segments as it is depicted in Figure 7.11. A specific combination of a segment from each variable defines an electric load event. Such an event ε_i is illustrated in Figure 7.11. We then consider the conditional probability of the electric load given that the electric load belongs to the electric load event ε_i . Subsequently, we consider the conditional expected value of the electric load given that the load belongs to event ε_i . The operating conditions of the system at the conditional expected value are determined by simulation of the electric power network. Then the linearized model of the system is computed around this operating point. Finally, the conditional (given event ε_i) performance of the system in terms of distributions of bus voltage magnitudes, circuit flows and total operating cost are derived from the linearized model and the known conditional electric load model. The procedure is applied to all possible electric load events and the results are weighted with the probabilities of the electric load events and summarized into an overall probabilistic model. It is important to note that at each expected value of a load event congestion management or any other type of remedial actions can be applied, if necessary, as well as the effect of possible contingencies can be accounted for.

The basis of this idea is depicted in Figure 7.11. Three stochastic load variables are assumed, namely v_1 , v_2 and v_3 following some probability distribution in the interval [a,b]. This interval is divided into three sections, and the expected value of each load random variable is calculated in each section. The triplet of such expected values of each load variables defines a specific load profile and therefore a base case operating point. Furthermore, a triplet of such sections, one for each variable, defines a possible event, i.e., event ε of Figure 7.11 is defined as:

$$\varepsilon_i = \{v_1 \in (c_2, b) \cap v_2 \in (c_1, c_2) \cap v_3 \in (c_1, c_2)\} \quad (7.23)$$

For each electric load event, the base case conditions of the electric power network are computed as well as the linearized model around the base case conditions. These procedures are described in the next section.

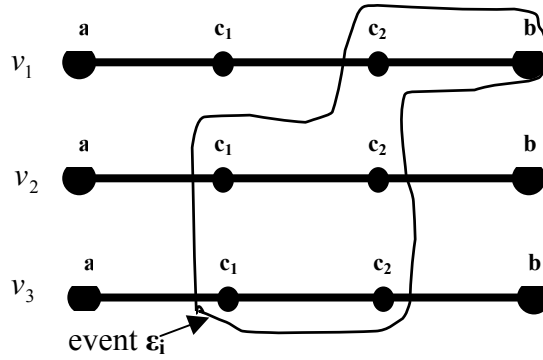


Figure 7.11. Schematic representation of non-conforming load sectionalization.

Furthermore an improved linearization approach that can also incorporate congestion management or any other major operating practice is used around each one of the defined base-case operating points. The model is based on the economic dispatch operation.

The problem of allocating the power output of each generating unit in a power system is known as economic dispatch problem. Each unit i has a cost function f_i depending on the active power output P_{gi} . f_i is usually a quadratic function of P_{gi} . The purpose of economic dispatch is to allocate the active output of each unit, minimizing the total cost. This is a non-linear constrained minimization problem, since the total load demand needs to be satisfied, the unit limits need to be obeyed and the network equations need to be taken into consideration. Furthermore, additional network constraint may need to be satisfied to deal with issues such as congestion management. If all these constraints are taken into account the problem is referred to as the constrained optimal power flow problem. In mathematical terms the problem is stated as follows:

$$\text{Min} \sum_{i=1}^M f_i(P_{gi}) \quad (7.24)$$

subject to :

$$G(x, u, p, P_g, v) = 0 \quad (7.25)$$

$$\sum_{k=1}^n \sum_{i=1}^L p_{dk}^i v_k - P_{total} = 0 \quad (7.26)$$

$$\sum_{i=1}^M P_{gi} - w = 0 \quad (7.27)$$

$$P_{gi, \min} \leq P_{gi} \leq P_{gi, \max}, \quad i = 1, \dots, M \quad (7.28)$$

$$V_{k, \min} \leq |V_k| \leq V_{k, \max}, \quad k = 1, \dots, Z \quad (7.29)$$

$$|T_j| \leq T_{j, \max}, \quad j = 1, \dots, R \quad (7.30)$$

where:

- M : Number of generating units
- n : Number of stochastic load variables used
- L : Number of bus loads
- Z : Number of buses
- R : Number of circuits
- x : State vector of power flow equations (Nx1)
- p : Vector of system parameters
- u : Vector of remedial action controls
- P_g : Vector of generating unit active power output (Mx1)
- v : Vector of stochastic load variables (nx1)
- P_{dk}^i : Load variable coefficient for load i and variable k
- P_{total} : Total active load
- w : Total active generation
- $P_{gi,min}$: Minimum active power output for unit i
- $P_{gi,max}$: Maximum active power output for unit i
- $V_{k,min}$: Minimum acceptable bus voltage level at bus k
- $V_{k,max}$: Maximum acceptable voltage level at bus k
- $T_{j,max}$: Maximum apparent power flow at circuit j
- $|V_k|$: Voltage magnitude at bus k
- $|T_j|$: Apparent power flow at circuit j

Equation (7.25) represents the set of the network quadratic power flow equations. Equations (7.26) and (7.27) are scalar equations defining the total system load and the total system generation. Relations (7.28) through (7.30) are network operating inequality constraints that deal with unit limits, voltage constraints and line congestion constraints. The remedial actions may involve a variety of system adjustments as those listed in Table 7.4.

Table 7.4. List of congestion management actions.

| | Congestion Management Action | Relative Cost |
|----|------------------------------|---------------|
| 1 | Shunt Capacitor Switching | Low |
| 2 | Shunt Reactor Switching | Low |
| 3 | Phase Shifter Adjustment | Low |
| 4 | MVAR Generation Adjustment | Low |
| 5 | Generation Bus Voltage | Low |
| 6 | Transformer Taps | Low |
| 7 | FACTS Controls | Low |
| 8 | Load Transfer | Low |
| 10 | Area Interchange | High |
| 11 | Interruptible Load | High |
| 12 | Firm Load | High |
| 13 | Critical Load | High |

The economic dispatch problem, or more general the optimal power flow problem, is a well known power system problem. Several well known solution methodologies have been applied to this problem, including (a) successive linear programming, (b) reduced gradient method, (c) Lagrange multipliers in combination with Kuhn-Tucker conditions, and (d) interior point methods. A good review of these methodologies can be found in [25] and [26].

In this work we assume that the problem is solved, using any of the methods mentioned, at any of the base cases described. Then we will use linearization around each base case operating point to express any quantity as a linear function of the probabilistic control variables. The idea is that since the segments of the v_i 's are relatively small, the linearized model will be relatively accurate within each segment.

Assume that the optimal power flow problem is solved at the base case condition. Then if the Lagrangian multipliers method is assumed the necessary optimality conditions are satisfied at the solution. For the application of the Lagrangian multiplier method the inequality constraints (7.28) through (7.30) are replaced with equality constraints by introducing slack variables:

$$P_{gi} + s_{i,sl.} - P_{gi,max} = 0, \quad i = 1, \dots, M \quad (7.31)$$

$$P_{gi} - s_{i,sur.} - P_{gi,min} = 0, \quad i = 1, \dots, M \quad (7.32)$$

$$|V_k| + V_{k,b} - V_{k,max} = 0, \quad k = 1, \dots, Z \quad (7.33)$$

$$|V_k| - V_{k,a} - V_{k,max} = 0, \quad k = 1, \dots, Z \quad (7.34)$$

$$|T_j| - q_j - T_{j,max} = 0, \quad j = 1, \dots, R \quad (7.35)$$

with the additional non-negativity constraints:

$$s_{i,sl.} \geq 0, \quad i = 1, \dots, M \quad (7.36)$$

$$s_{i,sur.} \geq 0, \quad i = 1, \dots, M \quad (7.37)$$

$$V_{k,b} \geq 0, \quad k = 1, \dots, Z \quad (7.38)$$

$$V_{k,a} \geq 0, \quad k = 1, \dots, Z \quad (7.39)$$

$$q_j \geq 0, \quad j = 1, \dots, R \quad (7.40)$$

$s_{i,sl.}$, $s_{i,sur.}$, $V_{k,b}$, $V_{k,a}$, q_j are new variables that are introduced in order to transform the inequality constraints to equality constraints (slack variables). The Lagrangian of the problem is:

$$\begin{aligned}
L = & \sum_{i=1}^M f_i(P_{gi}) - \lambda^T \cdot G(x, p, P_g, v) \\
& - \rho \cdot \left(\sum_{k=1}^n \sum_{i=1}^L P_{dk}^i v_k - P_{total} \right) - \sigma \cdot \left(\sum_{i=1}^M P_{gi} - w \right) \\
& - \sum_{i=1}^M \mu_{i,sl.} (P_{gi} + s_{i,sl.} - P_{gi,max}) \\
& - \sum_{i=1}^M \mu_{i,sur.} (P_{gi} - s_{i,sl.} - P_{gi,min}) \\
& - \sum_{k=1}^Z \beta_{k,b} (|V_k| + V_{k,b} - V_{k,max}) \\
& - \sum_{k=1}^Z \beta_{k,a} (|V_k| - V_{k,a} - V_{k,max}) \\
& - \sum_{j=1}^R \vartheta_j (|T_j| - q_j - T_{j,max})
\end{aligned} \tag{7.41}$$

where vector λ^T , ρ , σ , $\mu_{i,sl.}$'s, $\mu_{i,sur.}$'s, $\beta_{k,b}$'s, $\beta_{k,a}$'s and ϑ_j 's are the Lagrangian multipliers.

The necessary conditions for optimality are obtained by setting the partial derivatives of the Lagrangian with respect to all the unknowns and the Lagrangian multipliers equal to zero. After performing the differentiations and reordering the terms we get the set of necessary conditions:

$$G(x, p, P_g, v) = 0 \tag{7.42}$$

$$\frac{\partial f_i}{\partial P_{gi}} - \lambda^T \frac{\partial G}{\partial P_{gi}} - \sigma - \mu_{i,sl.} - \mu_{i,sur.} = 0 \tag{7.43}$$

for $i = 1, \dots, M$

$$\sum_{k=1}^n \sum_{i=1}^L P_{dk}^i v_k - P_{total} = 0 \tag{7.44}$$

$$\sum_{i=1}^M P_{gi} - w = 0 \tag{7.45}$$

$$P_{gi} + s_{i,sl.} - P_{gi,max} = 0, \quad i = 1, \dots, M \tag{7.46}$$

$$P_{gi} - s_{i,sur.} - P_{gi,min} = 0, \quad i = 1, \dots, M \tag{7.47}$$

$$|V_k| + V_{k,b} - V_{k,max} = 0, \quad k = 1, \dots, Z \tag{7.48}$$

$$|V_k| - V_{k,a} - V_{k,max} = 0, \quad k = 1, \dots, Z \tag{7.49}$$

$$|T_j| - q_j - T_{j,max} = 0, \quad j = 1, \dots, R \tag{7.50}$$

$$\rho = 0 \tag{7.51}$$

$$\sigma = 0 \tag{7.52}$$

$$\mu_{i,sl.} = 0, i = 1, \dots, M \quad (7.53)$$

$$\mu_{i,sur.} = 0, i = 1, \dots, M \quad (7.54)$$

$$\beta_{k,b} = 0, k = 1, \dots, Z \quad (7.55)$$

$$\beta_{k,a} = 0, k = 1, \dots, Z \quad (7.56)$$

$$\vartheta_j = 0, j = 1, \dots, R \quad (7.57)$$

The non-negativity constraints, (7.36) to (7.40) are also appended to the above set of equations.

The optimality conditions are subsequently linearized around the solution with respect to the unknown variables of the optimal power flow problem. If the unknown vector is called \vec{y} the optimal solution is \vec{y}^* then for sufficiently small perturbations of \vec{y} around \vec{y}^* , $\Delta\vec{y} = \vec{y} - \vec{y}^*$ the linearized model of (7.58) should be valid.

$$A \cdot \Delta\vec{y} = B \cdot \Delta v \quad (7.58)$$

where:

A is an $m \times m$ matrix of linearization coefficients, with m being the number of unknown variables,

$\Delta\vec{y}$ is an $m \times 1$ perturbation vector of the solution,

Δv is the deviation vector of the n stochastic load variables, which are the inputs to the model,

B is an $m \times n$ matrix of stochastic load variable coefficients.

Equation (7.58) is obtained by reordering the terms of the linearized equations and moving the terms of the input variables to the right hand side of the equation.

Equation (7.58) can be re-written in the form

$$\Delta\vec{y} = C \cdot \Delta v \quad (7.59)$$

assuming that A is invertible. This equation allows the computation the each generating unit power output, as well as of any other system quantity, for small perturbations of the stochastic load variables around their base case values.

Note that this generation scheduling observes the economic dispatch operation, as well as network constraints and congestion constraints. If some equation of (7.59) results in a violation of a non-negativity constraint, then this equation is replaced by the one with the variable that violated the constraint set to zero. The rest of the equations remain unchanged and $\Delta\vec{y}$ is recalculated based on the new model. Therefore, any constraint violation, such as generator overloading or occurrence of line congestion is immediately taken into consideration. The methodology is also applicable to any other additional operating constraints that may be of interest.

In the case of a generation limit constraint violation then the output of the violating unit can be set to the bound value, making thus a model switching, and (7.59) can be resolved. However, if a transmission system operational constraint is violated, like for example there is congestion on a line or over or under voltage at a bus special congestion management actions or remedial actions in general should be performed to bring the system back to an acceptable state.

The transmission system quantities, like circuit currents and power flows as well as bus voltages are linearized with respect to the stochastic load variables based on the described linearization model. The procedure for calculating their statistic, after the linearized models are constructed around each operating point is quite straightforward and is similar to the one described in section 7.3.

8. Example of Overall Reliability Evaluation

This section presents an example of overall reliability evaluation with the proposed methodology. The example test system is the IEEE RTS 24 bus system. The results are presented in a step by step process to illustrate the steps of the computations.

The IEEE RTS 24 bus system has been described elsewhere in the report. For this system three basic reliability indices are computed for varying level of contingencies, i.e., first level and second level.

Table 8.1 illustrates the three basic reliability indices as computed at the end of the first level contingency evaluation. Table 8.3 illustrates the first level unit contingencies (independent) and the effects analysis results. Note that only one unit contingency required remedial actions. Table 8.4 illustrates the first level circuit contingencies (independent) and the effects analysis results. Note that several circuit contingencies required remedial actions. Finally, Table 8.5 illustrates the first level common mode outages and the effects analysis results. Note that some required remedial actions including load shedding. Table 8.1 summarizes the results. Note also that two computational algorithms have been utilized. One that applies remedial actions to determine whether the system is adequate to serve the load. The other algorithm does not apply remedial actions – in this case if the analysis shows no solution, it is counted as a “failure”. The reliability indices with remedial actions are much lower than those without remedial actions.

Table 8.2 illustrates the three basic reliability indices as computed at the end of the second level contingency evaluation. Tables 8.6, 8.7, 8.8, 8.9, 8.10, 8.11, 8.12 and 8.13 illustrate examples of second level contingencies (independent and common mode) and the effects analysis results. Note that each table illustrates one node of the wind-chime scheme. One should notice the increased complexity of the enumeration scheme as it moves to the second level. Table 8.2 summarizes the results. Note also that two computational algorithms have been utilized. One that applies remedial actions to determine whether the system is adequate to serve the load. The other algorithm does not apply remedial actions – in this case if the analysis shows no solution, it is counted as a “failure”. The reliability indices with remedial actions are much lower than those without remedial actions.

Table 8.1. Reliability indices of IEEE-RTS (first level and common mode contingencies).

| | With RAs | Without RAs |
|-----------------------------|--------------------|--------------------|
| Service Failure Probability | 0.0016 | 0.0121 |
| Service Failure Frequency | 0.5440 (per year) | 2.616 (per year) |
| Service Failure Duration | 26.5112 (hrs/year) | 40.5978 (hrs/year) |

Table 8.2. Reliability indices of IEEE-RTS (first level, second level and common mode contingencies).

| | With RAs | Without RAs |
|-----------------------------|--------------------|--------------------|
| Service Failure Probability | 0.0049 | 0.0296 |
| Service Failure Frequency | 1.4011 (per year) | 6.0733 (per year) |
| Service Failure Duration | 30.4086 (hrs/year) | 42.7154 (hrs/year) |

Table 8.3. Table of first level generator unit outages.

| Unit No. | Outage Components | Constraints Violations (Yes/No) | RAs without Load Shedding (Yes/No) | Load Shedding (Yes/No) |
|----------|-------------------|---------------------------------|------------------------------------|------------------------|
| 1 | G10_1 | N | | |
| 2. | G10_2 | N | | |
| 3 | G10_3 | N | | |
| 4 | G10_4 | N | | |
| 5 | G20_1 | N | | |
| 6 | G20_2 | N | | |
| 7 | G20_3 | N | | |
| 8 | G20_4 | N | | |
| 9 | G70_1 | N | | |
| 10 | G70_2 | N | | |
| 11 | G70_3 | Y | Y | |
| 12 | G130_1 | N | | |
| 13 | G130_2 | N | | |
| 14 | G130_3 | N | | |
| 15 | G150_1 | N | | |
| 16 | G150_2 | N | | |
| 17 | G150_3 | N | | |
| 18 | G150_4 | N | | |
| 19 | G150_5 | N | | |
| 20 | G150_6 | N | | |
| 21 | G160 | N | | |
| 22 | G180 | N | | |
| 23 | G210 | N | | |
| 24 | G220_1 | N | | |
| 25 | G220_2 | N | | |
| 26 | G220_3 | N | | |
| 27 | G220_4 | N | | |
| 28 | G220_5 | N | | |
| 29 | G220_6 | N | | |
| 30 | G230_1 | N | | |
| 31 | G230_2 | N | | |
| 32 | G230_3 | N | | |

Table 8.4. Table of first level circuit outages.

| Circuit No. | Outage Components | Constraints Violations (Yes/No) | RAs without Load Shedding (Yes/No) | Load Shedding (Yes/No) |
|--------------------|--------------------------|--|---|-------------------------------|
| 1. | TL10-20 | N | | |
| 2 | TL10-30 | Y | | Y |
| 3 | TL10-50 | N | | |
| 4 | TL20-40 | Y | | Y |
| 5 | TL20-60 | Y | Y | |
| 6 | TL30-240 | Y | | Y |
| 7 | T30-90 | Y | | Y |
| 8 | TL40-90 | N | | |
| 9 | TL50-100 | N | | |
| 10 | TL60-100 | Y | | Y |
| 11 | TL70-80 | COM | | |
| 12 | TL80-90 | COM | | |
| 13 | TL80-100 | COM | | |
| 14 | TL90-110 | Y | | Y |
| 15 | TL90-120 | Y | Y | |
| 16 | TL100-110 | N | | |
| 17 | TL100-120 | N | | |
| 18 | TL110-140 | N | | |
| 19 | TL110-130 | COM | | |
| 20 | TL120-130 | COM | | |
| 21 | TL120-230 | N | | |
| 22 | TL130-230 | N | | |
| 23 | TL140-160 | Y | Y | |
| 24 | TL150-160 | N | | |
| 25 | TL150-240 | Y | | Y |
| 26 | TL150-210 | COM | | |
| 27 | TL150-210 | COM | | |
| 28 | TL160-170 | N | | |
| 29 | TL160-190 | N | | |
| 30 | TL170-180 | N | | |
| 31 | TL170-180 | COM | | |
| 32 | TL180-210 | COM | | |
| 33 | TL180-210 | COM | | |
| 34 | TL190-200 | COM | | |
| 35 | TL190-200 | COM | | |
| 36 | TL200-230 | COM | | |
| 37 | TL200-230 | COM | | |
| 38 | TL220-210 | COM | | |

Table 8.5. Table of first level common mode outages.

| No. | Outage Components | Constraints Violations (Yes/No) | RAs without Load Shedding (Yes/No) | Load Shedding (Yes/No) |
|------------|---------------------------|--|---|-------------------------------|
| 1.(A) | TL220-210 TL220-170 | N | | |
| 2.(B) | TL230-200 TL230-200 | N | | |
| 3.(C) | TL180-210 TL180-210 | N | | |
| 4.(D) | TL150-210 TL150-210 | Y | Y | |
| 5.(E) | TL130-110 TL130-120 | Y | Y | |
| 6.(F) | TL80-90 TL80-100 | Y | | Y |
| 7.(G) | TL190-200 TL190-200 | N | | |
| 8 | TL70-80 G70_1,2,3, L70 | Y | | Y |

Table 8.6. Second level contingencies based on set 1.

Generator G70_3 + another generator on outage.

| Unit No. | Outage Components | Constraints Violations (Yes/No) | RAs without Load Shedding (Yes/No) | Load Shedding (Yes/No) |
|-----------------|--------------------------|--|---|-------------------------------|
| 1. | G70_3, G10_2 | Y | | |
| 2 | G70_3, G10_3 | Y | | |
| 3 | G70_3, G10_4 | Y | | |
| 4 | G70_3, G20_1 | Y | | |
| 5 | G70_3, G20_2 | Y | | |
| 6 | G70_3, G20_3 | Y | | |
| 7 | G70_3, G20_4 | Y | | |
| 8 | G70_3, G70_1 | Y | Y | |
| 9 | G70_3, G70_2 | Y | Y | |
| 10 | G10_1, G70_3 | Y | | |
| 11 | G70_3, G130_1 | Y | | |
| 12 | G70_3, G130_2 | Y | | |
| 13 | G70_3, G130_3 | Y | | |
| 14 | G70_3, G150_1 | Y | | |
| 15 | G70_3, G150_2 | Y | | |
| 16 | G70_3, G150_3 | Y | | |
| 17 | G70_3, G150_4 | Y | | |
| 18 | G70_3, G150_5 | Y | | |
| 19 | G70_3, G150_6 | Y | | |
| 20 | G70_3, G160 | Y | | |
| 21 | G70_3, G180 | Y | | |
| 22 | G70_3, G210 | Y | | |
| 23 | G70_3, G220_1 | Y | | |
| 24 | G70_3, G220_2 | Y | | |
| 25 | G70_3, G220_3 | Y | | |
| 26 | G70_3, G220_4 | Y | | |
| 27 | G70_3, G220_5 | Y | | |
| 28 | G70_3, G220_6 | Y | | |
| 29 | G70_3, G230_1 | Y | | |
| 30 | G70_3, G230_2 | Y | | |
| 31 | G70_3, G230_3 | Y | | |

Table 8.7. Second level contingencies based on Set 1.

Generator G70_3 + one transmission line on outage.

| Circuit No. | Outage Components | Constraints Violations (Yes/No) | RAs without Load Shedding (Yes/No) | Load Shedding (Yes/No) |
|--------------------|--------------------------|--|---|-------------------------------|
| 1. | G70_3, TL10-20 | Y | Y | |
| 2 | G70_3, TL10-30 | Y | | Y |
| 3 | G70_3, TL10-50 | Y | Y | |
| 4 | G70_3, TL20-40 | Y | | Y |
| 5 | G70_3, TL20-60 | Y | Y | |
| 6 | G70_3, TL30-240 | Y | | Y |
| 7 | G70_3, T30-90 | Y | | Y |
| 8 | G70_3, TL40-90 | Y | Y | |
| 9 | G70_3, TL50-100 | Y | Y | |
| 10 | G70_1, TL60-100 | Diverge | | |
| 11 | G70_3, TL70-80 | Com | | |
| 12 | G70_3, TL80-90 | Com | | |
| 13 | G70_3, TL80-100 | com | | |
| 14 | G70_3, TL90-110 | Y | Y | |
| 15 | G70_3, TL90-120 | Y | Y | |
| 16 | G70_3, TL100-110 | Y | Y | |
| 17 | G70_3, TL100-120 | Y | Y | |
| 18 | G70_3, TL110-140 | Y | Y | |
| 19 | G70_3, TL110-130 | Com | | |
| 20 | G70_3, TL120-130 | Com | | |
| 21 | G70_3, TL120-230 | Y | Y | |
| 22 | G70_3, TL130-230 | Y | Y | |
| 23 | G70_3, TL140-160 | Y | Y | |
| 24 | G70_3, TL150-160 | Y | Y | |
| 25 | G70_3, TL150-240 | Y | | Y |
| 26 | G70_3, TL150-210 | Com | | |
| 27 | G70_3, TL150-210 | Com | | |
| 28 | G70_3, TL160-170 | Y | Y | |
| 29 | G70_3, TL160-190 | Y | Y | |
| 30 | G70_3, TL170-180 | Y | Y | |
| 31 | G70_3, TL170-220 | Com | | |
| 32 | G70_3, TL180-210 | Com | | |
| 33 | G70_3, TL180-210 | Com | | |
| 34 | G70_3, TL190-200 | Com | | |
| 35 | G70_3, TL190-200 | Com | | |
| 36 | G70_3, TL200-230 | Com | | |
| 37 | G70_3, TL200-230 | Com | | |
| 38 | G70_3, TL220-210 | Com | | |

Table 8.8. Second level contingencies based on set 1.

Transmission line 20-60 + one generator on outage.

| Unit No. | Outage Components | Constraints Violations (Yes/No) | RAs without Load Shedding (Yes/No) | Load Shedding (Yes/No) |
|-----------------|--------------------------|--|---|-------------------------------|
| 1 | G10_1 | Y | Y | |
| 2. | G10_2 | Y | Y | |
| 3 | G10_3 | Y | Y | |
| 4 | G10_4 | Y | Y | |
| 5 | G20_1 | Y | Y | |
| 6 | G20_2 | Y | Y | |
| 7 | G20_3 | Y | Y | |
| 8 | G20_4 | Y | Y | |
| 9 | G70_1 | Y | Y | |
| 10 | G70_2 | Y | Y | |
| 11 | G70_3 | Y | Y | |
| 12 | G130_1 | Y | Y | |
| 13 | G130_2 | Y | Y | |
| 14 | G130_3 | Y | Y | |
| 15 | G150_1 | Y | Y | |
| 16 | G150_2 | Y | Y | |
| 17 | G150_3 | Y | Y | |
| 18 | G150_4 | Y | Y | |
| 19 | G150_5 | Y | Y | |
| 20 | G150_6 | Y | Y | |
| 21 | G160 | Y | Y | |
| 22 | G180 | Y | Y | |
| 23 | G210 | Y | Y | |
| 24 | G220_1 | Y | Y | |
| 25 | G220_2 | Y | Y | |
| 26 | G220_3 | Y | Y | |
| 27 | G220_4 | Y | Y | |
| 28 | G220_5 | Y | Y | |
| 29 | G220_6 | Y | Y | |
| 30 | G230_1 | Y | Y | |
| 31 | G230_2 | Y | Y | |
| 32 | G230_3 | Y | Y | |

Table 8.9. Second level contingencies based on set 1.

Transmission line 20-60 + another transmission line on outage.

| Circuit No. | Outage Components | Constraints Violations (Yes/No) | RAs without Load Shedding (Yes/No) | Load Shedding (Yes/No) |
|--------------------|--------------------------|--|---|-------------------------------|
| 1. | TL10-20 | Y | Y | |
| 2 | TL10-30 | Y | | Y |
| 3 | TL10-50 | Y | Y | |
| 4 | TL20-40 | Y | | Y |
| 5 | TL20-60 | | | |
| 6 | TL30-240 | Y | | Y |
| 7 | T30-90 | Y | | Y |
| 8 | TL40-90 | Y | Y | |
| 9 | TL50-100 | Y | Y | |
| 10 | TL60-100 | N | | |
| 11 | TL70-80 | COM | | |
| 12 | TL80-90 | COM | | |
| 13 | TL80-100 | COM | | |
| 14 | TL90-110 | Y | | Y |
| 15 | TL90-120 | Y | | Y |
| 16 | TL100-110 | Y | Y | |
| 17 | TL100-120 | Y | Y | |
| 18 | TL110-140 | Y | Y | |
| 19 | TL110-130 | COM | | |
| 20 | TL120-130 | COM | | |
| 21 | TL120-230 | Y | Y | |
| 22 | TL130-230 | Y | Y | |
| 23 | TL140-160 | Y | Y | |
| 24 | TL150-160 | Y | Y | |
| 25 | TL150-240 | Y | | Y |
| 26 | TL150-210 | COM | | |
| 27 | TL150-210 | COM | | |
| 28 | TL160-170 | Y | Y | |
| 29 | TL160-190 | Y | Y | |
| 30 | TL170-180 | Y | Y | |
| 31 | TL170-220 | Com | | |
| 32 | TL180-210 | Com | | |
| 33 | TL180-210 | Com | | |
| 34 | TL190-200 | Com | | |
| 35 | TL190-200 | Com | | |
| 36 | TL200-230 | Com | | |
| 37 | TL200-230 | Com | | |
| 38 | TL220-210 | Com | | |

Table 8.10. Second level contingencies based on set 1.

Transmission line 90-120 + one generator on outage.

| Circuit No. | Outage Components | Constraints Violations (Yes/No) | RAs without Load Shedding (Yes/No) | Load Shedding (Yes/No) |
|--------------------|--------------------------|--|---|-------------------------------|
| 1 | G10_1 | Y | Y | |
| 2. | G10_2 | Y | Y | |
| 3 | G10_3 | Y | Y | |
| 4 | G10_4 | Y | Y | |
| 5 | G20_1 | Y | Y | |
| 6 | G20_2 | Y | Y | |
| 7 | G20_3 | Y | Y | |
| 8 | G20_4 | Y | Y | |
| 9 | G70_1 | Y | Y | |
| 10 | G70_2 | Y | Y | |
| 11 | G70_3 | Y | Y | |
| 12 | G130_1 | Y | Y | |
| 13 | G130_2 | Y | Y | |
| 14 | G130_3 | Y | Y | |
| 15 | G150_1 | Y | Y | |
| 16 | G150_2 | Y | Y | |
| 17 | G150_3 | Y | Y | |
| 18 | G150_4 | Y | Y | |
| 19 | G150_5 | Y | Y | |
| 20 | G150_6 | Y | Y | |
| 21 | G160 | Y | Y | |
| 22 | G180 | Y | Y | |
| 23 | G210 | Y | Y | |
| 24 | G220_1 | Y | Y | |
| 25 | G220_2 | Y | Y | |
| 26 | G220_3 | Y | Y | |
| 27 | G220_4 | Y | Y | |
| 28 | G220_5 | Y | Y | |
| 29 | G220_6 | Y | Y | |
| 30 | G230_1 | Y | Y | |
| 31 | G230_2 | Y | Y | |
| 32 | G230_3 | Y | Y | |

Table 8.11. Second level contingencies based on Set 1.

Transmission line 90-120 + another transmission line on outage.

| Circuit No. | Outage Components | Constraints Violations (Yes/No) | RAs without Load Shedding (Yes/No) | Load Shedding (Yes/No) |
|--------------------|--------------------------|--|---|-------------------------------|
| 1. | TL10-20 | Y | Y | |
| 2 | TL10-30 | Y | | Y |
| 3 | TL10-50 | Y | Y | |
| 4 | TL20-40 | Y | | Y |
| 5 | TL20-60 | Y | | Y |
| 6 | TL30-240 | Y | | Y |
| 7 | T30-90 | Y | | Y |
| 8 | TL40-90 | Y | Y | |
| 9 | TL50-100 | Y | Y | |
| 10 | TL60-100 | Y | | Y |
| 11 | TL70-80 | COM | | |
| 12 | TL80-90 | COM | | |
| 13 | TL80-100 | COM | | |
| 14 | TL90-110 | Y | | Y |
| 15 | TL90-120 | | | |
| 16 | TL100-110 | Y | Y | |
| 17 | TL100-120 | Y | | Y |
| 18 | TL110-140 | Y | | Y |
| 19 | TL110-130 | COM | | |
| 20 | TL120-130 | COM | | |
| 21 | TL120-230 | Y | Y | |
| 22 | TL130-230 | Y | Y | |
| 23 | TL140-160 | Y | Y | |
| 24 | TL150-160 | Y | Y | |
| 25 | TL150-240 | Y | | Y |
| 26 | TL150-210 | COM | | |
| 27 | TL150-210 | COM | | |
| 28 | TL160-170 | Y | Y | |
| 29 | TL160-190 | Y | Y | |
| 30 | TL170-180 | Y | Y | |
| 31 | TL170-220 | COM | | |
| 32 | TL180-210 | COM | | |
| 33 | TL180-210 | COM | | |
| 34 | TL190-200 | COM | | |
| 35 | TL190-200 | COM | | |
| 36 | TL200-230 | COM | | |
| 37 | TL200-230 | COM | | |
| 38 | TL220-210 | COM | | |

**Table 8.12. Second level contingencies based on set 1.
Transmission line 140-160 + one generator on outage.**

| Unit No. | Outage Components | Constraints Violations (Yes/No) | RAs without Load Shedding (Yes/No) | Load Shedding (Yes/No) |
|-----------------|--------------------------|--|---|-------------------------------|
| 1 | G10_1 | Y | Y | |
| 2. | G10_2 | Y | Y | |
| 3 | G10_3 | Y | Y | |
| 4 | G10_4 | Y | Y | |
| 5 | G20_1 | Y | Y | |
| 6 | G20_2 | Y | Y | |
| 7 | G20_3 | Y | Y | |
| 8 | G20_4 | Y | Y | |
| 9 | G70_1 | Y | Y | |
| 10 | G70_2 | Y | Y | |
| 11 | G70_3 | Y | Y | |
| 12 | G130_1 | Y | Y | |
| 13 | G130_2 | Y | Y | |
| 14 | G130_3 | Y | Y | |
| 15 | G150_1 | Y | Y | |
| 16 | G150_2 | Y | Y | |
| 17 | G150_3 | Y | Y | |
| 18 | G150_4 | Y | Y | |
| 19 | G150_5 | Y | Y | |
| 20 | G150_6 | Y | Y | |
| 21 | G160 | Y | Y | |
| 22 | G180 | Y | Y | |
| 23 | G210 | Y | Y | |
| 24 | G220_1 | Y | Y | |
| 25 | G220_2 | Y | Y | |
| 26 | G220_3 | Y | Y | |
| 27 | G220_4 | Y | Y | |
| 28 | G220_5 | Y | Y | |
| 29 | G220_6 | Y | Y | |
| 30 | G230_1 | Y | Y | |
| 31 | G230_2 | Y | Y | |
| 32 | G230_3 | Y | Y | |

Table 8.13. Second level contingencies based on set 1.
Transmission line 140-160 + another transmission line on outage.

| Circuit No. | Outage Components | Constraints Violations (Yes/No) | RAs without Load Shedding (Yes/No) | Load Shedding (Yes/No) |
|--------------------|--------------------------|--|---|-------------------------------|
| 1. | TL10-20 | Y | Y | |
| 2 | TL10-30 | Y | | Y |
| 3 | TL10-50 | Y | Y | |
| 4 | TL20-40 | Y | | Y |
| 5 | TL20-60 | Y | Y | |
| 6 | TL30-240 | Y | | Y |
| 7 | T30-90 | Y | | Y |
| 8 | TL40-90 | Y | Y | |
| 9 | TL50-100 | Y | Y | |
| 10 | TL60-100 | Diverge | | |
| 11 | TL70-80 | Com | | |
| 12 | TL80-90 | Com | | |
| 13 | TL80-100 | Com | | |
| 14 | TL90-110 | Y | | Y |
| 15 | TL90-120 | Y | Y | |
| 16 | TL100-110 | Y | Y | |
| 17 | TL100-120 | Y | Y | |
| 18 | TL110-140 | Y | Y | |
| 19 | TL110-130 | Com | | |
| 20 | TL120-130 | Com | | |
| 21 | TL120-230 | Y | Y | |
| 22 | TL130-230 | Y | Y | |
| 23 | TL140-160 | | | |
| 24 | TL150-160 | Y | Y | |
| 25 | TL150-240 | Y | | Y |
| 26 | TL150-210 | Y | Y | |
| 27 | TL150-210 | Y | Y | |
| 28 | TL160-170 | Y | Y | |
| 29 | TL160-190 | Y | Y | |
| 30 | TL170-180 | Y | Y | |
| 31 | TL170-220 | com | | |
| 32 | TL180-210 | Com | | |
| 33 | TL180-210 | com | | |
| 34 | TL190-200 | com | | |
| 35 | TL190-200 | Com | | |
| 36 | TL200-230 | Com | | |
| 37 | TL200-230 | Com | | |
| 38 | TL220-210 | Com | | |

9. Conclusions

The report has presented a comprehensive reliability assessment method for transmission systems. The method is based on a number of computational algorithms that identify the system states that contribute to system unreliability. A by-product of the method is the determination of the sequence of events, if it exists, that may trigger system collapse. The methodology supports any user selected failure criteria.

The methodology has also created a number of improved analysis tools. Among them they are: (a) the single phase quadratized power flow, (b) improved contingency selection method, (c) a comprehensive and efficient remedial actions method and (d) an accurate and efficient stochastic power flow. One common characteristic of these tools is the quadratized model of the electric power system. Specifically, the mathematical model of the electric power system has been reformulated to be expressed in terms of mostly linear equations with few nonlinear equations of degree no higher than two. The quadratization is easily achieved with the introduction of additional state variables. It has been observed that the quadratized model yields more efficient solution procedures. For this reason, it is recommended that this general approach be further investigated and developed.

One very important issue that is facing the industry today is the handling of reliability issues in an open power market operation. Because the reliability assessment models are so complex, the introduction of these models into market operations is problematic. There is a need to integrate reliability issues into market operations. This is a very difficult task. Conceptually, the techniques developed in this research project can be applied to assess system reliability under real time operation in an open market environment. The efficiency of the tools however may present serious obstacles. On the other hand it is recognized that in real time operations the probabilities of outage events are quite different and simplifying modifications can be made based on the event probabilities. This type of approach should be investigated in the future.

References

- [1] J. Endrenyi, *Reliability Modeling in Power Systems*, John Wiley & Sons, 1978.
- [2] Koeunyi Bae and James S. Thorp, "An Importance Sampling Application: 179 Bus WSCC System under Voltage Based Hidden Failures and Relay Misoperations," in Proceedings of the IEEE Hawaii International Conference on System Sciences, January 6-9, 1997, Kona, Hawaii.
- [3] A.G.Phadke and James S. Thorp, "Expose Hidden Failures to Prevent Cascading Outages," IEEE Computer Application in Power, July 1996, pp. 20-23.
- [4]. A. P. Sakis Meliopoulos, *Power System Modeling, Analysis and Control*, ECE6320 Class Notes, Georgia Institute of Technology, 2002.
- [5] Roy Billinton and Ronald N. Allan, *Reliability Evaluation of Power Systems*, Plenum Press, New York, 1996.
- [6] A. P. Sakis Meliopoulos, N. D. Reppen, R. Kovacs, M. P. Bhavaraju, N. J. Balu, M. Lauby, and R. Billinton, "A Probabilistic Method for Transmission Planning," in Proceedings of the 1998 International Conference on Probabilistic Methods Applied to Power Systems (PMAPS), Oakland, California, September 1998.
- [7] A. P. Sakis Meliopoulos, Carol S. Cheng, and Feng Xia, "Performance Evaluation of Static Security Analysis Methods," IEEE Transactions on Power Systems, vol. 9, no. 3, August 1994, pp.1441-1449.
- [8] Allen J. Wood and Bruce F. Wollenberg, *Power Generation, Operation, and Control*, John Wiley & Sons, Inc. 1984.
- [9] Roy Billinton and Wenyuan Li, *Reliability Assessment of Electric Power Systems Using Monte Carlo Methods*, Plenum Press, New York, 1994.
- [10] M.Mazumdar, "Importance Sampling in Reliability Estimation," *Reliability and Fault Tree Analysis*, SIAM, Philadelphia, 1975, pp.153-163.
- [11] E. Khan, R. Billinton, "A Hybrid Model for Quantifying Different Operating States of Composite Power Systems," IEEE Transactions on Power Systems, vol.7, no.1, February 1992.
- [12] C. Singh, J.Mitra, "Composite System Reliability Evaluation using State Space Pruning", IEEE Transactions on Power Systems, vol. 12, no. 1, February 1997, pp 471-479.

- [13] Sun Wook Kang, A.P. Meliopoulos, “Contingency Selection via Quadratized Power Flow Sensitivity Analysis,” in Proceedings of the IEEE 2002 Power Engineering Society Summer Meeting, vol.3, pp.1494-1499.
- [14] K. A. Clements, B. P. Lam, D. J. Lawrence, N. D. Reppen, “Computation of Upper and Lower Bounds on Reliability Indices for Bulk Power Systems,” IEEE Transactions on Power Apparatus and Systems, vol. PAS-103, no.8, August 1984, pp. 2318 – 2325.
- [15] George Stefopoulos, Fang Yang and A. P. Sakis Meliopoulos, “An Improved Contingency Ranking Method”, in Proceedings of the 35th North America Power Symposium (NAPS), Rolla MO, October, 2003.
- [16] David G. Luenberger, Linear and Nonlinear Programming, Addison-Wesley, 1989.
- [17] Fang Yang, A. P. Sakis Meliopoulos, George J. Cokkinides, “A Bulk System Reliability Assessment Methodology”, in Proceedings of the 8th International Conference on Probabilistic Methods Applied to Power Systems (PMAPS), Ames, Iowa, September 12-16, 2004, pp. 44-49.
- [18] A. P. Meliopoulos, A. G. Bakirtzis, R. Kovacs, “Power system reliability evaluation using stochastic load flows,” IEEE Transactions on Power Apparatus and Systems, vol. PAS-103, no. 5, pp. 1084–1091, May 1984.
- [19] A. P. Sakis Meliopoulos, George J. Cokkinides, Xing Yong Chao, “A new probabilistic power flow analysis method,” IEEE Transactions on Power Systems, vol. 5, no. 1, pp. 182–190, February 1990.
- [20] A. P. Meliopoulos, X. Chao, George J. Cokkinides, R. Monsalvatge, “Transmission loss evaluation based on probabilistic power flow,” IEEE Transactions on Power Systems, vol. 6, no. 1, pp. 364–371, February 1991.
- [21] George K Stefopoulos, A. P. Meliopoulos and George J. Cokkinides, “Probabilistic Power Flow with Non-Conforming Electric Loads,” in Proceedings of the 8th International Conference on Probability Methods Applied to Power Systems (PMAPS), Ames, Iowa, September 12-16, 2004, pp. 525-531.
- [22] A. P. Meliopoulos, George J. Cokkinides, Fang Yang and George K. Stefopoulos, “Probabilistic Simulation of Power Grids via Multi-Point-Linearization,” submitted to the 43rd IEEE Conference on Decision and Control (CDC), Atlantis, Paradise Island, Bahamas, December 14-17, 2004.
- [23] George K. Stefopoulos, A. P. Meliopoulos and George J. Cokkinides, “Comparison of Linearized Stochastic Power Flow and Monte Carlo Simulation”, presented at the 36th Annual North American Power Symposium (NAPS), Moscow, Idaho, August 9-10, 2004.

- [24] IEEE Committee Report, "IEEE Reliability Test System," IEEE Transactions on Power Apparatus and Systems, vol. PAS-98, no. 6, pp. 2047–2054, November/December 1979.
- [25] James A. Momoh, M. E. El-Hawary, Ramababu Adapa, "A Review of Selected Optimal Power Flow Literature to 1993 Part I: NonLinear and Quadratic Programming Approaches," IEEE Transactions on Power Systems, vol. 14, no. 1, February 1999, pp. 96-104.
- [26] James A. Momoh, M. E. El-Hawary, Ramababu Adapa, "A Review of Selected Optimal Power Flow Literature to 1993 Part II: Newton, Linear Programming and Interior Point Methods," IEEE Transaction on Power Systems, vol. 14, no. 1, February 1999, pp. 105-111.
- [27] A.P.Sakis Meliopoulos, Sun Wook Kang, George Cokkinides, "Probabilistic Transfer Capability Assessment in a Deregulated Environment," in Proceedings of the 33rd IEEE Hawaii International Conference on System Sciences, January 2000.
- [28] Sun Wook Kang, A New Approach for Power Transaction Evaluation and Transfer Capability Analysis, Ph.D. Thesis, Atlanta: Georgia Institute of Technology, 2001.